COMBUSTION SYNTHESIS OF DIAMOND FILMS

By

SRIHARI NANDYAL

Bachelor of Engineering

Karnataka Regional Engineering College

Surathkal, India

1985

Submitted to the Faculty of the
Graduate College of the
Oklahoma State University
in partial fulfillment of
the requirements for
the Degree of
MASTER OF SCIENCE
December, 1991

COMBUSTION SYNTHESIS OF DIAMOND FILMS

Thesis Approved:

R Kossandueri

Thesis Adviser

C E Eline

Don A. Lucca

Norman N Durham

Dean of the Graduate College

PREFACE

Diamond films were synthesized using an oxy-acetylene flame on a polished molybdenum substrate. The effect of different parameters such as gas flow rates, ratio of oxygen to acetylene, separation of the inner cone from the substrate, and acetylene cylinder pressure were studied. The morphological characteristics of the diamond films were then examined under a scanning electron microscope and their quality assessed using μRaman spectroscopy.

A growth mechanism is proposed which explains the evolution of different crystalline forms of diamond from the cauliflower-like structures. The use of this hypothesis could enable the synthesis of diamond crystallites with a preferred orientation. The effect of the acetylene cylinder pressure on the transparency of the diamond films grown has been addressed and a plausible cause for the improvement in film quality is given. A method for growing uniform films has been proposed based on the shape of the stagnation zone in the flame.

This project has been funded by MOST Chair funds and a grant from the Oklahoma Center for Integrated Design and Manufacturing (OCIDM).

I wish to express my sincere gratitude to my adviser, Professor Ranga Komanduri, whose inspiration, guidance, and constant encouragement kept me motivated during this project. I am also grateful to my other committee members, Dr. C. E. Price and Dr. D. A. Lucca, for their advise during the course of this work.

This project is a part of the research efforts of the Oklahoma CVD Diamond Research group. The author acknowledges the many contributions of this group towards the completion of the project.

Special thanks are due to Drs. James Lange and J. P. Wicksted of the Physics Department for their interest in the diamond film project and in enabling the use of the μRaman facility. Thanks are also due to Mr. Chuck Hasty and Mr. Steve Wang of the Physics Department for spending considerable time and providing the Raman spectrum of large number of samples. Thanks are also due to Dr. Lionel Raff, Dr. Paul Geno, and Mr. Tim Smith of the Chemistry Department for the analysis of gas samples. I would also like to express my gratitude to Dr. K. A. M. Gasem for his interest in this work and to Mr. Charles Baker, Lab Manager, of the Chemical Engineering Department for assistance during the course of this investigation.

I am greatly indebted to Drs. L. L. Hoberock and C. E. Price of the Mechanical and Aerospace Engineering Department for the financial support during the course of this study.

To all my wonderful colleagues in the Manufacturing Processes Group, I extend my sincere thanks. Special thanks are due to Ron Markum and other members of the MAE Research Laboratory who helped me in setting up the apparatus.

To my parents, Mr. Seshasayan and Mrs. Vijayalakshmi, and sisters, Mrs. Vyjayanthi and Ms. Vydehi, I owe a deep sense of gratitude for patiently providing moral support and encouragement throughout my graduate study at Oklahoma State University.

TABLE OF CONTENTS

LIST OF TABLES

LIST OF FIGURES

Figure Page

CHAPTER I

INTRODUCTION TO DIAMOND SYNTHESIS

Nature of Diamond

The many unique properties of diamond have made it one of the most fascinating materials on earth. Its extreme hardness (~8000 kg/mm^2) unmatched by any other material, high thermal conductivity (5 times that of copper), high wear resistance, low friction, and bewitching optical properties have always aroused man's curiosity to know the composition of diamond and to explore possibilities of synthesizing this exquisite gem. Appendix A gives the various properties of diamond. In the medieval ages, diamond was used solely as a precious gem and lapidarys had perfected the art of diamond cutting even at that time. However, the scientific work on this fascinating material got an impetus when Newton [1] suggested that diamond was probably an unctuos coagulated substance. In 1772, Lavoisier [2] burnt diamonds in a closed bell-jar by focusing sunlight on the diamonds and examined the resulting gas. He observed that the gas had properties similar to carbon-dioxide which was also the end product of the combustion of charcoal. He conjectured that diamond and charcoal were probably of the same chemistry.

In 1797, Smithson Tennant [3] conducted a series of experiments to validate Lavoisier's theory. He observed that the amount of carbon-dioxide that was produced by burning known weights of diamond was exactly same as obtained by the combustion of same weight of charcoal. He concluded that diamond was a crystalline form of charcoal. Allen and Pepys [4] consolidated Tennant's work when they found that the carbon-dioxide produced by the combustion of similar weights of diamond and different types of charcoal was passed through lime water, equal weights of calcium carbide precipitated out. They

summarized that diamond and all other carbonaceous substances were alike, only differing in their state of aggregation. This was also confirmed by Davy in 1814 [5].

Diamond Growth Under High-Pressure Conditions

The realization that diamond, which was now known to be a dense form of carbon, could be synthesized under high-pressure and high-temperature conditions occurred during the later part of the 19th century. During this period the South African diamond mines were discovered suggesting that diamonds were possibly developing inside the earth under high-pressure and high-temperature conditions existing there. This observation fuelled innumerable attempts to synthesize diamonds under these conditions.

In 1880, J. B. Hannay [6] claimed to have made diamonds by heating a mixture of hydrocarbons, bone oil, and lithium at red heat in sealed wrought iron tubes. Out of the eighty tubes used, only three did not explode and were found to contain crystalline carbon which looked exactly like diamond. Carbon analysis of the crystals showed that they contained 97.85% carbon. However, Hannay's experiments were very unreliable and present knowledge indicates that the temperatures used by Hannay and the reaction pressures in the tubes were too low for the synthesis of diamond.

In 1894, a French chemist Henri Moissan [7] dissolved sugar-charcoal in molten iron and quenched the solution in cold water. This caused the carbon to crystallize under the high pressure generated by the contraction of the mass as it cooled from the outside. Moissan extracted transparent crystals when he dissolved the metal from the solidified melt, which he claimed as 'diamonds'. These crystals were reported to have good optical properties and produced carbon-dioxide on combustion.

Moissan's synthesis method was attempted by Sir William Crookes [8], Sir Charles Parsons [9] and J. W. Hershey [10] without much success. Parsons assiduously worked for thirty years using his own techniques as well as Moissan's to synthesize diamonds, but

meticulous examination of the transparent crystals he synthesized revealed that they were either magnesia or alumina and were not combustible.

The development of thermodynamics in the early part of the twentieth century and the availability of high-pressure technology [11] along with the P-T equilibrium diagram of carbon (Fig. 1), culminated finally in the successful synthesis of man made diamonds from graphite by researchers at General Electric Company [12] in 1955. Using a molten transition metal catalyst-solvent in a high temperature (~ 1500° C) and high pressure (~ 50 kbar) press, diamonds were successfully synthesized. It can be seen from Figure 1, at these conditions diamond is the thermodynamically stable form of carbon. Since then plants in many countries using this high pressure-high temperature (HP-HT) method produce about 30 to 40 tons of synthetic diamond grit per year for abrasive use.

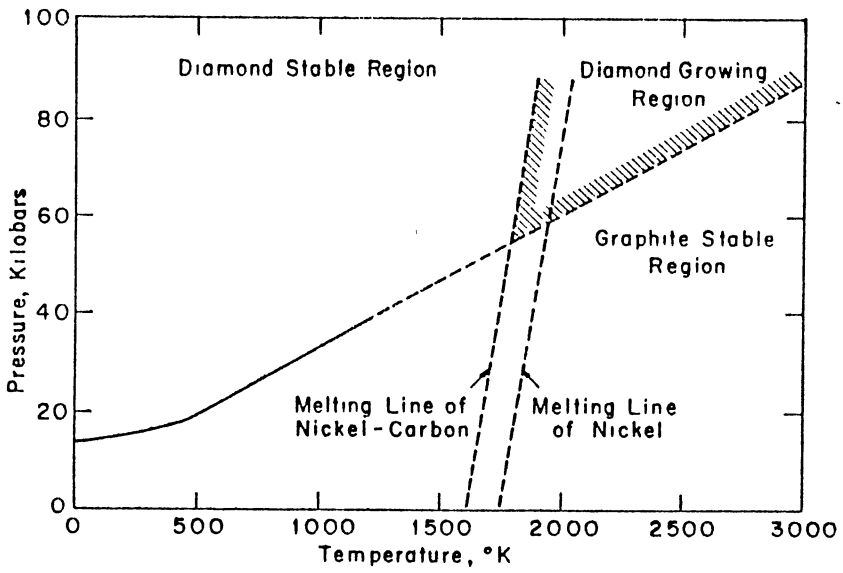

Figure 1. P-T Diagram of Carbon showing the Diamond Stable Region [13]

In 1961, De Carli and Jamieson [14] using intense-shock compression of graphite reported the formation of very fine crystallites (upto a few hundred Angstroms) of diamond. In this technique, graphite is subjected to pressures of the order of 300 kbar instantaneously at an estimated temperature of 1200° C.

Diamond Synthesis Under Low-Pressure Conditions

The methods of synthesizing diamond mentioned thus far utilize temperature and pressure conditions where diamond is the stable form of carbon. Under normal atmospheric conditions, graphite is the stable form of carbon and exists along with diamond, which is metastable (Fig. 1). This co-existence is possible because their is an activation or kinetic barrier which prevents the spontaneous transformation of diamond to the more stable phase.

Though diamond is the metastable form of carbon under low pressure or atmospheric conditions, this does not preclude its crystallization under these conditions. This is because the free energy of carbon in the diamond form is slightly higher than in the graphite form in the graphite stable region. Under suitable experimental conditions, it is possible to grow diamonds by using compounds such as methane, CO, carbon vapor, etc., in which the free energy of the carbon atoms is higher than the carbon in diamond [15]. If the carbon atoms during their fall from a state of higher free energy could pause at the lower level of diamond instead of going all the way down to that of graphite, diamond could be crystallized. This possibility of synthesizing diamonds in the graphite stable region was also acknowledged by Bridgman [16].

The earliest documented effort on the growth of diamonds from low pressure gases was as far back as 1911 by von Bolton [17]. He reported the epitaxial growth on diamond seed crystals from illuminating gas (acetylene) decomposition in the presence of mercury vapor at 100° C.

However, the first successful work was that of Eversole [18] of Union Carbide using thermal pyrolysis method for the vapor deposition of diamond. This work was contemporaneous with that of the high pressure-high temperature process and consisted of passing a carbon containing gas (preferably with methyl group) over seed crystals at a temperature of about 1000° C and a pressure of a few torr. New diamond was formed on the seeds until it was hampered by the accumulation of graphite, which was then removed by heating the diamond-deposited seed crystals in a hydrogen gas atmosphere at about 1000° C and 50 atmospheres. For continuous diamond growth, this deposition-cleaning cycle was repeated. The growth rates, however, were extremely low (a few Angstroms /hour) and impractical for serious considerations for commercial use. Consequently, there was much scepticism about this process.

Later, Angus and co-workers [19-21] at Case Western Reserve University conducted basic CVD diamond studies and confirmed Eversole's findings but could not improve upon the low growth rates (angstroms/hr) substantially. The process was plagued by the co-deposition of graphite along with diamond, thus necessitating time consuming graphite removal operations. However, Angus realized that atomic hydrogen had a very important role to play in the removal of co-deposited graphite [22]. Taking this lead Deryagin, Fedoseev, Spitsyn and co-workers [23-24] at the Institute of Physical Chemistry in Moscow demonstrated this aspect. They observed that super-equilibrium concentrations of atomic hydrogen obtained by decomposing molecular hydrogen during the deposition process, acted as a "solvent" for graphite but did not affect the diamond growth. They, therefore, suggested that by activating the gas by hot-filament or arc discharge, the growth of graphite could be impeded because of the simultaneous etching of graphite during growth. They reported that they grew diamond at a rate of 3-5 μm/hr using the chemical transport reaction method. Details of this process, however, were not revealed.

The substantially improved growth rates reported by the Russian workers prompted researchers all around the world and especially in Japan to explore methods for effectively

decomposing the precursor gases. A spate of activation techniques were reported, each method differing only in the manner in which the constituent gases were decomposed. Lux and Haubner [25] have classified these techniques as follows:

1. Activation by High Temperatures.
   - Hot filament
   - Laser heating
   - Arc discharge and arc plasma jets
   - Combustion flames
2. Activation by Electric or Electromagnetic Discharge.
   - Microwave and radio frequency gas discharge
   - DC and AC glow discharges
3. Plasma Jet Methods
   - R.F.
   - Microwave
   - D.C.
4. Combined Activation
   - Hot filament + Microwave
   - Hot filament + DC discharge
   - Hot filament + BIAS

In 1988 Hirose [26] of Japan, announced a simple method of synthesizing diamond films based on oxy-acetylene combustion flame with a slightly fuel rich mixture. This technique offers a very simple and economical means of synthesizing diamond films at growth rates of 60-150 μm/hr. As the diamond growth takes place under atmospheric conditions, expensive vacuum chambers and equipment are not required. The flame provides its own environment for diamond growth and the quality of the film is dependent on such process variables as the gas flow rates, gas flow ratios, substrate temperatures,

and purity of the gases. This interesting new technique is yet to be fully exploited and is the subject of this investigation.

Applications of Diamond Films

The unique combination of properties bestowed upon diamond has enabled its use in a variety of applications. Diamond is the hardest material existing on this planet and its density, room-temperature thermal conductivity, elastic modulus, and wear resistance are unmatched by any known material. Its high refractive index and optical dispersion properties are the best known. It also has a high resistance to chemical attack. Appendix C compares the properties of diamond with cubic boron nitride (cBN), the next hardest material. Figure 2 lists the unique properties of diamond together with current or potential applications [27].

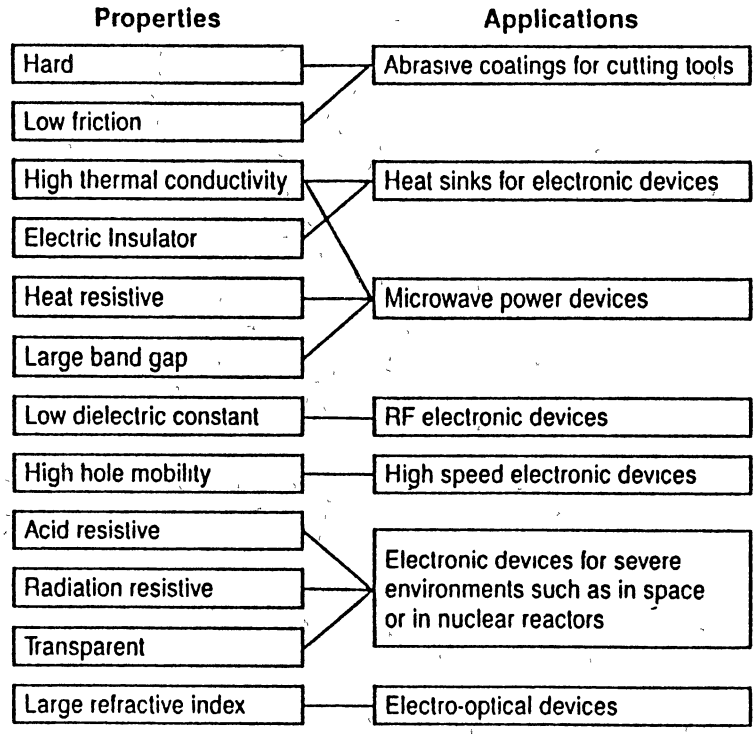

Figure 2. Relationship Between the Unique Properties of Diamond and its Current or Potential Applications [27]

The ability to deposit diamond films over large areas, has enhanced the use of diamond as a wear resistant coating for tribological applications. It's extreme hardness, excellent lubricity, and low coefficient of friction has favored its use as abrasive grains and as coatings on cutting tools, wire drawing dies, and bearing surfaces. It may also be possible to employ diamond coatings as impact-protection coatings for rain erosion and small particle impact. Diamond's excellent sound propagation qualities have already found use in audio speaker diaphragms to improve the dynamic range of the speaker.

Windows for high power lasers may take advantage of diamonds high thermal conductivity, low coefficient of expansion, and strength. The high thermal conductivity has led to the use of diamond as a heat sink material in electronic applications. Other possible applications of diamond which take advantage of its optical properties are as coatings on optical elements and infrared lenses.

Diamond electronics is another area where the semiconducting nature of diamond can be exploited. Diamond is a wide band gap semi-conductor (5.5 eV) and, furthermore, has a breakdown voltage ($\sim 10^7$ V/cm) and a saturation velocity (2.7×10^7cm /s) higher than silicon, GaAs or InP. Electron and hole mobilities are approximately 1900 and 1200 cm^2/V-sec respectively. However, the use of vapor grown diamond as an active electronic component will require greater crystalline perfection than is now available.

Summing up, the unique properties of diamond and now the ability to deposit diamond films on a variety of substrates using low pressure CVD techniques vastly expands the potential application areas for these materials over that possible with high-pressure, high-temperature method. These developments herald a new era in diamond technology opening economic opportunities for a range of manufacturing, tribological and optical applications.

CHAPTER II

LITERATURE REVIEW

In this chapter a critical review of the synthesis and related aspects of the activated chemical vapor deposition (CVD) of polycrystalline diamond films is presented. Emphasis will be on the combustion synthesis method of diamond growth as this process is the subject of this investigation. Excellent reviews of the historical development of CVD diamond may be found in the papers by Devries [28], Angus and Hayman [29] and Spear [30].

In the following, various techniques used for the synthesis of diamond films will be described. A detailed review of the work on the combustion synthesis technique will then be followed by the morphological and characterization aspects, growth mechanisms, and the chemical aspects of diamond film growth. The importance of the roles of hydrogen and oxygen in the preferential etching of co-deposited graphite is also described.

On the Synthesis of Diamond Films by Various Activated CVD Techniques

The versatility of chemical vapor deposition and the realization that diamond can be grown under metastable conditions has enabled the use of this technique in the successful synthesis of diamond films. Early attempts using thermal pyrolysis [18] and vapor transport reactions [24] were fraught with difficulties and extremely low deposition rates (angstroms/hr). These low growth rates were a result of the codeposition of graphite along with diamond. However, the observation of Angus et. al.[22] and the subsequent demonstration by Deryaguin et. al.[23] of the beneficial effects of atomic hydrogen in the

preferential removal of co-deposited graphite increased the growth rates of diamond to the order of a few microns per hour. Since then a number of activation techniques based on CVD methods have been announced [25], Figure 3, each method differing principally in the means used to decompose the source gases.

Matsumoto and co-workers [31-32] at the National Institute for Research in Inorganic Materials (NIRIM) in Japan were among the first to demonstrate the use of a hot filament in a closed CVD system. In this simple technique, a dilute solution of CH_4 (~1%) in hydrogen is decomposed by passing it over a tungsten filament heated to about 2000° C. Growth rates of ~1 μm/hr were reported. Since then this process has been studied and used with great success by many researchers around the world [33-41]. Different materials such as Si, Mo, Ta, and W have been successfully coated and higher growth rates (~8-10 μm/hr) using organic compounds such as acetone, trimethylamine and alcohols have been achieved [35]. Though contamination of the growing film by filament metal evaporation is a problem in this method, it has found applications in areas where ultraclean films are not required and has been successfully used to coat large areas .

The first successful use of a microwave plasma assisted method to activate the gas for growing polycrystalline diamond was reported by Kamo and co-workers [42]. Microwave radiation at a frequency of 2.45 GHz was used to dissociate the precursor gases (~1% CH_4 and ~99% H_2), depositing high quality diamond films at rates of 1-2 μm/hr. The advantage of the microwave plasma deposition over other diamond fabrication methods is its stability and reliability. The system can be easily run for days without any problems and metal contamination of the film by hot electrodes or filaments is not involved. As a result this technique has been the most extensively studied with the objective of reducing the deposition temperatures [43-44], to coat cutting tools [45] and optical materials [43], and to increase the deposition area [46].

Other activated CVD approaches to diamond film growth include arc discharge or direct current plasma jets [44-51] where growth rates of 80 μm/hr have been reported.

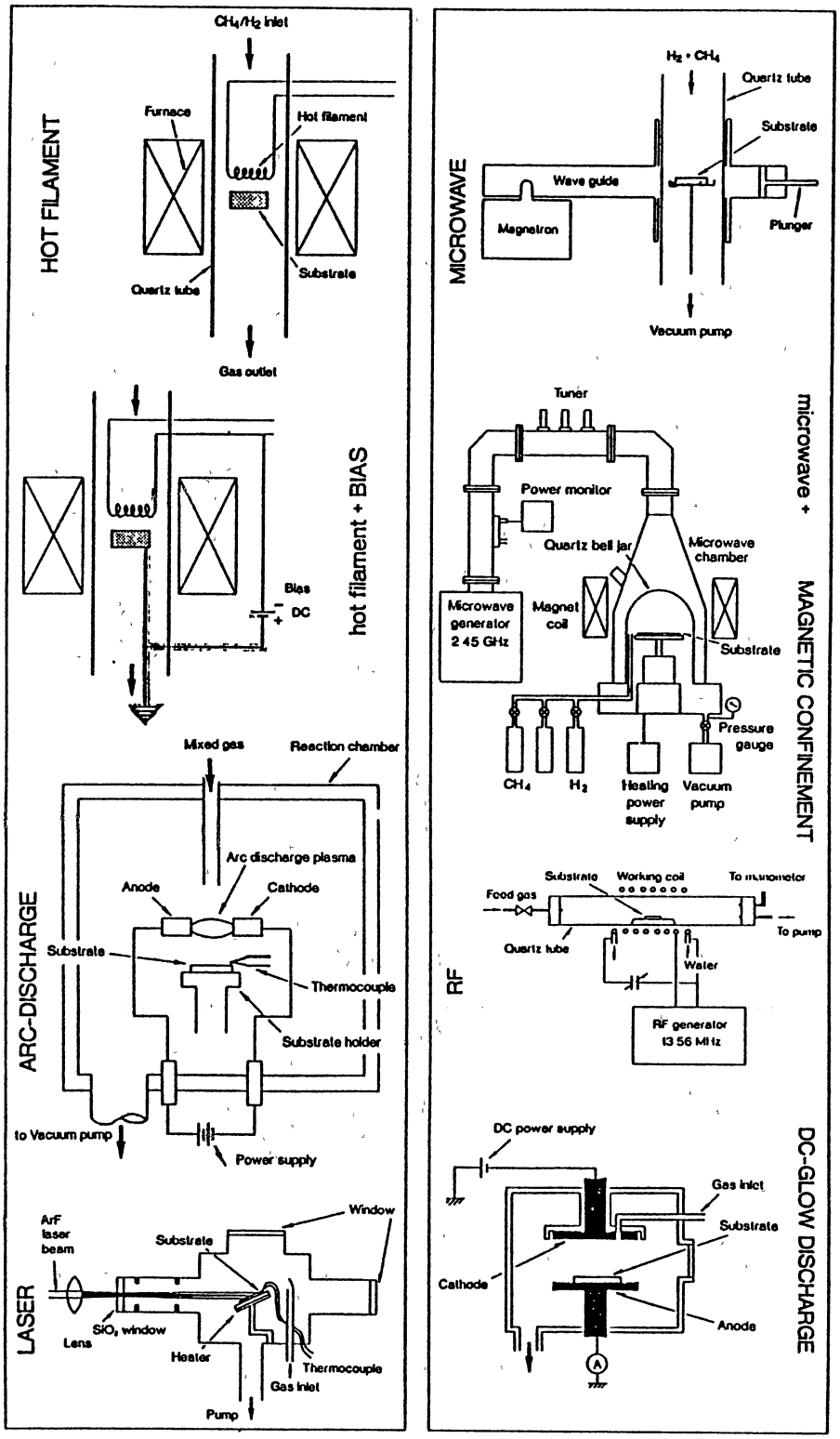

Figure 3. Activated CVD Processes [25]

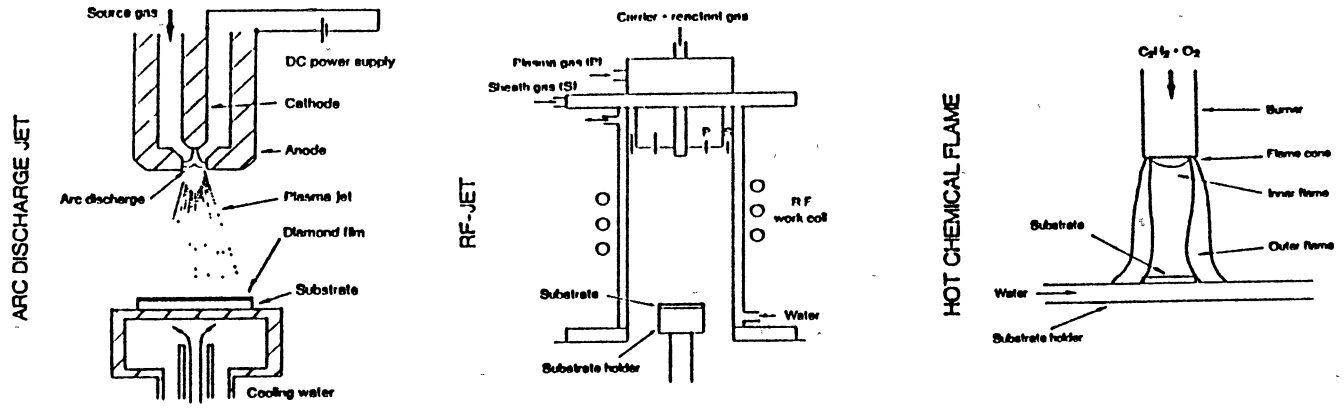

Figure 3. Activated CVD Processes (Contd.)

Recently, Ohtake and Yoshikawa [51] using an arc discharge plasma jet reported growth rates of 930 μm/hr. In this method, a d.c. arc discharge plasma torch is used to generate a plasma jet consisting of argon and hydrogen, to which methane is added. This plasma jet is then sprayed onto a cooled substrate resulting in diamond deposition. Diamond growth rates by this method are an order of magnitude closer to that obtainable by high-temperature and high-pressure synthesis. The use of radio frequency [52-55], laser [56] and electron assisted [57-58] processes have also been reported.

In 1988 Hirose [26] of Japan announced a simple method of diamond synthesis using an oxygen-acetylene welding torch. With a slightly fuel rich (acetylene) flame and a substrate mounted on a water-cooled copper block, films were deposited with a growth rate of 50-150 μm/hr. The uniqueness of this process was its ability to grow diamond films under atmospheric conditions without a vacuum chamber. Hirose coined this newly developed technique as "combustion flame technology". This method has since been confirmed in many laboratories [59-68] and is the subject of this investigation. The effect of various parameters such as substrate temperature, substrate position in the flame, gas flow rates and ratios on the film quality have been reported [59, 67]. High quality diamond films have been synthesized by Tzeng et. al. [60] and Hirose et. al.[65]. Yarbrough and co-workers [59] at Pennsylvania State University have studied the effects of low pressure conditions on the quality of the film grown in a vacuum chamber. Even single crystals of 100-150 μm size have been grown by Komanduri et. al. [63-64] and Ravi et. al. [61] enhancing the possible use of this technique to produce abrasive grains.

These constructive studies have reaffirmed the faith in these exciting new techniques of diamond synthesis, which till the late 1970's was looked upon with much scepticism because of the very low growth rates involved. Figure 4 shows how the technology is evolving in terms of growth rates. At the time of Eversoles' announcement the growth rate was only 20 Å/hour (the average size of an atom is 3 Å in diameter). But

since the demonstration by the Russians in 1981 of the usefulness of atomic hydrogen, the growth rates have leaped from about 1-2 μm/hr in 1982 to 1000 μm/hr in 1989.

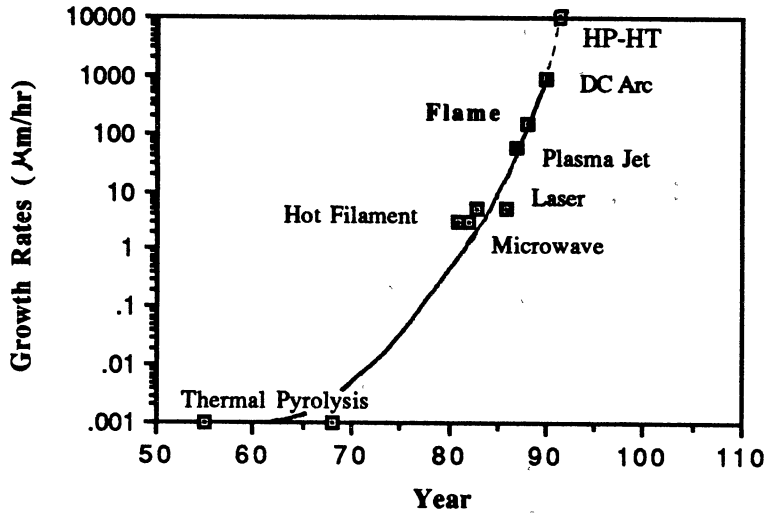

Figure 4. Trend in Growth Rates

Combustion Synthesis of Diamond

The simplicity of and high growth rates achievable in the combustion flame technique has excited the diamond film community recently [26, 68]. Though the process still lacks homogeneity of crystal growth, it shows potential for a wide range of applications because of its low cost of operation. In this section, the work done on the combustion synthesis of diamond will be reviewed. Detailed discussions on the morphology and mechanisms of diamond growth will be addressed in the succeeding sections.

The "combustion flame technology" uses a simple gas welding torch with a slightly fuel rich oxy-acetylene flame to synthesize diamond. Hirose [26] who introduced this

technique in 1988 reasoned that as flames are sources of short-lived radicals, the radicals from flames might stabilize the growth of diamond crystals. This expectation was fulfilled by using the apparatus shown in Figure 5 to synthesize diamond at growth rates of about 100-150 μm/hr. Hirose reported that in order to grow diamond, an acetylene rich

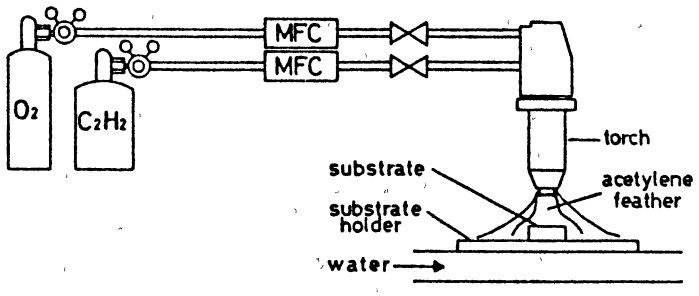

Figure 5. Schematic of the Apparatus for Combustion Synthesis of Diamonds [26]

oxy-acetylene flame should be used. In this flame, three zones are apparent, the inner cone, the acetylene feather, and the outer luminous zone. Diamond growth was observed only in the second zone, namely the acetylene feather. No vacuum chamber was required as the experiment was conducted under atmospheric conditions. As the flame temperatures were high, the substrate was cooled by mounting it on a water cooled copper block.

Hanssen et. al. [66-67] confirmed Hirose's work and extended it to study the effects of key parameters such as the substrate to inner cone distance, gas flow ratios and substrate temperatures on the diamond film quality. They grew polycrystalline diamond films for 10 minutes on Si(100) and (111) wafers, BN, Mo(100), Nb(100), Ta foil, TiC (100) and Cu rod. Diamond crystal growth was observed throughout the entire region of the C_2H_2 feather. It was also observed that the growth rates dropped off with increasing

radial distance from the center. This was attributed to the existence of temperature gradients of 150-200° C across the substrate surface, from the center to the edge, resulting in changes in morphology. The temperature distribution across the substrate surface shown in Figure 6 was recorded using a thermal imaging camera. The morphology was found to vary from well faceted particles with minimal amounts of secondary growth at the center to ball-like particles towards the edge. In between, the morphology displayed increasing secondary growth features. For samples grown at different gas ratios and substrate temperatures, the particle morphology did not change with position, but the average particle size and nucleation density varied radially. This indicated that the radial variation of the deposit was mainly due to the radial distribution of the flame species even though temperature had an influence.

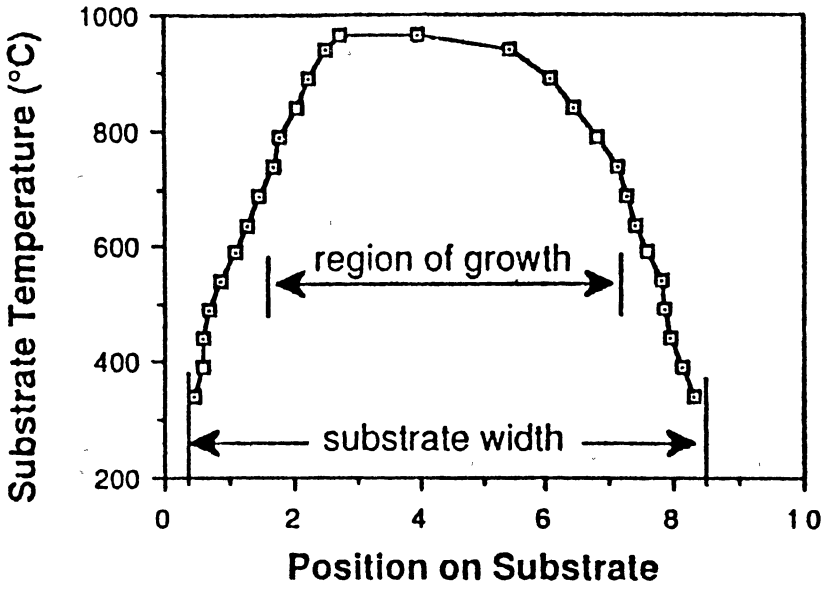

Figure 6. Substrate Temperature Profile Measured With Thermal Imaging Camera [62]

Oakes et. al. [62] studied the effects of hydrogen addition to the O_2/C_2H_2 flame. They used hydrogen in two different ways; in the first method, the O_2/C_2H_2 ratio was fixed at 1.03 and hydrogen was added to the flame. In the second method, the ratio $[O_2/(C_2H_2 + H_2)]$ was fixed at 1.03 and hydrogen was substituted for acetylene. It was observed that the diamond growth density decreased significantly as the ratio, (H_2/C_2H_2), exceeded 0.25. However, there was a marked improvement in diamond quality as a result of hydrogen addition.

The effect of low pressure conditions, when the diamond was grown in a vacuum chamber, was studied by Yarbrough et. al.[59]. They reported that stoichiometric ratios of O_2 and C_2H_2 (R=1) which readily produced diamond in the atmospheric pressure experiments, produced only graphite at lower pressures. Diamond deposition occurred at O_2 to C_2H_2 ratios of 1.16-1.18 under these conditions. The addition of H_2 did not have any effect. They also observed, that nucleation densities on silicon scratched with diamond paste was about 10^6 cm^{-2} which was lower than the 10^8 cm^{-2} value in the low pressure plasma or hot filament technique.

As in all other methods of diamond synthesis, the growth of pure diamond films exhibiting a Raman spectrum with a peak only at 1332 cm^{-1} and absence of any defects is the ultimate goal in the flame deposition technique. This task is difficult because of the existence of radial gradients of temperatures and flame species concentrations which result in a highly non-uniform morphology. However, Tzeng et. al. [60] and Hirose et. al. [65] have recently reported on the successful synthesis of high purity diamond films. Tzeng et. al. taking advantage of the oxygen rich periphery of the acetylene feather reported the synthesis of high quality crystallites using a flame tilted at 70 degrees to the substrate normal. By using this approach, they conjectured that the effects of the radial gradients of temperatures and flame species could be minimized. Hirose et. al. using a similar approach synthesized high quality diamond at low substrate temperatures of 500-750° C. These diamond films which were synthesized on TiN and Mo at gas ratios close to unity were

optically transparent with few defects. X-ray diffraction and Raman analysis of the crystals indicated that the diamond was of very high quality with good crystallinity. Defects such as stacking faults and twinning were few in number. They also reported that the maximum growth rates of these optically transparent diamond films occurred between gas ratios, R, of 0.9-0.93.

The various activated CVD techniques used in the synthesis of diamond films utilize low pressure conditions in a reaction chamber. This restricts the size of the substrate to be coated and long or large area substrates cannot be coated easily. This disadvantage of the CVD techniques is easily circumvented by the flame deposition method and was effectively demonstrated by Hirose and co-workers [69]. Figure 7 shows the apparatus used for coating a 50 mm long × 10 mm wide WC- Co alloy substrate. The torch was mounted on a movable table operated with an electric motor. Two types of diamond coatings were made: type (a) consisted of a ball-like structure, and type (b), was of a crystalline nature. The main problem encountered during the coating operation was the graphitization of the already deposited diamond by the trailing outer flame. Scraper-type adhesion tests showed that the film exhibited an uniform adherence distribution along the majority (80%) of the length of the substrate.

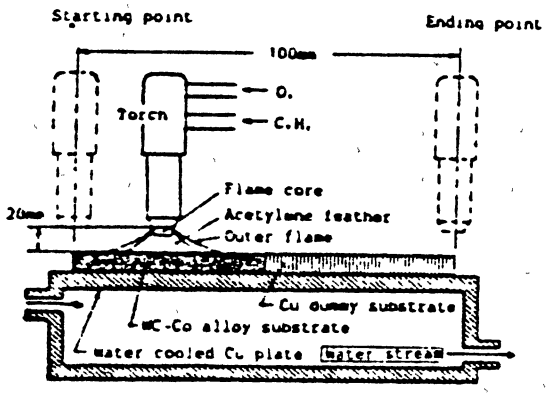

Figure 7. Large Area Deposition Using the Flame Technique [69]

Another advantage of the flame technique which has been cleverly exploited in the growth of large single crystals is the growth rate. Komanduri et. al. [64] and Ravi et. al. [61] have reported on the synthesis of large single crystals of 100-150 μm dimensions at high temperatures of ~1200° C. The growth of these large crystals have opened new avenues for use of low pressure diamonds as abrasive grains and in electronic applications.

Morphology of Low Pressure Diamond Films

A characteristic of the diamonds synthesized by CVD is that they have well-defined crystal habits, which depend on the experimental conditions. Matsumoto and Matsui [70] have observed that the morphology of vapor deposited crystallites is dominated by cube {100} and octahedral {111} surfaces. Multiple twinned and cubo-octahedra exhibiting both {100} and {111} surfaces are also common. However, the appearance of a {110} surface is rare. In addition, cauliflower-like growth (crystals resembling cauliflowers) has also been reported [67]. Although the origin of this is not clear, in this thesis we propose that the cauliflower-like growth leads to octahedral to cubic form of diamond under favorable conditions.

In combustion synthesis of diamond, the morphology of the crystals is a strong function of the gas flow rates, gas flow ratios, substrate temperature, and purity of the gases. Hanssen et. al. [66, 67] have observed that when the gas flow ratio, R, of O_2 to C_2H_2 was less than 0.9 ball-like structures grew (Figure 8(a)). As the ratio R was varied between 0.9 and 1.2 well faceted cubo-octahedral crystals some of them exhibiting five fold symmetry were observed (Figure 8(b)). Beyond R =1.2, no growth was seen. They have classified the deposit morphologies into three categories: "ball-like" growth, faceted growth and intermediate growth. Figure 9 shows the deposition conditions at the center of growth as a function of substrate temperatures and oxygen to acetylene ratios. Kobashi et. al.[71] observed similar trends in their microwave CVD diamond synthesis experiments.

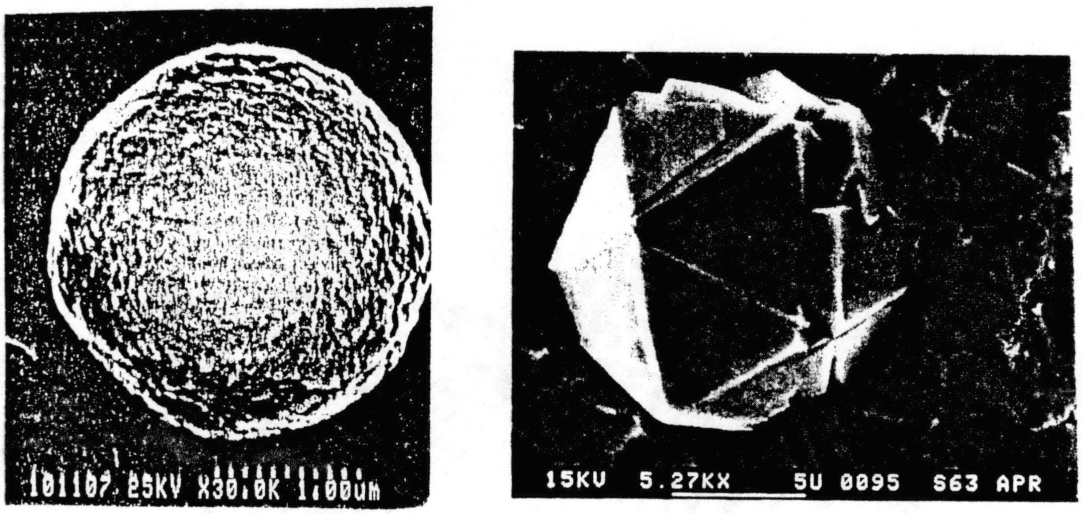

(a) (b)

Figure 8 (a) SEM photographs of a ball-like particle grown in an oxyacetylene flame with R =0.85, [67]and (b) a fivefold twinned crystallite at R = 1 [27]

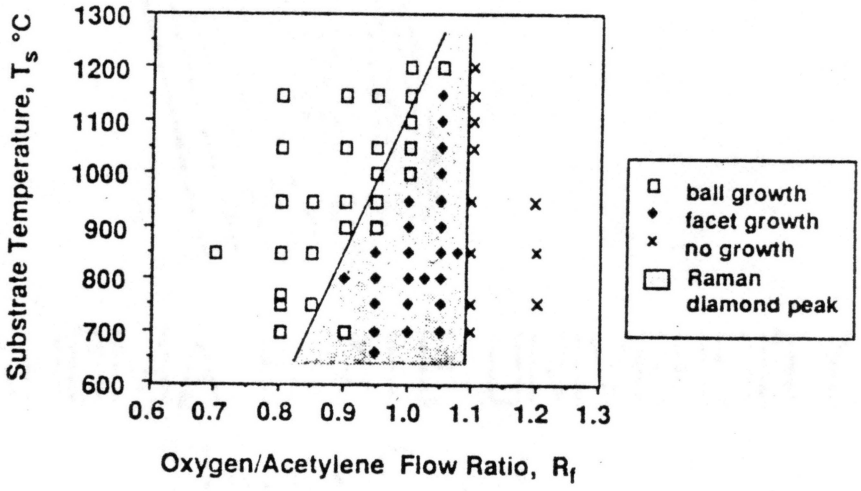

Figure 9 Deposit Morphology as a Function of Oxygen to Acetylene Ratio and Substrate Temperatures [66]

They reported the dominance of {111} faces for methane concentrations less than 0.4 % and {100} faces for concentrations between 0.4 % to 1.2 %.

A peculiar characteristic in the flame deposition method is the growth of high quality diamond crystallites along an annular region of the diamond film, where the outer boundary of the feather intersects the substrate [59-60]. The growth of these crystallites, observed only in a vertically blowing oxygen-acetylene flame has been attributed to the higher oxygen to carbon ratio in the periphery of the flame. Radial gradients of the substrate temperature, concentrations of flame species, and the residence time of the species also seem to contribute to this phenomena. It has also been reported [67] that the morphology of the film is highly non-uniform with non-diamond carbon growing in the central portion of the film immediately below the inner cone of the flame. With longer deposition times it was observed that a coarse columnar or particulate structure developed. In contrast Hirose et. al. [65] have grown high quality diamond in the central portion of the film. This has also been confirmed in the present investigation. Recently, Hanssen et. al. [66] have also confirmed the growth of high quality diamond in the center of the film, with the crystallite quality degrading away from the growth center and throughout the annular growth region. Crystallites outside the annulus of high growth showed a slight increase in quality when compared to crystallites within the edge of the annular high growth region. The growth density of the diamond crystallites was found to increase with the distance of the inner cone from the substrate.

The effect of temperature on the morphology of diamond films and crystals has not been resolved satisfactorily. Spitsyn et. al. [24] have reported on the predominance of cubic {100} habit at high temperatures and the prevalence of octahedral {111} faces at lower temperatures. Similar observations were made by Komanduri et. al. [64] and Tzeng et. al. [60] in their combustion synthesis experiments. However, Lux and Haubner [25] and Kobashi et. al. [71] have reported results which are not consistent with the above

observations, i.e., they observed octahedral morphology at higher temperatures and cubic at lower temperatures.

It has been noticed by many researchers [24, 70] that the {111} octahedral faces are very rough while the {100} faces are smooth. This phenomena has been explained by Kim et. al. [72] in terms of the relative growth rates of {111} to cubic {100} faces. They observed that the ratio of the apparent growth rate of the octahedral {111} faces to cubic {100} was twice the ratio estimated from surface energy considerations. This discrepancy was attributed to the separation of the {111} faces into {100} and {110} crystallographic planes. The roughening of the octahedral faces arose from the competing growths of the two constituent planes of {100} and {110}. However, Hirabayashi et. al. [73-75] contend that the roughness of the {111} planes occur not because of the presence of {100} and {110} faces but rather due to the existence of trigons on the {111} surfaces. These trigons are typically of a few nanometers in size and grow in a layer by layer manner. They are generated by multinucleation on the {111} surface. As the crystal grows larger, {110} surfaces appear at the corner of the {111} surfaces because of inhomogeneity of the effective carbon concentration on the {111} surface. The fact that {110} planes develop during growth has also been pointed out by Wild et.al. [76].

Growth Mechanisms of CVD Diamond

In spite of the numerous publications which appear in the area of diamond film synthesis, only a few discuss the mechanism of diamond growth . As a result, the growth mechanism of diamond films from its initiation to a preferred orientation is not very well understood. Russian researchers [23, 77-79] based on extensive experimental studies have argued that the growth of diamond from the vapor phase is controlled by kinetics. They proposed that the formation of diamond kinetically competes with the formation of graphite, the graphite growing via methyl radical addition, while diamond, atleast partially, via metastable radicals CH_5.

Tsuda et. al. [80] carried out quantum chemical calculations in order to determine the lowest energy path for a proposed mechanism of diamond growth on {111} surfaces that consisted of two steps. In the first step, the {111} plane of the diamond surface is covered by methyl groups via methylene insertion or hydrogen abstraction followed by methyl radical addition. In the second step, three neighboring methyl groups on the {111} plane are spontaneously bound to form the diamond structure following the single attack of a methyl cation and the subsequent loss of three hydrogen molecules. For epitaxial growth to be sustained [81], the surface should maintain a positive charge and there should be a constant supply of methyl radicals. This mechanism, however, does not explain the critical effect of hydrogen atom superequilibrium.

Frenklach and Spear [82] have proposed an alternative mechanism for the growth of the {111} surface of diamond. Acetylene was the main monomer growth species in this mechanism. The proposed mechanism basically consisted of two alternating steps : The first step is the activation by H-atom removal of a surface bonded hydrogen.

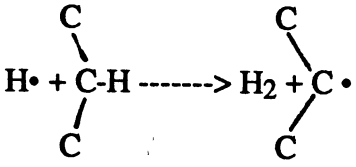

In the second step, this surface activated carbon radical then acts as a site for adding more carbons to the structure by reacting with acetylene.

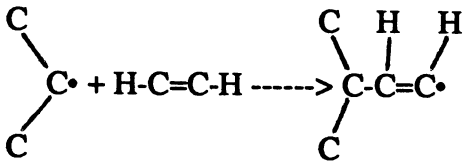

The propagation of a growth step on the {111} plane then proceeds by additional radical reactions. The propagation results in the addition of two acetylene molecules for one hydrogen abstraction step, with the resulting regeneration of the hydrogen atom which was consumed in forming the activated surface site.

In addition to the chemical mechanisms mentioned, physical mechanisms have also been proposed. In 1988, Kobashi et.al. [71] conducted detailed investigations on the growth of diamond films in a microwave plasma. With methane concentrations of 1.2% and growth periods spanning about 60 hours, periodic observations on the SEM revealed cyclic growths of microcrystallites of diamond along with the already developed facets. As these microcrystallites grew and developed into facets, new microcrystallites began to evolve and this process repeated. This indicated that diamond films grow cyclically through microcrystal formation due to the higher order growth followed by the formation of well-defined diamond faces. They have explained this restructuring process as follows:

1. increase of the areas of primary diamond faces,
2. overgrowth of small crystallites on well defined faces,
3. "fusion" of a group of small crystallites to form well-defined larger faces, and finally,
4. "absorption" of small crystallites into larger faces.

Ravi et.al. [61] have proposed a mechanism of diamond growth based on evidence of ledge growth and lateral epitaxy on nondiamond substrates. The {100} oriented crystals of diamond synthesized at high temperatures were observed to grow by the sideways propagation of ledges on the surface. These growth ledges on the surface of the {100} diamond crystals were observed to lie along the <100> directions. The propagation of the {100} faces was found to be enhanced by the presence of oxidizing species in the flame that preferentially removed nondiamond carbon from the deposits as well as etch the diamond surface to create growth ledges.

Characterization of Polycrystalline Diamond Films

With the successful vapor deposition of diamond films, the identification and assessment of the film's quality has become a very important issue. This is especially true because of the existence of another class of films known as diamond-like carbon (DLC) [83] films which have properties close to that of diamond. These DLC coatings are characterized by a high degree of sp^2 bonding and consist of a variety of noncrystalline carbonaceous materials ranging from amorphous to microcrystalline. It is therefore a necessity to differentiate between diamond and DLC films and identify techniques to characterize these materials. Messier et. al. [84] have suggested a working definition of diamond coatings produced by vapor deposition techniques which is as follows:

1. having a crystalline morphology discernible by electron microscopy;
2. having a single crystalline structure identifiable by X-ray and electron diffraction; and,
3. displaying a Raman peak typical of crystalline diamond.

As mentioned in the earlier section on morphology, diamond films exhibit highly developed facets of the {100} and {111} orientations when observed under the scanning electron microscope (SEM). These morphological characteristics are not discernible on a DLC film which mainly consists of an amorphous structure. Thus the SEM is a powerful tool to identify the crystalline nature of the deposited film.

Even though X-ray and electron diffraction have been used frequently for identifying the crystalline forms of carbon these techniques have an inherent disadvantage of not being able to identify the amorphous carbon phases even when they are dominant. Moreover, these techniques do not provide sufficient information regarding the nature of chemical bonding of carbon which is very essential to establish the film potential for various applications.

Raman spectroscopy on the other hand is very sensitive to both crystalline and non-crystalline phases and displays vibrational modes which are directly related to atomic

bonding and has been extensively used to characterize diamond films [85-87]. Well crystallized diamond exhibits only a single first order Raman peak at 1332 cm^{-1} [88]. This peak may be broadened by defects or may be shifted by as much as ±4 to 8 cm^{-1}, depending upon relative stresses in the coating [89]. Graphite displays two Raman peaks, one at 1580 cm^{-1} [90] and the other at 1350 cm^{-1} which corresponds to the highly disordered microcrystalline state. Diamond-like carbon exhibits a diffuse zone with a peak around 1500 cm^{-1}.

Figure 10 shows the Raman spectra of two diamond films grown on silicon substrates [30]. The peak at 1332 cm^{-1} is characteristic of diamond and the broad band occuring in the 1500 to 1600 cm^{-1} range are characteristic of disordered sp^2 type carbons in the deposit. The peak at 519 cm^{-1} is from the silicon substrate. The Raman spectra in Figure 10(a) is a typical pattern for a highly perfect diamond film. Such type of diamond has been synthesized by Hirose et. al. [65] using the flame technique recently. The pattern in Figure 10(b) is typical for an imperfect film of crystalline diamond with appreciable amounts of sp^2 carbon present as defects.

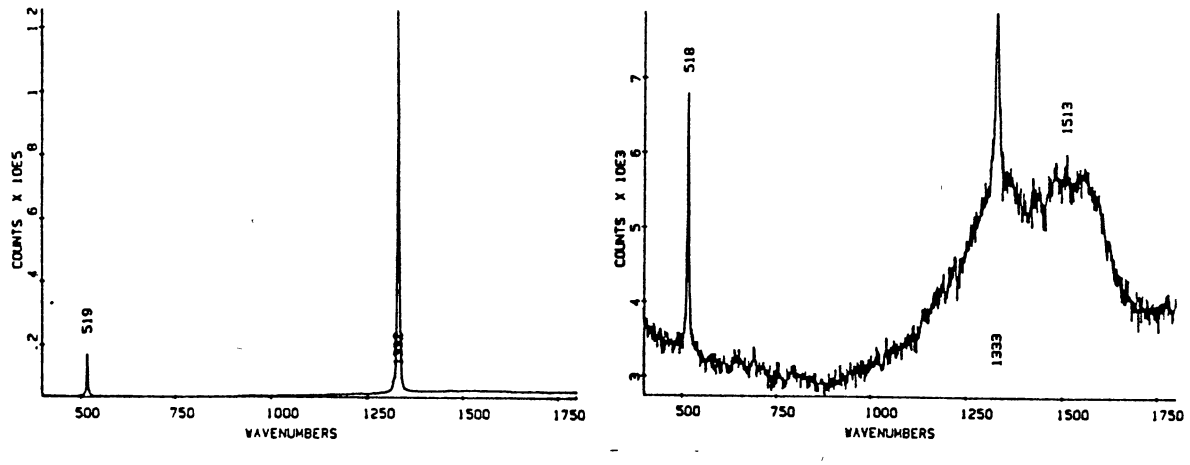

(a) (b)

Figure 10. Raman Spectra of Diamond Films [30]

The sensitivity of the Raman technique to the sp^2 bonded phases of carbon is approximately two orders of magnitude greater that that of the sp^3 bonded phase. Therefore, the relative intensities of the two peaks [1332 and ~1150 cm^{-1}] should not be interpreted as a measure of diamond quality. Consequently, the presence of a small peak at around 1550 cm^{-1} indicates very small quantities of the sp^2 bonded phase in the material.

An interesting aspect of the Raman spectrum is its sensitivity to the increase in the photon energy level. Wagner et. al. [91] while studying the effects of increasing photon energies on the Raman spectra of diamond observed that an increase in photon energy from 2.41 to 3.00 eV strongly reduced the photoluminescence background and caused the disappearance of the 1550 cm^{-1} peak of amorphous carbon. There was also an apparent increase in line width for the 1332 cm^{-1} line with increasing photon energy, which was attributed to the change in spatial resolution.

Knight and White [87] have conducted an extensive Raman study of diamond films and observed that films deposited on hard substrates such as alumina, WC, or SiAlON showed a shift in the Raman band in the range of 4-13 wave-numbers, with both positive and negative shifts being observed. The diamond line for films deposited on soft substrates such as silicon were exactly at the expected 1332 cm^{-1}. These shifts in wavenumbers were attributed to internal stresses in the film brought about by mismatch between diamond film and substrate. The negative shifts have been interpreted as films in tension and the positive shifts as films in compression.

Roles of Atomic Hydrogen and Oxygen

It is now a well established fact that good quality diamond films by activated CVD processes are obtained in entirely hydrogen atmosphere, with only small amounts of a hydrocarbon (1% or less) present in the reaction mixture. Several factors have been suggested to explain the role of the hydrocarbon dilution by hydrogen. First, is the preferential etching of graphite over diamond by atomic hydrogen [22, 24]. For this to

occur the hydrogen atoms should be in superequilibrium concentrations. According to Angus's work, graphite (or any other sp^2 carbon) which forms simultaneously with diamond in the low pressure synthesis is etched by atomic hydrogen present in superequilibrium concentrations, whereas diamond is very little affected. The second effect of hydrogen [22] is to satisfy the dangling bonds of surface carbon atoms, keeping them in the sp^3 configuration and thus preventing the diamond surface from reconstruction into graphite (or sp^2 structures). Frenklach [92] has suggested that the suppression of the formation of aromatic species in the gas phase by molecular hydrogen plays a key role in the hydrogen etching effect on graphite.

The influence of atomic hydrogen on the relative growth and etching rates for diamond and graphite in the range of 900-1000° C is shown in Figure 11 [93]. The etching rates of graphite, amorphous or glassy carbon, and diamond in a hydrogen plasma under typical activated growth conditions were reported by Setaka [94] to be 0.13, 0.11, and 0.006 mg/cm^2-hr respectively. This means that graphite is etched by atomic hydrogen nearly 20 times that of diamond.

Hirose and Terasawa [35] using oxygen containing hydrocarbons in a hot filament CVD system reported growth rates of 10 μm/hr which was an order of magnitude higher than reported earlier. However, they did not discuss the role of oxygen in facilitating the growth rates. Mucha et.al. [95] realizing the importance of this phenomenon conducted optical emission studies of oxygen additions to a CH_4/H_2 discharge to ascertain the cause for the increase in growth rates. They observed that the dominant effect of added oxygen is to facilitate an increase in the atomic hydrogen content of the discharge, suggesting that oxygen accelerates the removal of amorphous and graphitic carbon allotropes. Kawato and Kondo [96] reported that the addition of oxygen (0.4%) to a H_2-CH_4 system caused a decrease in acetylene concentration in the activated gas stream, thus suppressing the deposition of graphitic or amorphous carbon. This improved the quality of diamond

substantially, as determined by the decrease in the 1550 cm^{-1} Raman peak for amorphous carbon.

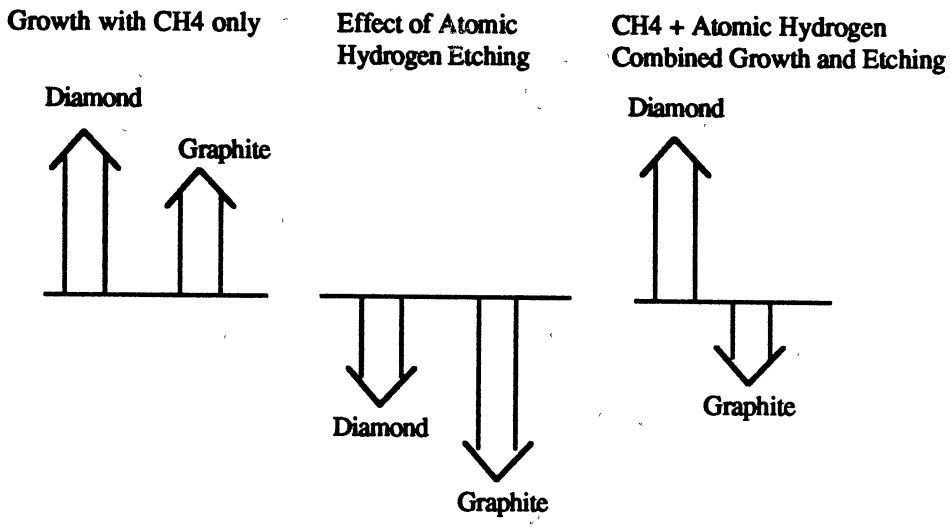

Figure 11. Effect of Atomic Hydrogen on the Growth Rates of Graphite and Diamond [93]

A clear indicator of the beneficial effects of O_2 is in the combustion flame technique of diamond deposition where large single crystals (~100 μm) at high growth rates have been reported [61, 64].

Diagnostics of Activated Gases in CVD Diamond Synthesis

Studies of the gas-phase environment in which diamond nucleation and growth occurs are of considerable interest, since a knowledge of the gas composition at the substrate may give important clues regarding the kinetic mechanism leading to diamond formation. Knowledge of these mechanisms could lead to better deposition process control, improved material quality and characteristics, and identification of the inherent

chemical constraints on growth conditions. At present, quantitative species concentrations have been reported using emission spectroscopy [97], infrared laser absorption spectroscopy [98] and mass spectroscopy [99]. Of the many gaseous diamond precursors which have been proposed, *in situ* concentration measurements in filament-assisted reactors, combined with kinetic arguments, have identified the most likely species as CH_3, C_2H_2, C_2H_4, and CH_4 [98-99]. Reactivity considerations suggest that of these, either the methyl radical or acetylene is the probable growth species.

In the combustion flame technique, however, laser induced fluorescence (LIF) and mass spectroscopic analysis by Matsui et.al. [100-101] have shown that CO and H_2 are the dominant gases in the feather, and that C_2H_2 and C-containing radicals (eg. C_2H, CH, C_n, n=1-3) are minor species whose concentrations are approximately equal to the equilibrium values near the burner. With increase in ratio R of O_2/C_2H_2 from 0.84 to 1, an increase in CO and H_2 mole fractions by approximately 20% was observed. When the overall reaction for R = 1.00 was expressed as

$$C_2H_2 + O_2 \quad \text{------>} \quad 2CO + H_2$$

it was observed that for R > 1.05, O containing radicals such as O and OH were so numerous that some parts of CO were oxidized to CO_2. On the other hand, the C-containing radicals increased rapidly for R < 0.96, as a result C_2H_2 and C_2H radicals were dominant and C_3, C, and C_2 were larger than CH_x (x = 1-3) radicals. Solid carbon appeared at about R < 0.87. LIF studies of the fuel rich flame indicated that the concentration of the C_2 radical decreased almost linearly with increasing height from the burner head. In the vicinity of the burner there was a rapid increase in C_2 towards the inner cone. The OH radicals were observed in the intermediate and outer zones and were distributed almost uniformly. Hydrogen atoms were abundant for all gas ratios.

Cappelli and Paul [102] however think that the absence of diamond and the presence of non-diamond carbon in the central region of the deposit might be explained by the absence of sufficient levels of atomic hydrogen. In the annular region where diamond is prevalent, it is possible that the OH radical and atomic oxygen play a similar role to that proposed for atomic hydrogen, since the concentration of OH and O within the secondary flame can be significantly increased through chain reactions with O_2, H, and H_2O. The rapid production of OH within the secondary flame zone should be accompanied by the rapid consumption of acetylene. If both acetylene and OH are required for diamond growth, then they maybe simultaneously present at sufficient quantities only within a narrow spatial region within the secondary flame. Alternately, it is conceivable that the reactive intermediates such as C_2H act as the dominant growth species.

The various aspects reviewed in this chapter indicate that the process of diamond synthesis involves a number of factors on which the quality of diamond depends. Knowledge of molecular dynamics, statistical mechanics, heat transfer, thermodynamics, materials science and chemical kinetics is therefore required to model the process from nucleation to growth and to predict the conditions for obtaining a desired morphology.

CHAPTER III

PROBLEM STATEMENT

Ever since Hirose [26] reported on the synthesis of diamond films using a combustion flame with growth rates of ~ 50 μm/hr, curiosity regarding this process has grown steadily. Many laboratories around the world [61, 64, 67] have confirmed Hirose's results. Although the growth rates are very high as compared to other activated CVD processes which are typically in the range of ~ 1 μm/hr, there are still several issues such as non-uniform morphology distribution, inconsistency of deposition, lack of transparency, etc., that need to be addressed. To address these issues an oxy-acetylene combustion synthesis apparatus, similar to the one used by Hanssen et. al.[67] was built as the first objective.

The combustion flame technique involves a number of parameters such as gas flow ratio, gas flow rates, substrate temperature, gas cylinder pressures, distance of the substrate from the inner cone, etc., which affect the quality of the film grown. The effect of these parameters on diamond film growth were studied as a second objective. Hanssen et. al. [67] and Yarbrough et. al. [59] have reported on the effects of some of these parameters. However, the effect of acetylene cylinder pressure on the diamond film quality has not been reported to date. The third objective is, therefore, to study systematically the effects of acetylene cylinder pressure on the quality of the diamond films and to ascertain the pressure range at which good diamond films can be grown.

There have been a number of reports on the growth of textured diamond films (i.e., films with preferred orientations)[109]. All these films were grown either epitaxially on diamond or on other oriented substrate materials, such as, Si {100} or Si {111}. There is

also a general consensus that {100} crystallites grow at high temperature and the {111} crystallites grow at lower temperatures. However, no indepth study on how these morphologies develop exists. Some researchers are of the opinion [60] that cauliflower-like growth features observed prominently on flame grown diamond films are formed as a result of deterioration of well formed {100} or {111} features. The fourth objective of this research, therefore, is to study the morphological variations existing on the diamond film surface in order to understand the growth process and propose a hypothesis for the same.

The growth of diamond films of uniform thickness and morphological behaviour has proved to be an elusive task. This is attributed to the large gradients of substrate temperature and flame species concentration existing during the deposition process [66]. It is therefore felt, that in order to grow good quality diamond films of uniform thickness over large area a close study of the flame characteristics as it impinges on the substrate is required. This will help in identifying the zones in the flame where uniform deposition could be possible. This is the fifth objective of the study.

The sixth objective of the study is to characterize the diamond films using scanning electron microscopy and μRaman spectroscopy. This will help in assessing the film quality and identify the synthesis conditions under which good quality films can be grown.

CHAPTER IV

EXPERIMENTAL SETUP, TEST PROCEDURES AND FILM CHARACTERIZATION

Introduction

The varied nature of the crystallites on a diamond film grown using combustion flames is unique to this process. Even though films from other CVD processes have exhibited morphologies of different nature, the individual films consist of a uniform crystalline structure which maybe cubic, octahedral or ball-like. In contrast, flame grown films have a diversity of crystallites ranging from ball-like to well developed structures in the same film. This variegated nature of deposits is a result of the existence of radial gradients of temperatures and species concentrations in the flame [66]. Other process parameters such as gas flow rates, ratio of oxygen to acetylene, substrate to inner cone distance, etc., have also been found to change the morphological characteristics considerably.

The primary objective, therefore, was to study the effect of different process parameters on the nucleation and growth of diamond using the combustion flame technique. It was also felt that a careful study of surface morphology could give a clue as to the evolution of the diamond crystallites. This would help in understanding the growth behavior and simplify the task of growing films with a preferred orientation and of uniform thickness. Moreover, the identification of zones within the flame where these morphologies are prevalent could help in growing films of a desired morphology.

For this purpose, an apparatus for oxy-acetylene combustion flame synthesis of diamond was constructed along the lines of Hanssen et. al. [67] to investigate the effects of :

1. Gas flow rates,
2. Gas flow ratios,
3. Substrate to inner cone distance, and
4. Acetylene cylinder pressure.

Some of these parameters were selected for analysis as they have been reported to profoundly affect the morphological behavior of the diamond crystallites. The significant effect of C_2H_2 cylinder pressure on the quality of diamond films, which we found in the investigation has, however, not been reported as yet.

The films grown under these varying conditions were then studied using scanning electron microscopy and μRaman spectroscopy.

In this chapter, a detailed description of the experimental setup is provided along with that of other supporting equipment used for the control of the gas flow rates and ratios and measurement of substrate temperatures. The procedure followed in the synthesis of the diamond films is described in the last section.

Experimental Set-up

Figure 12 is the schematic of the experimental setup [67] and Figures 13a&b are the photographs of the setup used in our laboratory. The combustion flame technique uses ordinary gas welding equipment consisting of commercial grade oxygen (purity level 99.995%) and acetylene (purity level 99.96%) gas cylinders connected via flexible hoses to a welding torch. The oxygen cylinders were nominally of 220 cubic feet capacity, with the gas stored at a pressure of 2500 psi. The acetylene cylinders had varying volumes of gas charged to a pressure of 250 psi. The acetylene in the cylinder comes dissolved in acetone contained in a porous filler of charcoal, infusorial earth, finely shredded asbestos and

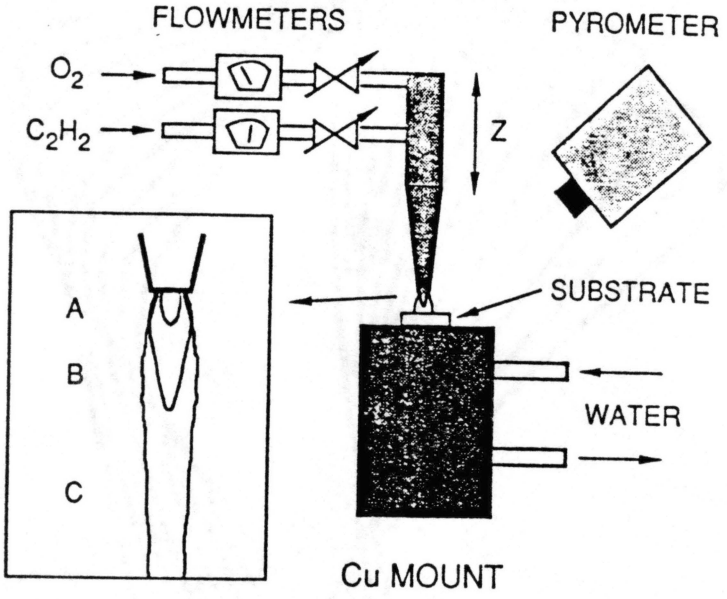

Figure 12. Schematic of the Experimental Set-Up Used [67]

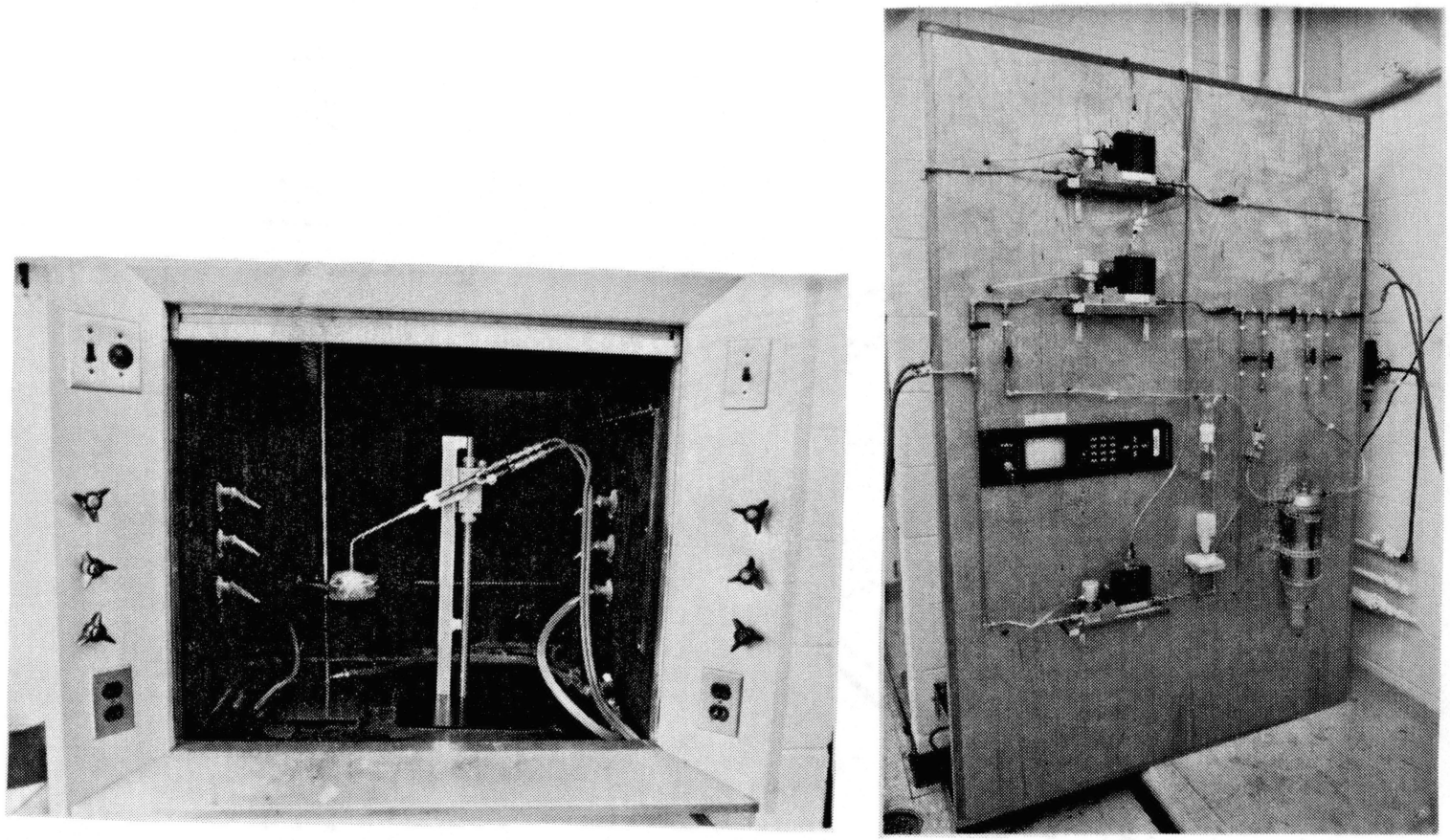

(a) (b)

Figure 13. Photographs of the Experimental Apparatus

Portland cement. Acetylene is passed through a scrubber-dryer and a methanol bubbler to remove moisture and other impurities.

The schematic of a typical welding torch is shown in Figure 14 [108]. In this mixer-type torch, acetylene enters through a central orifice while oxygen enters through a series of smaller holes around the mixer nozzle. In this investigation a Victor 100C brazing torch attached with a Type 2 (0.042" orifice diameter) or 4 (0.0635" orifice diameter) nozzle was used along with flash arrestors. This torch was then mounted on a vertically moving translation stage for accurate positioning of the torch relative to the surface on which the film was grown.

The oxy-acetylene flames are of three different types, neutral, carburizing, and oxidizing depending upon the ratio of oxygen to acetylene supplied through the torch. These flames are described in the following [108]:

1. Neutral Flame (Figure 15a): When the ratio, R, of oxygen to acetylene is equal to one (stoichiometric), the resulting flame has only two zones and is called a neutral flame. The small inner cone at the center varies in length from 1/16" to 1" long, depending upon the size of the nozzle and the gas flow rates. The inner cone is the region where CO and hydrogen are produced as a result of combustion of oxygen and acetylene. Here the acetylene breaks down into gaseous carbon and hydrogen, and then the carbon combines with an equal volume of oxygen to form CO. In the outer envelope the carbon monoxide and hydrogen combine with oxygen from the air to form carbon-dioxide and water. These reactions are expressed as

$$C_2H_2 \quad \text{------->} \quad 2C + H_2$$

$$2C + O_2 \quad \text{------->} \quad 2CO$$

$$CO + H_2 + O_2 \quad \text{------->} \quad CO_2 + H_2O$$

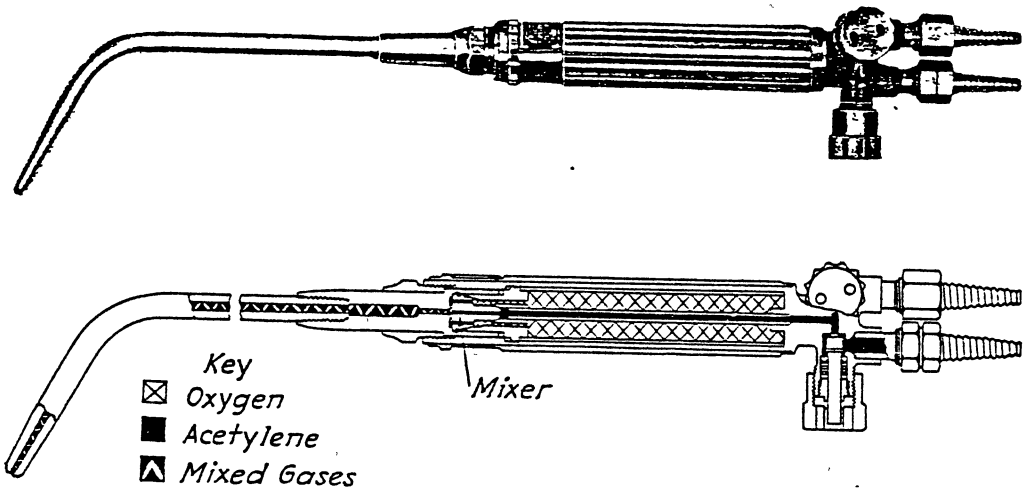

Figure 14. Schematic of the Welding Torch Used for Diamond Synthesis [108]

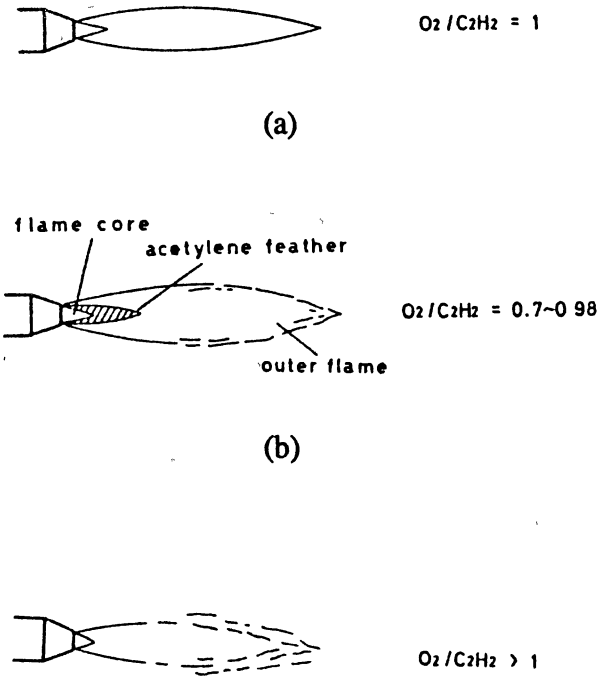

Figure 15. Three Types of Oxy-Acetylene Flames
(a) Neutral, (b) Carburizing and , (c) Oxidizing [65]

2. Carburising Flame (Figure 15b): When a slightly acetylene rich (fuel rich) mixture is used, the flame consists of three zones instead of the two existing in the neutral flame. An additional incandescent cone of whitish color is observed surrounding the inner cone. As acetylene is present in excess, the additional carbon generated in the inner cone burns with oxygen which diffuses into the flame from the surrounding air. This causes the formation of the "acetylene feather" between the inner cone and the outer luminous zone. ***It is in this acetylene feather region that diamond growth has been observed.***
3. Oxidizing Flame (Figure 15c): When oxygen is in excess in the mixture, the flame has two zones as in the case of a neutral flame, but unlike the neutral flame the inner cone is shorter and acquires a purplish tinge.

The flame temperature in the inner cone varies with the ratio, R, of O_2 to C_2H_2 gas flow, from 3162° C for R = 1.5 to 2960° C for R = 0.8 [103].

As the quality of the films depend sensitively on the gas compositions and uniformity of flow, precise control of the gas flow rates is required. To achieve this, mass flow controllers (MKS Type 2259C) were used to meter the gas flow rates of oxygen and acetylene to within 0.1% of the desired rates. A mass flow programmer (MKS 147B) was used to program the flow rates desired and control the individual mass flow controllers. The specifications for these instruments are given in the Appendix B.

A polished molybdenum screw scratched with 6 μm diamond paste was used as the surface for deposition. Scratching with diamond paste has been found to enhance the nucleation density of diamond crystallites. As the flame temperatures are very high, efficient cooling of the substrate is required. Therefore, the substrate was mounted on a water cooled copper block and the temperatures monitored using a Williamson Tempmatic 8000 series dual wavelength infrared pyrometer. This pyrometer is insensitive to flame emission and has the capability to measure temperatures in extremely hostile environments

such as those encountered in the combustion experiments. The specifications for the pyrometer are given in Appendix B.

Scanning Electron Microscopy

As the diamond crystallites in the film are of the order of microns in size, a SEM is required to study the morphological features. For this purpose an ISI-ABT32 digital scanning electron microscope with a resolution of 5 nm was used. In this instrument the accelerating voltage can be adjusted for 2, 5, 10, 15, 20, 25, and 30 kV depending on the sample material and the depth of field required. Magnifications from 15x to 300,000x can be achieved. The SEM also has a built-in polaroid camera for taking micrographs of the specimens.

Before the samples were examined on the SEM, a thin conducting coating of gold-palladium was deposited on the surface. A Ladd SC502 vacuum sputter coater was used to coat the samples.

Micro-Raman Spectroscopy

A common technique used to characterize diamond films is μRaman spectroscopy. For this purpose a RAMANOR U 1000 (Instruments SA Inc., Edison NJ) double monochromator, designed for spectroscopic applications was used. In all the scans, the Argon ion laser wavelength was set at 5145 Å with a laser power of 150 mW. Specifications of this instrument are given in the Appendix B.

A schematic of the system used to measure the μRaman spectra is shown in Figure 16. The system interfaces an Olympus model BH-2 optical microscope with a Ramanor U 1000 double monochromator. The detector is a Burle C31034A Photomultiplier tube. Conventional Raman spectroscopy was performed with the argon ion laser focussed to a 30 μm diameter spot size on a substrate. The addition of a microscope to the system decreased

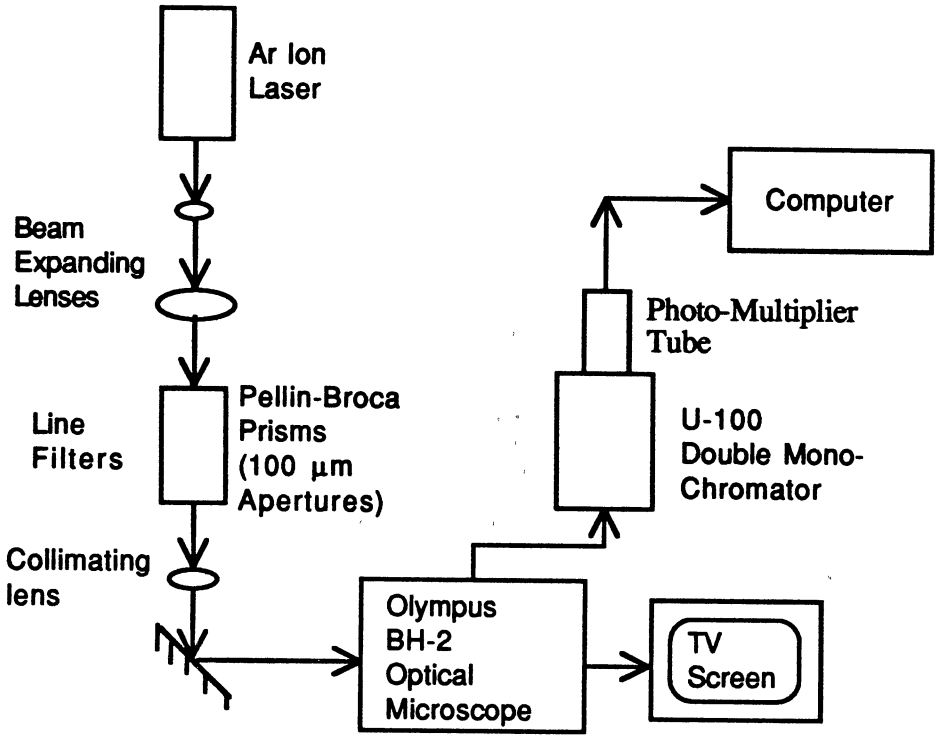

Figure 16. Schematic of the System used to Measure the micro-Raman Spectra

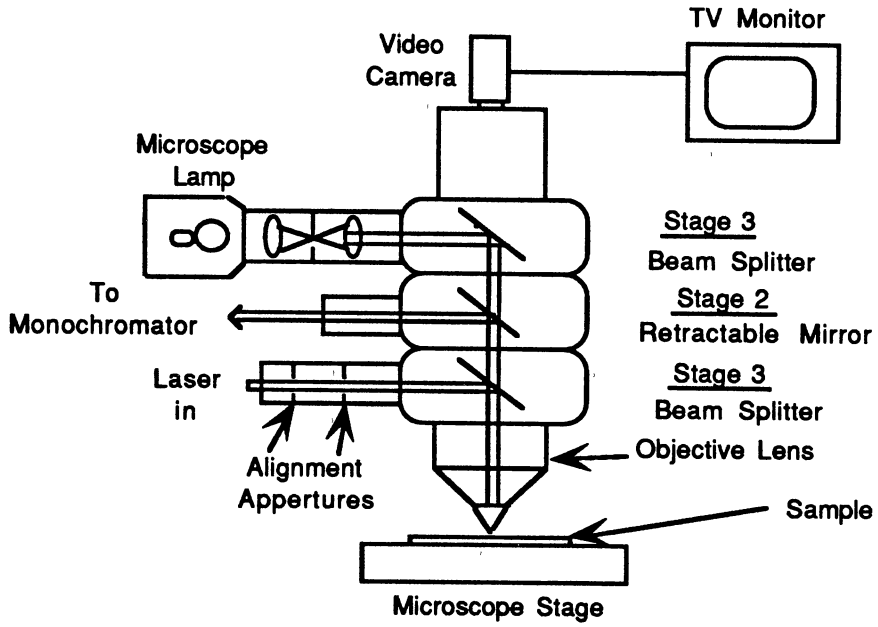

Figure 17. Schematic of the Microscope as Interfaced to the Raman System

the laser spot size to about 1 μm and improved the spatial resolution and reproducibility to approximately 1 mm.

A schematic cross-section of the microscope configured for use in μRaman spectroscopy is shown in Figure 17. The laser beam (~2 mm diam) enters the microscope through the first of two added stages of the microscope. This stage houses alignment apertures and a 50% beam splitter. After reflecting off the beam splitter, the laser light is focused on a crystallite of interest by attenuating the laser and retracting the sliding mirror which is housed in the second stage of the microscope. The sample plane is then viewed by reflected light illumination from the third stage. The laser spot on the substrate is observed on a monitor screen via a Javelin camera. The substrate is translated on the microscope stage until the laser strikes the position of interest. To record a Raman spectrum, the sliding mirror is moved back into position and the laser power is increased. The laser power at the sample was typically 150 mW. A fraction of the scattered light is collimated by the objective lens which passes through the beam splitter and strikes the mirror mounted on the sliding stage which directs the light to the monochromator and is imaged upon the Photo Multiplier Tube. The resolution (full width at half maximum, FWHM) of the spectrometer with a 1800 line/mm grating is 1 cm^{-1}.

Experimental Procedures

Polycrystalline diamond films were synthesized using an oxy-acetylene flame under normal atmospheric pressure conditions. These films were grown on a molybdenum screw, which had been polished and then scratched with a 6 μm diamond paste to enhance the nucleation of diamond. The molybdenum substrate was mounted on a water cooled copper block. Because of the size of the flame, the substrate was restricted to 5/16" diameter. The diamond films can be grown effectively on any carbide forming substrates (Si, Mo, W), as the nucleation density on such materials is one to two orders of magnitude higher than on substrates that do not form carbides (Cu, Au) [24].

While conducting the experiments the flow ratio of oxygen to acetylene, R, was adjusted such that three regions in the flame were noticeable. These regimes are shown in Figure 15b. The flame was then positioned over the substrate in such a manner that the acetylene feather covered the whole substrate. The feather is the region where diamond growth has been observed.

The temperature of the substrate was maintained constant by moving the flame relative to the molybdenum screw or by varying the flow rates of water through the copper block. An infrared pyrometer was used to monitor the substrate temperatures during the deposition.

The following are typical test conditions used:

O_2 to C_2H_2 ratio	:	0.9 - 1.1
Separation of the inner cone from the substrate	:	1 - 8 mm
Temperature of the substrate	:	750 - 1100° C
Duration of the tests	:	1 - 2 hours
Gas flow rates	:	1.5 - 4 standard liters per min (slm)
Gas line pressures	:	20 psi for O_2 and 10 psi for C_2H_2

The morphology of the surface and cross-sections of the samples were studied using a scanning electron microscope. μRaman spectroscopy was used to characterize the diamond films grown as this technique is very sensitive to crystalline diamond and exhibits a first order phonon mode at 1332 cm^{-1} which is unique for diamond.

CHAPTER V

EXPERIMENTAL RESULTS AND DISCUSSION

Introduction

The quest for high quality, defect free, transparent diamond films is yet to be realized. Even though Hirose et. al. [26] and Tzeng et. al. [60] have reported on the synthesis of high purity diamonds in their laboratories, it appears that they have grown films with only a small area of good crystallinity. However, there is still no clear insight into the growth mechanisms of flame formed diamonds even as researchers report on the successful synthesis of good quality films. An understanding of the growth mechanism is therefore a prime requirement for achieving a large number of unaccomplished objectives.

Hanssen et. al. [67] had reported on the observations of cauliflower-like growth features as well as well formed crystals of octahedral and cubic orientations. Though these observations have been confirmed by other researchers also, there are no reports on the initiation and growth of these "cauliflower-like" structure or how octahedral or cubic structure development takes place. There is however, a general agreement that the octahedral features dominate at lower temperatures and the cubic at higher temperatures.

In order to grow high quality films of uniform thickness, preferred crystal orientation, etc., a fundamental approach to the growth mechanism is needed. Hence, a systematic analysis was conducted under different parametric conditions to observe the morphological changes produced as a result. In this chapter, SEM micrographs showing the surface morphological characteristics are supplemented by μRaman spectra to evaluate the diamond film quality. A detailed study of the growth features is reported and based on it a hypothesis for the growth process is proposed. It is proposed that multinucleation of

diamond leads to cauliflower-like growth. This cauliflower-like growth then transforms into octahedral at high temperatures and into cubic at still higher temperatures. Further development of the film takes place in a cyclic manner which is similar to the phenomena observed by Kobashi et. al. [71].

For the development of good quality diamond coatings on a variety of substrate materials, it is necessary to maintain low, uniform substrate temperatures. Many researchers [60, 62, 66] have reported the morphology of the diamond surface to be dependent on substrate temperature and concentration of flame species. Thus octahedral features were observed at lower temperatures (~ 750° C) and cubic morphologies at higher temperatures (~ 1100° C). What we propose here which is rather unique, is to deposit diamond films at low substrate temperature and modify the surface morphology of the films by changing the ratio of O_2 to C_2H_2. By utilizing the oxidation of diamond and its ability to alter the crystal morphology, we propose to tailor films of any morphology.

A plausible reason for the growth of high quality diamond films at low cylinder pressure of acetylene is also given. The significance of the "stagnation zone" in the growth of diamond films of uniform thickness and morphology is also brought to light in the foregoing discussions.

Effect of Gas Flow Ratio on Diamond Morphology

To study the effect of nominal gas flow ratios, the flow rate of acetylene was maintained at 2 standard liters per minute (slm) and the duration of deposition was 2 hours in all the experiments. The substrate temperature was approximately 850° C and the distance of the inner cone from the substrate was maintained at 2 mm. The effect of varying flow ratios on the diamond morphology is shown in Figure 18. All the micrographs are at the center of the specimens. Crystalline deposition was observed between nominal flow ratios of 0.92 to 1.02. For ratios less than 0.92 ball-like growth was observed and for ratios greater than 1.02 no deposit was noticed. Between R = 0.92

and 1.02, the morphology of the crystals changed from badly formed octahedral crystals at R = 0.92 (Fig. 18(a)) to cubo-octahedrons at R = 1 (Fig. 18(d)). There was also a perceptible increase in crystal size with increase in R. At R = 0.94, the crystals were octahedral of about 2 μm in size whereas at R = 1.02 (Fig. 18(e)), the crystals were cubo-octahedral and ~ 6 μm in size. Also, with increase in nominal flow ratios, the number of facetted particles increased in number with large areas of the film being occupied by these crystallites. The range of gas ratios for diamond growth varied depending on the process conditions. For e.g., at higher flow rates diamond deposition was observed even at R = 1.1.

The Raman spectra of the films are shown in Figure 19. It can be observed that with an increase in oxygen content in the gas stream better films are obtained. The best films were observed at R ≈ 1. This may be due to the higher temperature prevailing in the feather and the etching of any non-diamond carbon by the excess oxygen.

Effect of Gas Flow Rate on Diamond Morphology

The following experimental conditions were used while studying the effect of flow rates: nominal gas ratio, R = 0.98; size of nozzle used, No. 4; substrate temperature ~850-900° C; and deposition time of 2 hours. The flow rates were varied from 2 slm to 4 slm at increments of 0.5 slm. The inner cone distance was maintained at 1 mm. Below 2 slm, the growth rates were very low and the film cracked frequently after deposition or got burnt. The upper limit of the flow rate was restricted by the full scale range of the mass flow meters. Figure 20 shows the SEM micrographs of the films deposited at varying flow rates. No clear morphological trend was observed in the deposits. This may be due to the variation in the acetylene cylinder pressure. The most transparent film was obtained at flow rates of 4 slm, but the morphology did not show a distinct orientation. The thickness of the films decreased with increase in flow rates from ~10 μm at 2 slm (Fig. 21(a)) to ~ 6 μm at 4 slm (Fig. 21(d)). This suggests that the diamond film was probably getting etched

(a) R = 0.92

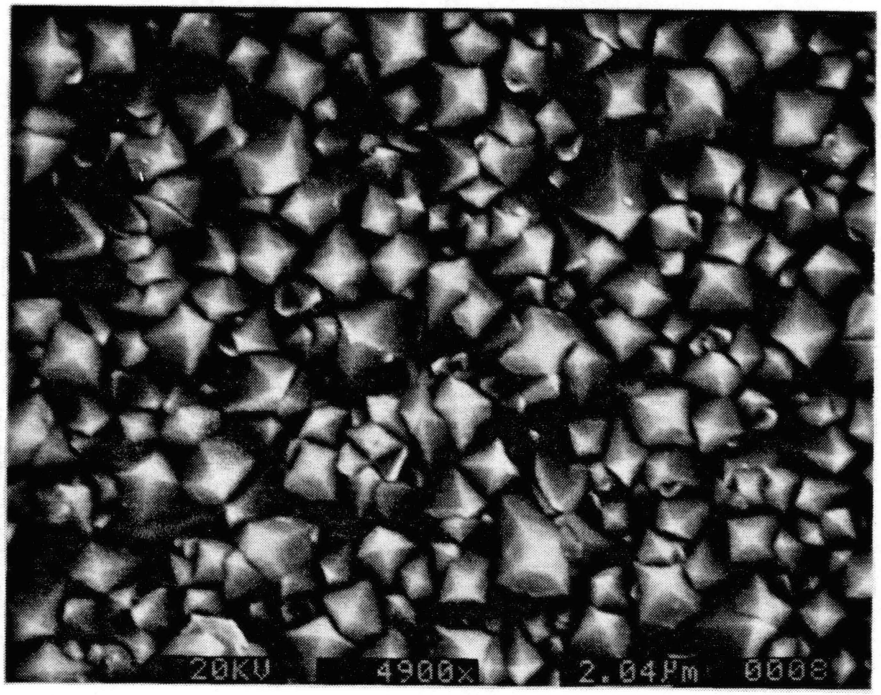

(b) R = 0.94

Figure 18. Effect of Gas Flow Ratio

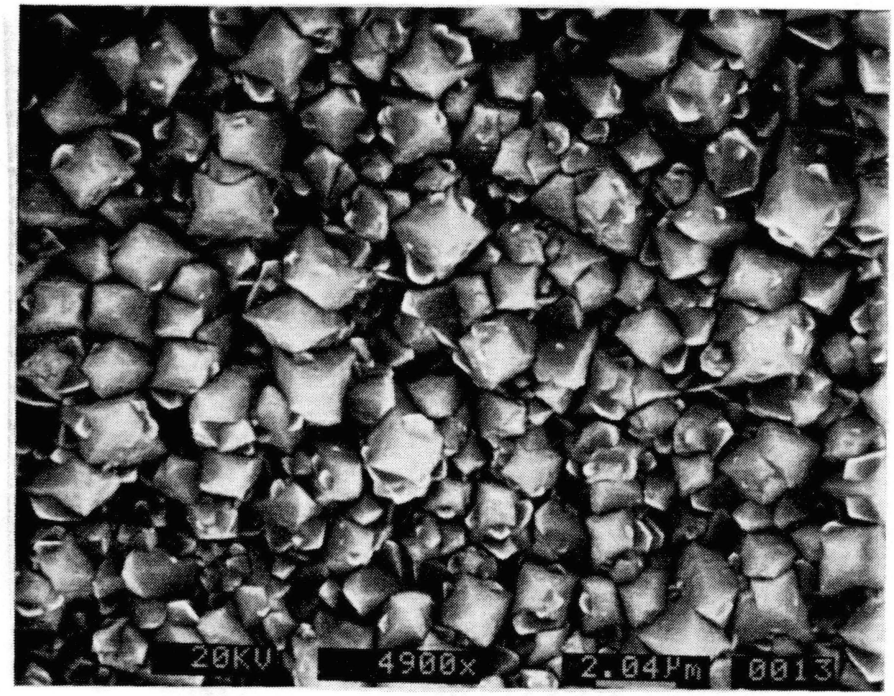

(c) R = 0.96

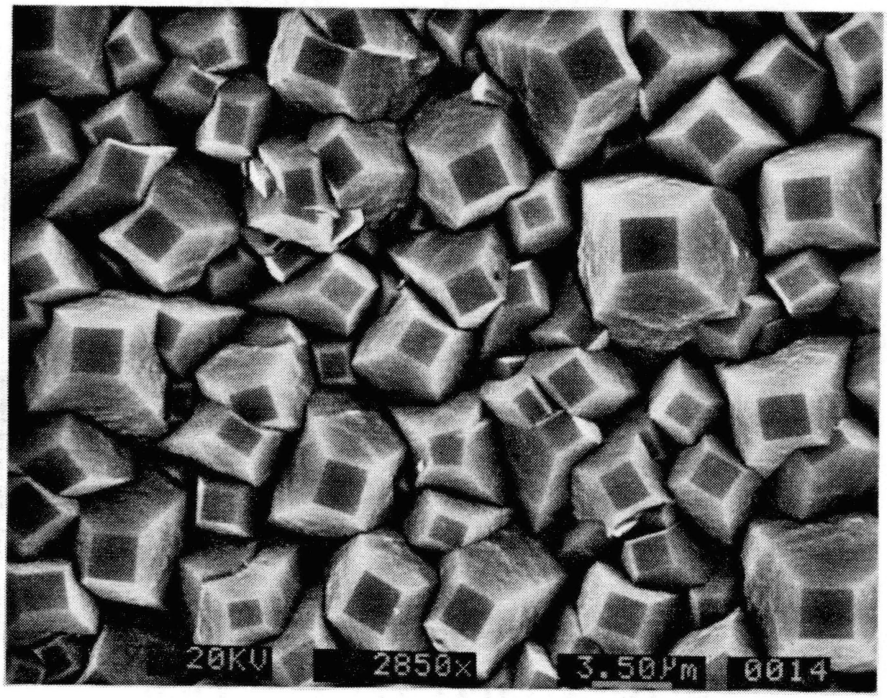

(d) R = 1.0

Figure 18. Effect of Gas Flow Ratio (contd.)

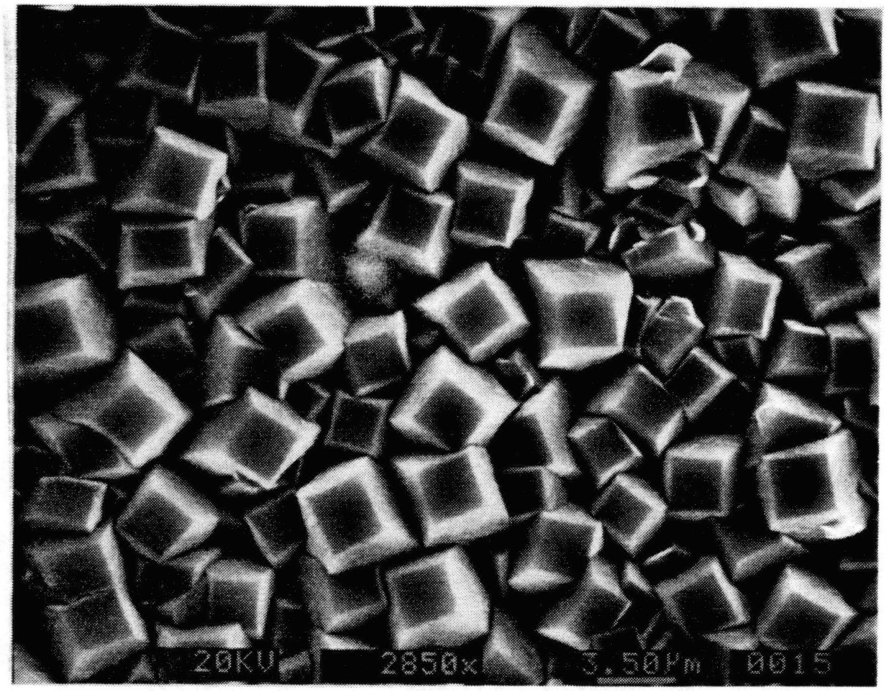

(e) R = 1.02

Figure 18. Effect of Gas Flow Ratio (contd.)

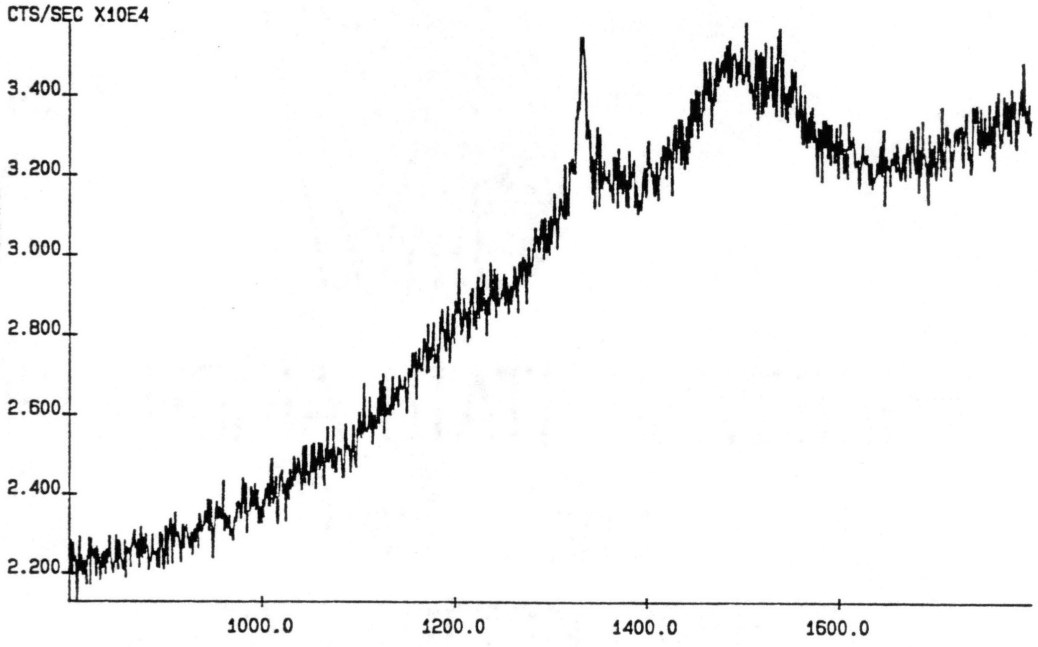

(a) R = 0.92

Figure 19. Raman Spectra of Films for Different Gas Ratios

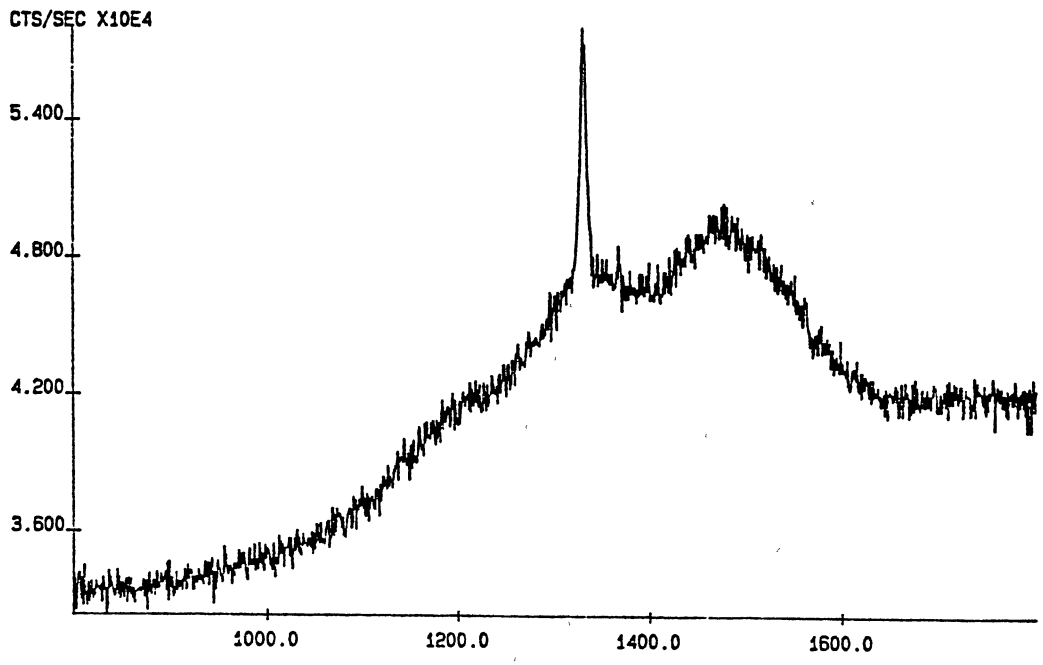

(b) R = 0.94

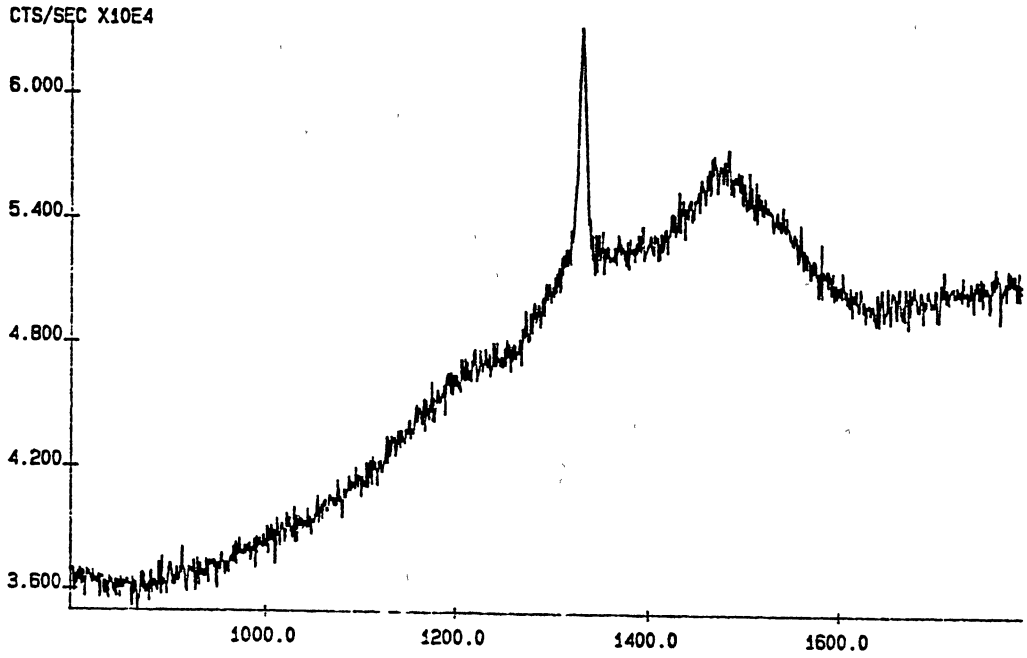

(c) R = 0.96

Figure 19. Raman Spectrum of Films for Different Gas Ratios

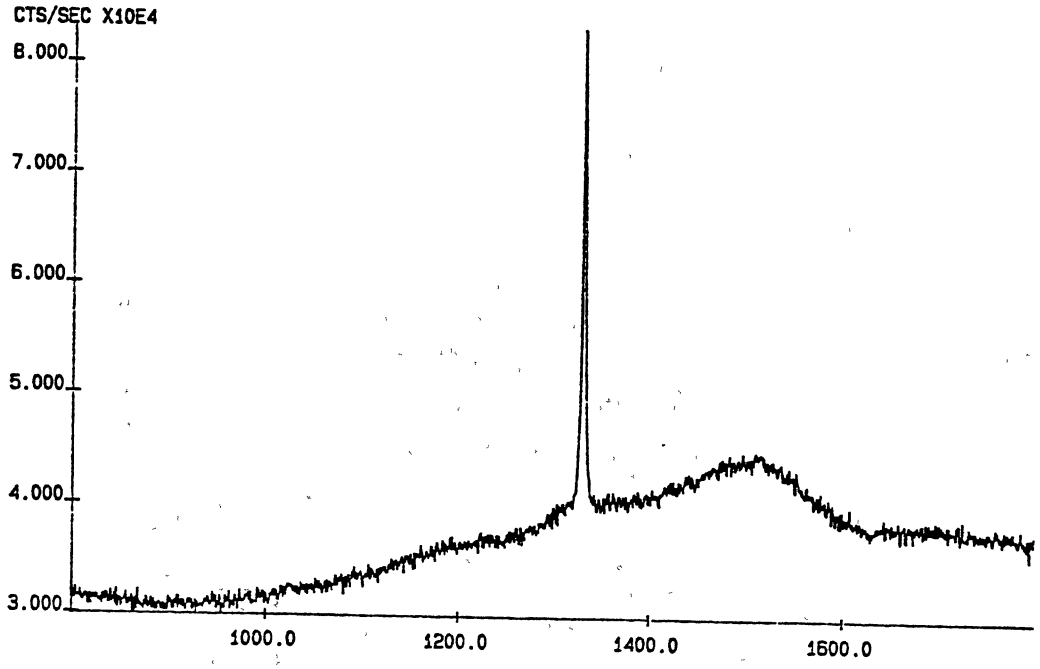

(d) R = 1

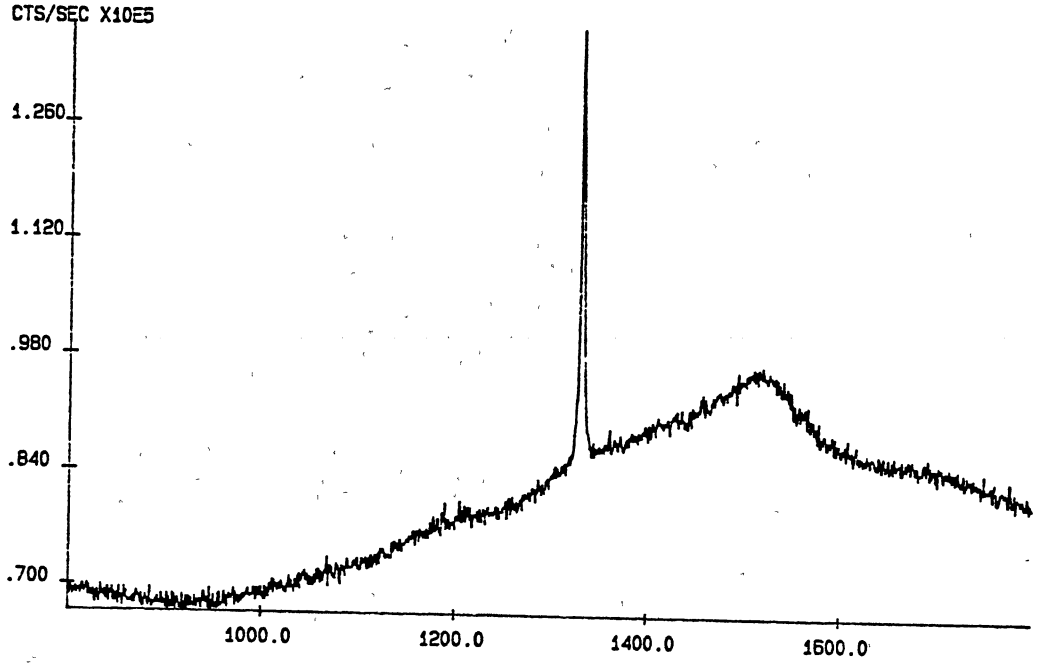

(e) R = 1.02

Figure 19. Raman Spectra of Films at Different Gas Ratios (Contd.)

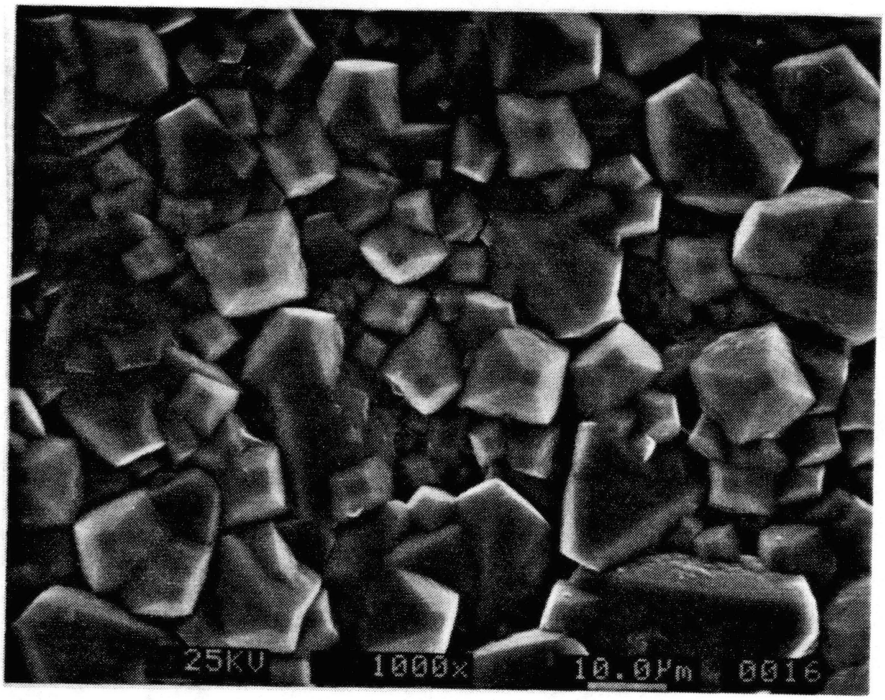

(a) Flow Rate = 2 slm

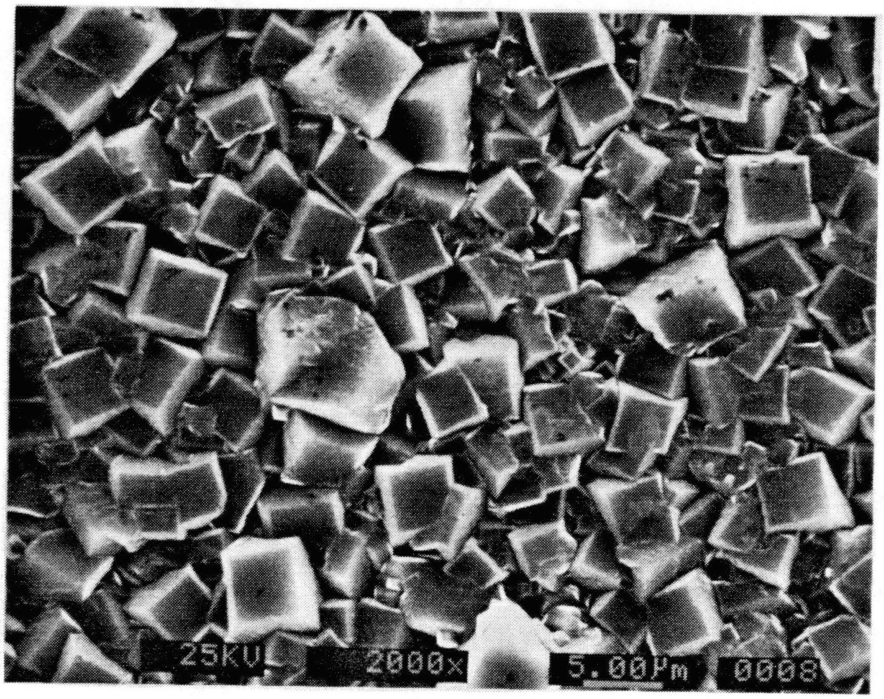

(b) Flow Rate = 3 slm

Figure 20. Effect of Gas Flow Rate

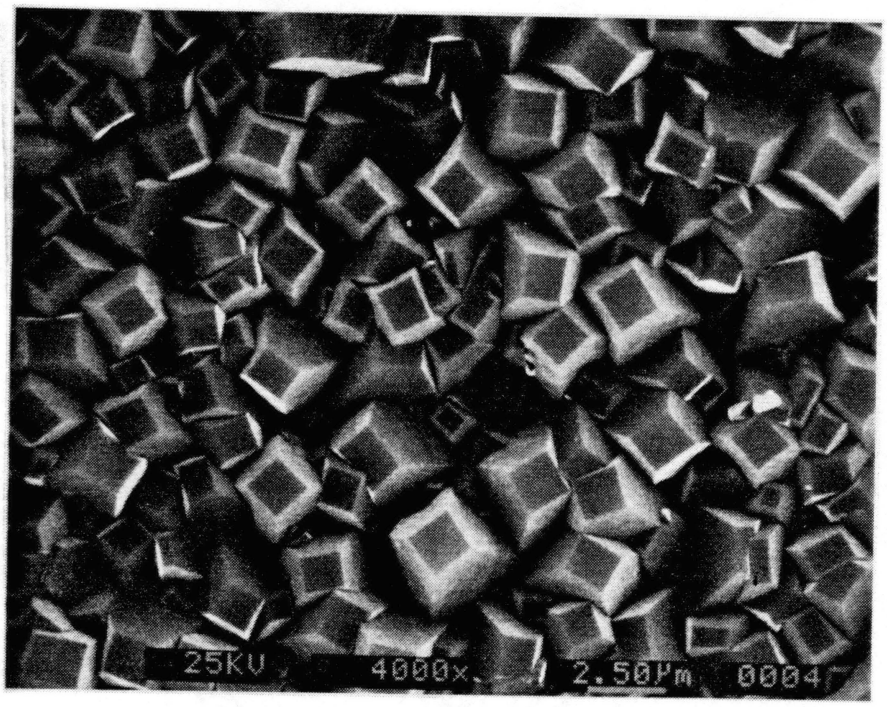

(c) Flow Rate = 3.5 slm

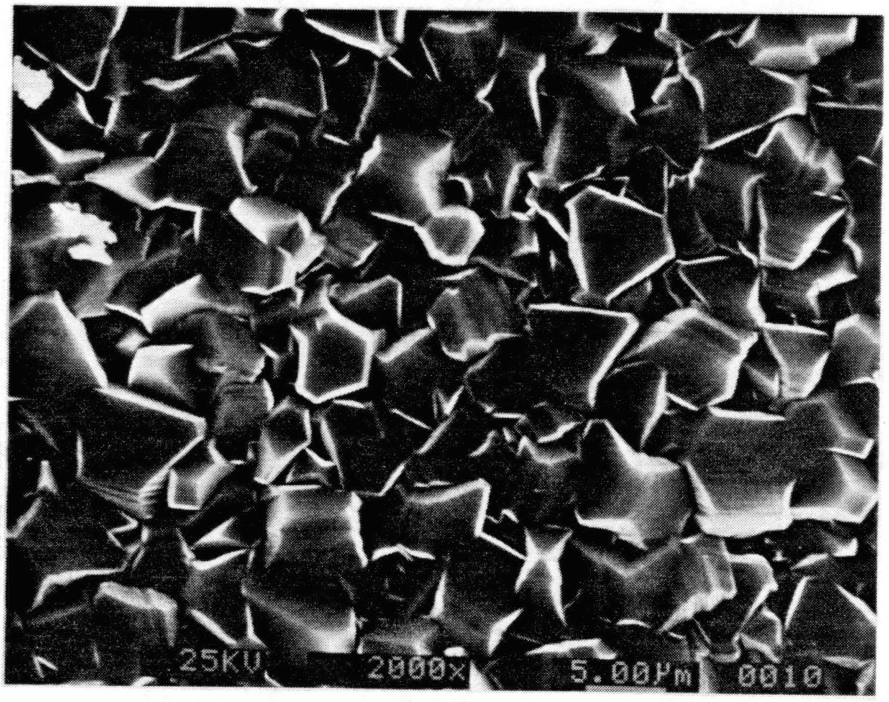

(d) Flow Rate = 4.0 slm

Figure 20. Effect of Gas Flow Rate (Contd.)

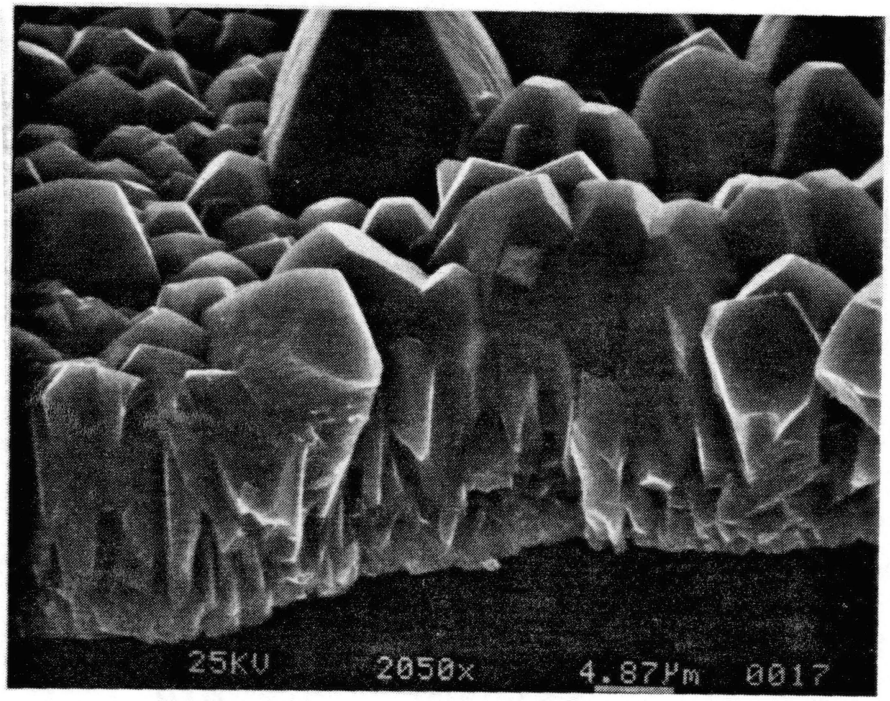

(a) Flow Rate = 2 slm

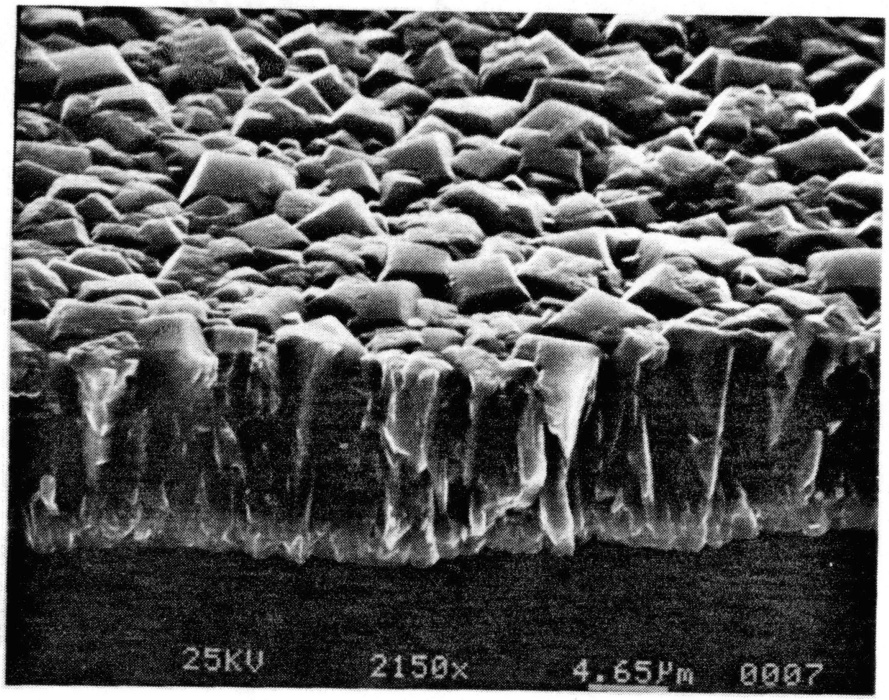

(b) Flow Rate = 3 slm

Figure 21. Cross-sectional view of Films Grown at Different Flow Rates

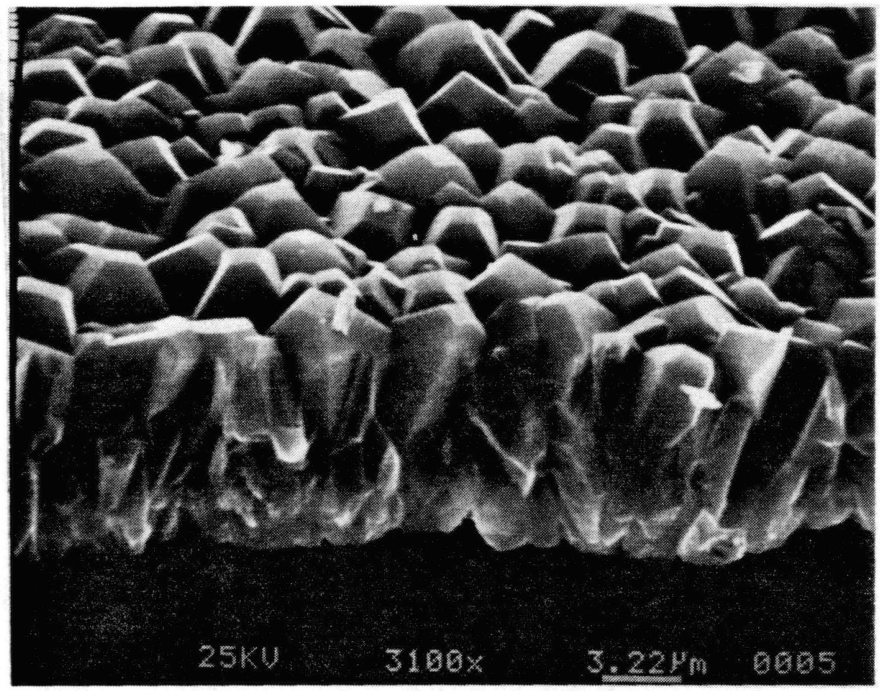

(c) Flow Rate = 3.5 slm

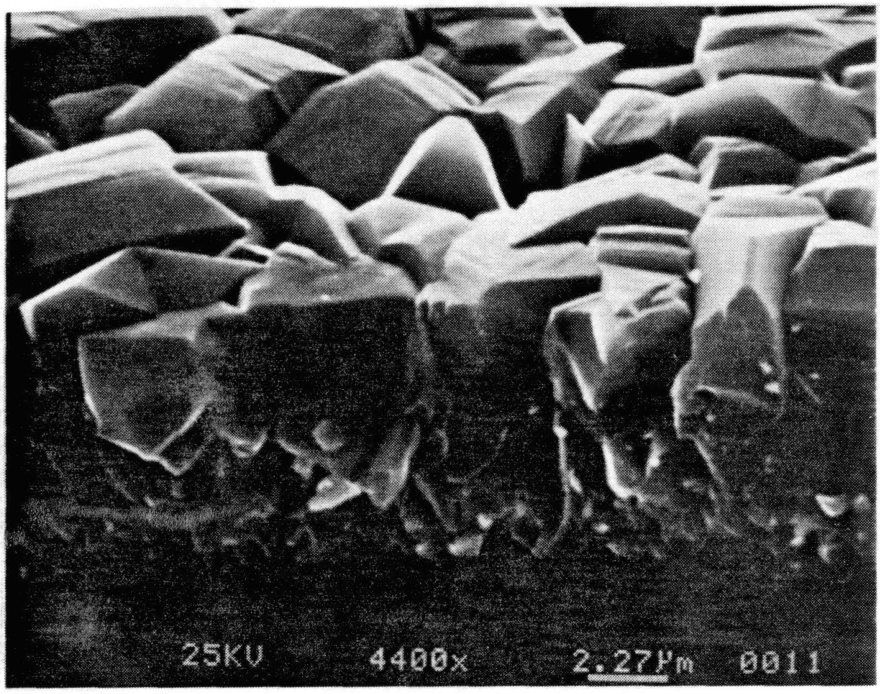

(d) Flow Rate = 4.0 slm

Figure 21. Cross-sectional view of Films Grown at Different Flow Rates (Contd.)

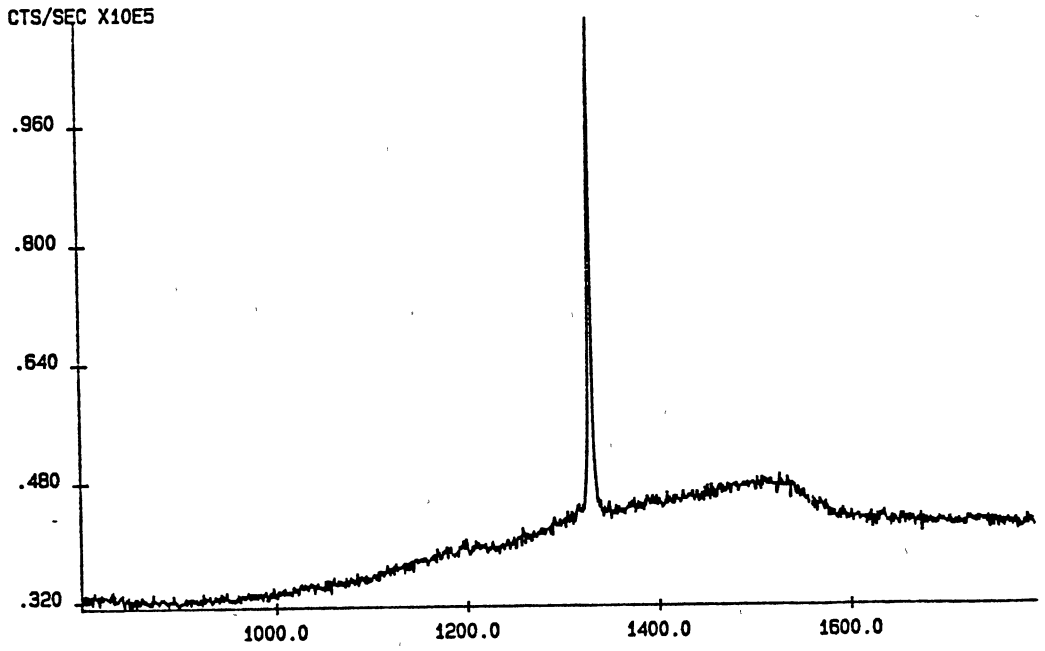

(a) Flow Rate = 2 slm

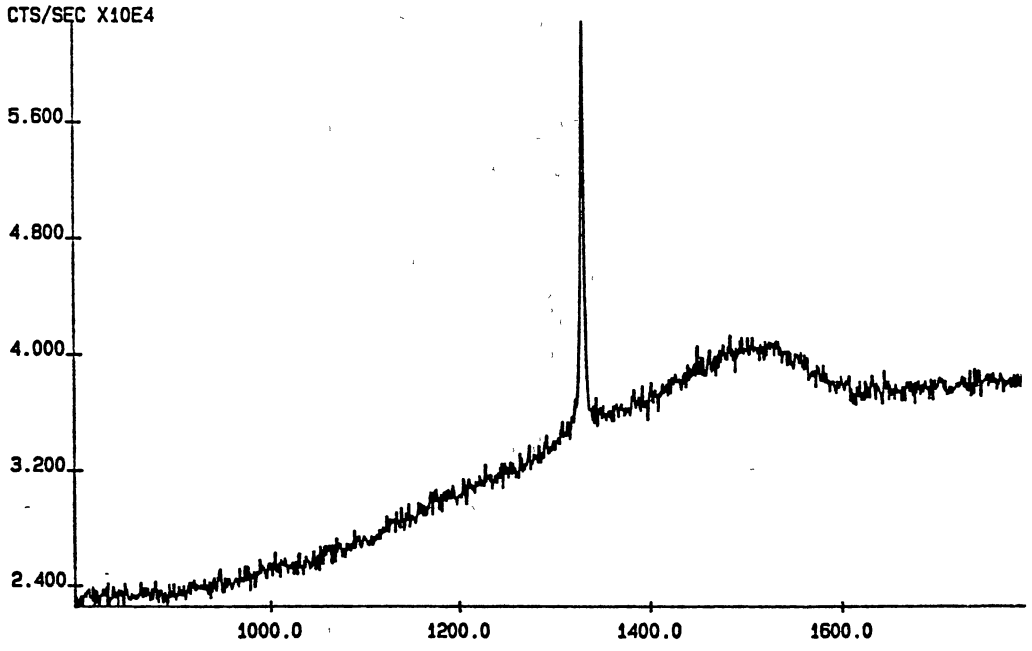

(b) Flow Rate = 3 slm

Figure 22. Raman Spectra of Films Grown at Different Gas Flow Rates

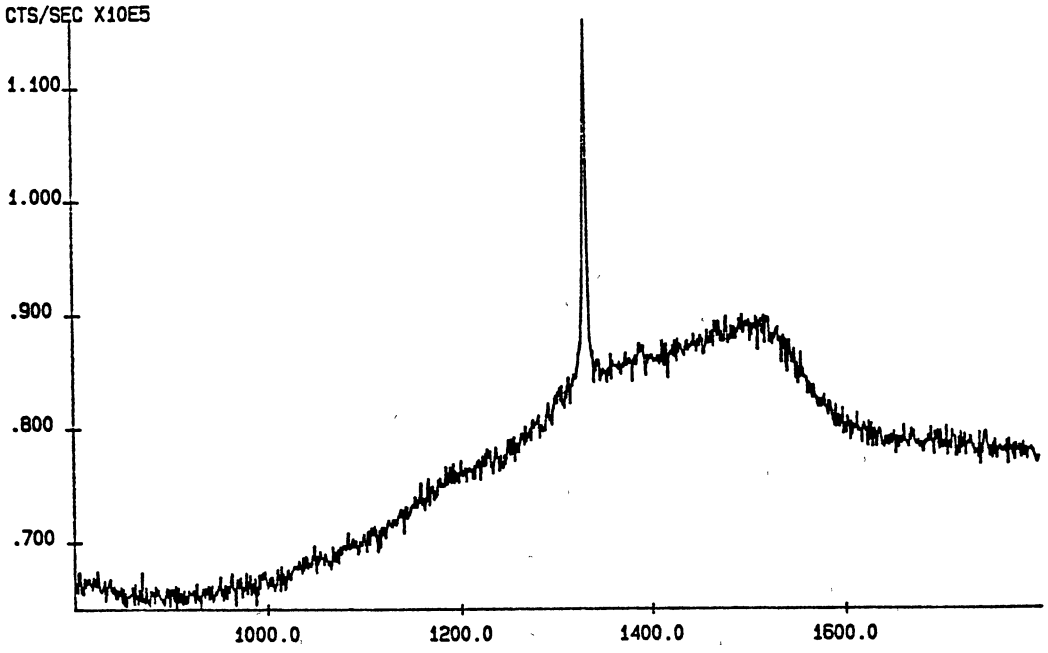

(c) Flow Rate = 3.5 slm

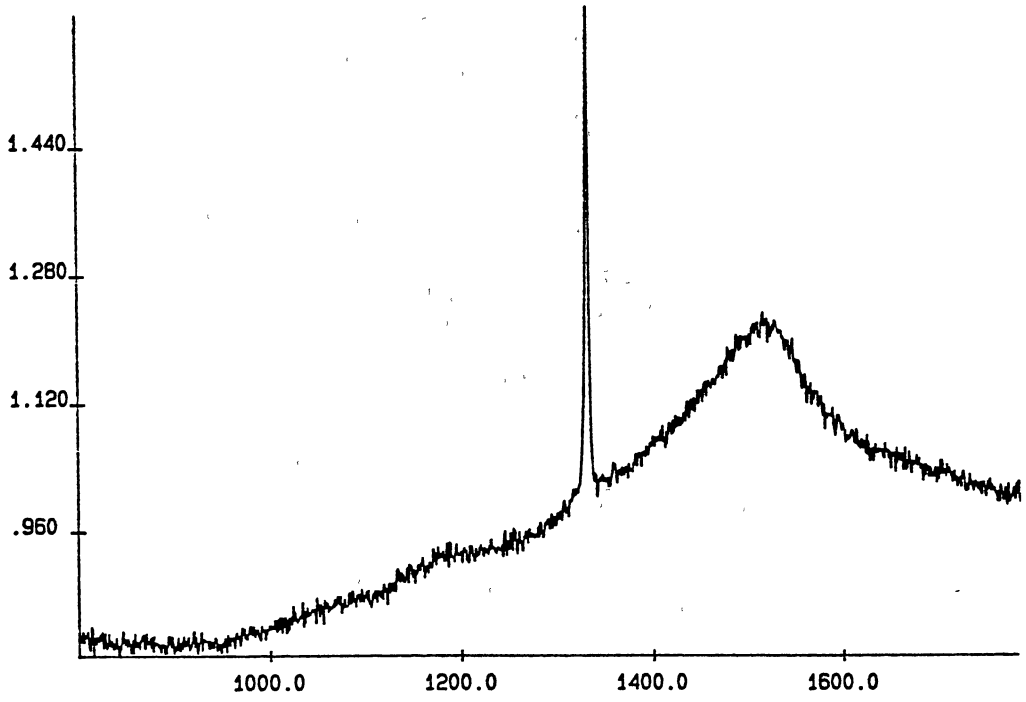

(d) Flow Rate = 4.0 slm

Figure 22. Raman Spectra of Films Grown at Different Flow Rates

during the growth process. Also as the inner cone was longer and hence temperatures in the feather higher, the cubic morphology dominated at higher flow rates. The Raman spectra of the films at 2, 3, 3.5 and 4 slm are shown in the Figure 22. The best quality film with the lowest non-diamond carbon content was obtained at 2 slm. With increase in flow rates, the broad band between 1500-1600 cm^{-1} increased signifying an increase in non-diamond carbon.

Effect of Distance of the Innercone From the Substrate

The experimental conditions used were as follows: Acetylene flow rates of 2 slm, nominal gas ratios of 0.98, No. 2 size nozzle, substrate temperature of ~850° C, and deposition time of 2 hours. In all the experiments, the acetylene feather length was approximately 25 mm. Four distances of the inner cone from the substrate were studied: 1, 2, 4, and 8 mm. The SEM micrographs for the different conditions are shown in the Figure 23. At lower distances the film was whitish in complexion and showed very good translucency. The morphology was very well defined and well developed crystals were noticed in the area below the inner cone. The micrograph shown in Figure 23(a), however, does not exhibit a well developed morphology as the acetylene cylinder pressure was high. This aspect will be discussed in the next section. With increase in separation the area of transparency reduced dramatically and at 8 mm distance the film was dark with only cauliflower-like growth present. Also, the growth rates of the film dropped as the separation increased and the films were very thin at large separations. Figure 24 shows how the Raman signature of the films change as the distance is increased. At lower separations there was only a small difference in quality of the films, however, the area of deposition of good crystallites was found to increase with decrease in separation.

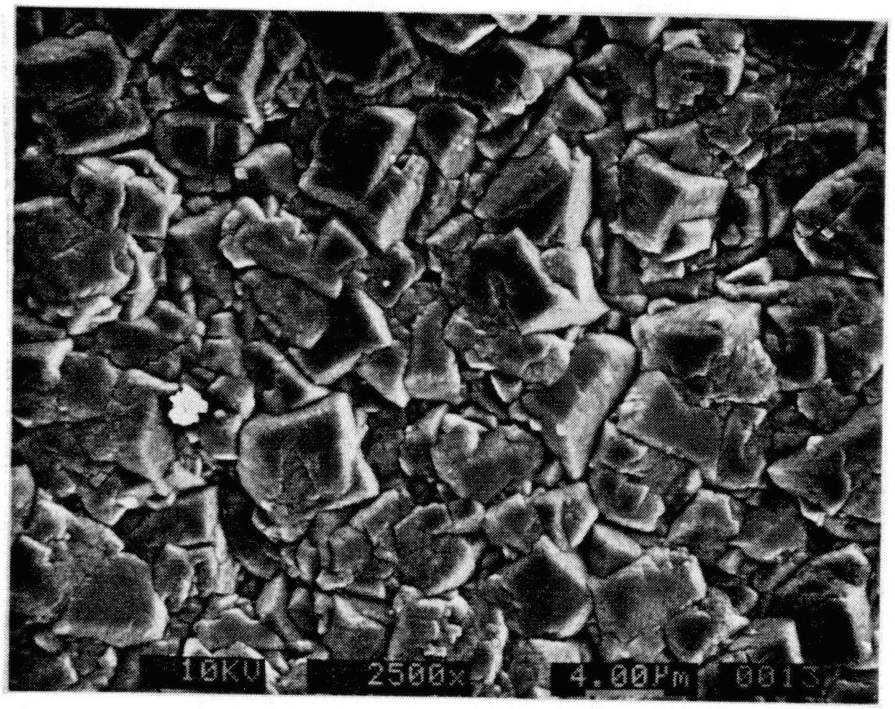

(a) Inner Cone Distance = 1 mm

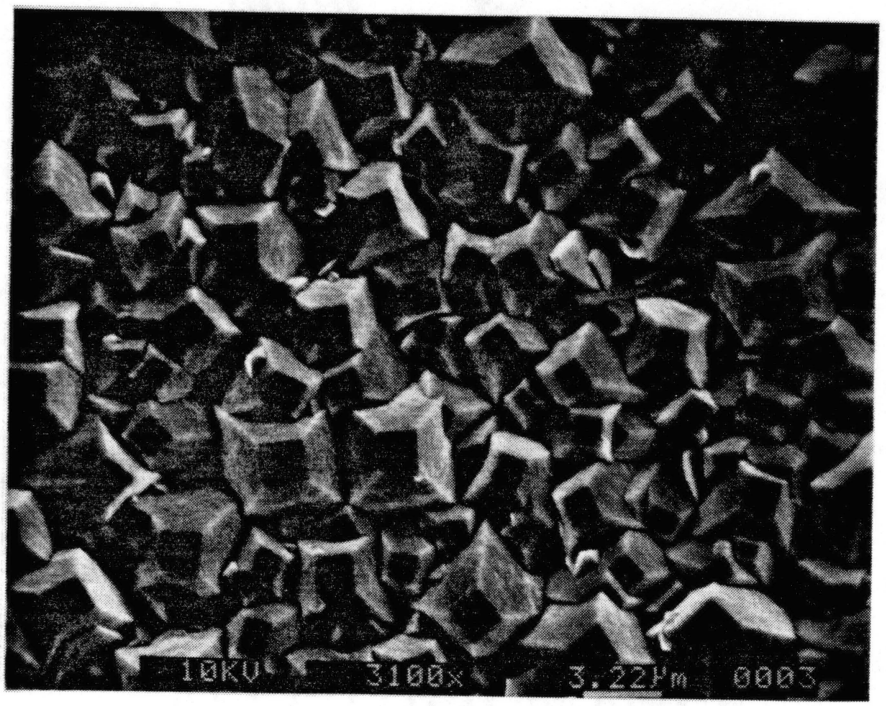

(b) Inner Cone Distance = 2 mm

Figure 23. Effect of Inner Cone Distance

(c) Inner Cone Distance = 4 mm

Figure 23. Effect of Inner Cone Distance (Contd.)

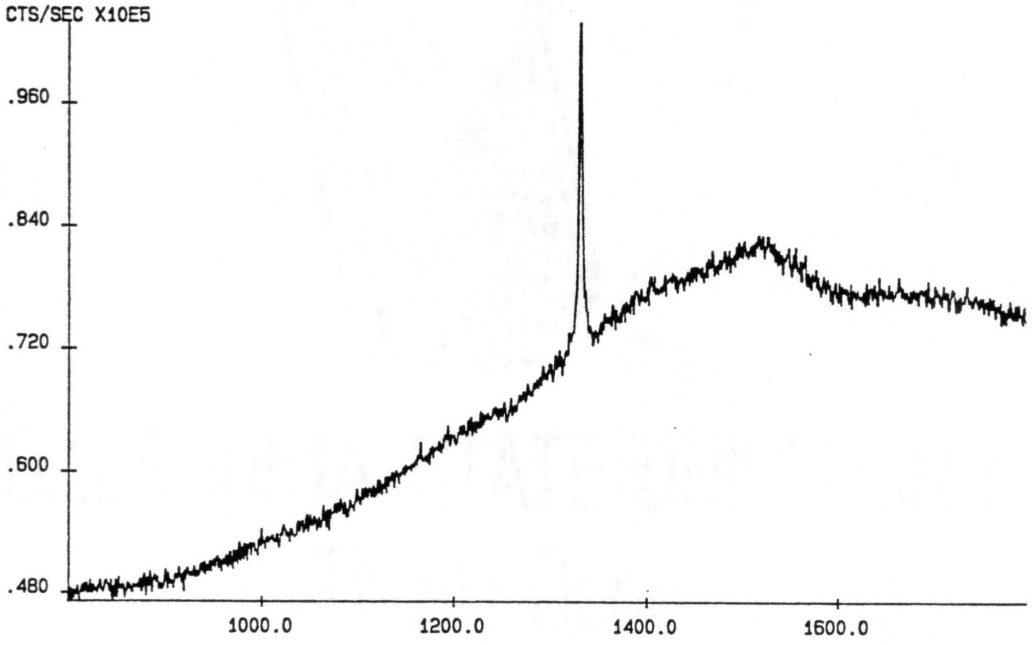

(a) Inner Cone Distance = 1 mm

Figure 24. Raman Spectra of Film at Different Inner Cone Distances

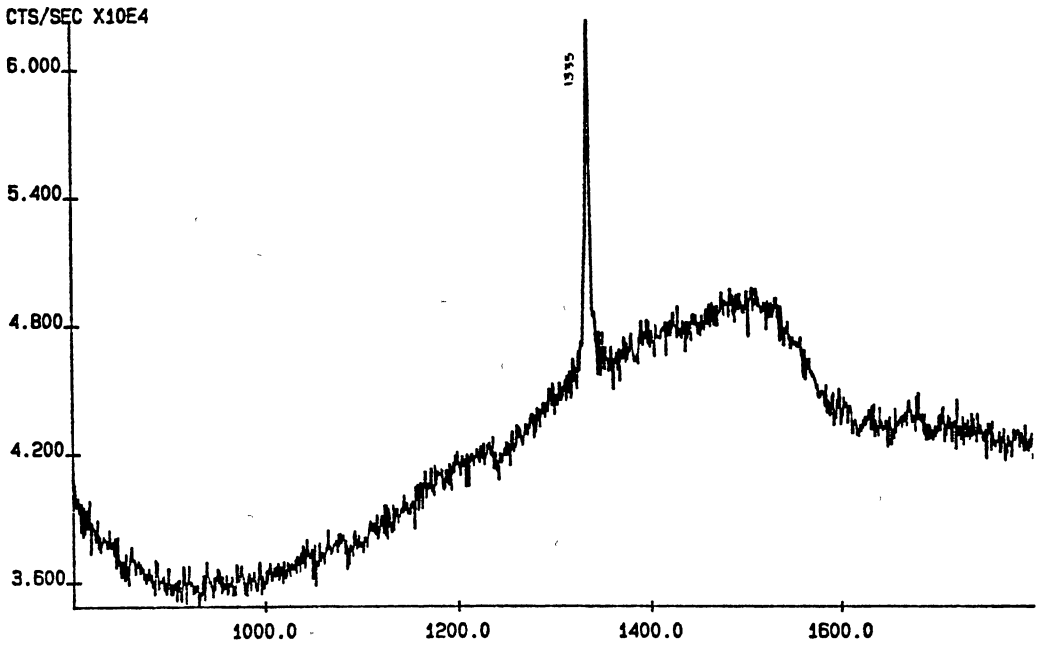

(b) Inner Cone Distance = 2 mm

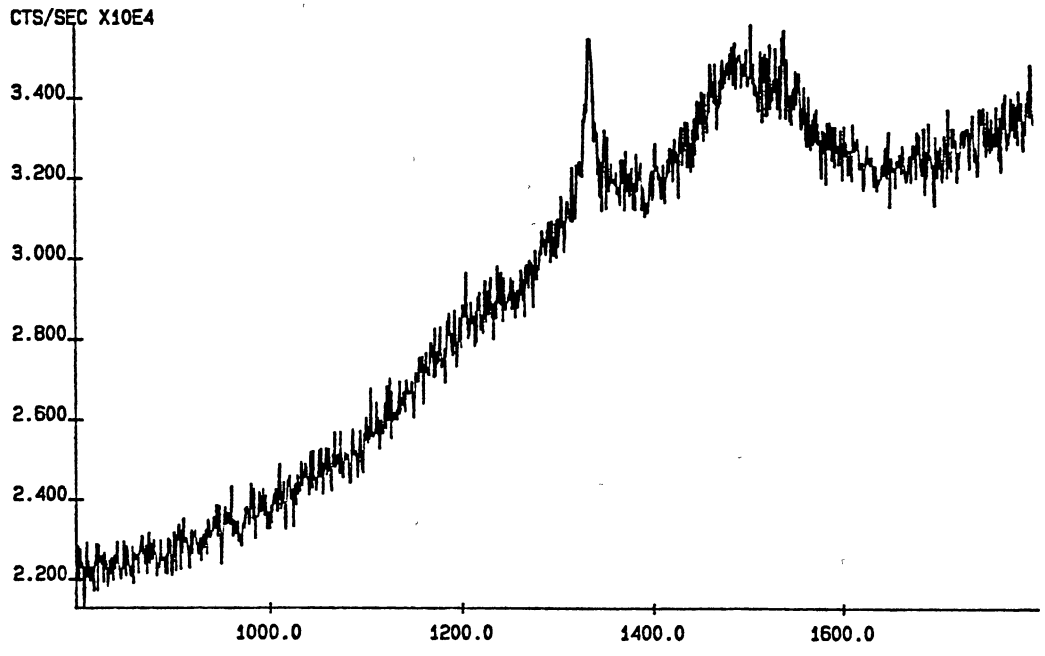

(c) Inner Cone Distance = 4 mm

Figure 24. Raman Spectra of Film at Different Inner Cone Distances (Contd.)

Effect of Acetylene Cylinder Pressure on Diamond Film Quality

The effect of variation in C_2H_2 cylinder pressure has not been reported in the literature as yet. It was found during the course of this investigation, that the pressure of the acetylene in the cylinder had a marked influence on the quality of the film grown. The cylinder pressure effected the quality to such an extent that the film transformed from a noncrystalline state at high pressures to a transparent high quality deposit at low cylinder pressures.

In order to study the nature of deposits as a function of cylinder pressure a systematic analysis was conducted where only the cylinder pressure was the variable and all other factors were held constant. The following growth conditions were used during the study: C_2H_2 gas flow rates of 3.2 slm; nominal gas ratios of ~1; substrate to inner cone distance of 1 mm; and duration of the run was 2 hours. Figure 25 shows the morphology of diamond films as a function of the cylinder pressure at five different values. It was very surprising to note that dark, dirty looking films consisting only of cauliflower-like structures at high cylinder pressures (215 psi) transformed into transparent films consisting of well formed crystallites at low values of cylinder pressure (98 psi). The Raman spectra (Fig. 26) of the films, however, does not indicate a large difference in the diamond content. The transparency of the films started to improve at C_2H_2 cylinder pressures of approximately 100 psi. At 40 psi, the film was very transparent and when placed over news print the letters in the background could be read easily.

To summarize, the morphology of the diamond films was found to be sensitively dependent on the different processing conditions. It was observed that the morphology varied from cauliflower-like structures to well formed crystallites depending on the conditions used. The pressure in the acetylene cylinder was found to have a profound effect on the quality of the film grown, with the quality and transparency improving with decrease in cylinder pressure.

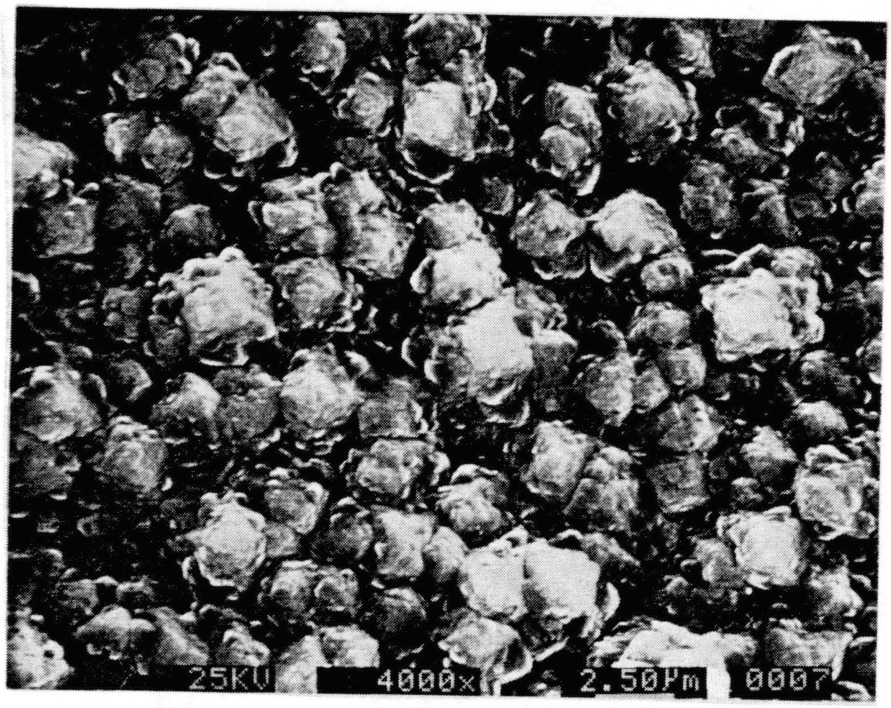

(a) Pressure = 215 psi

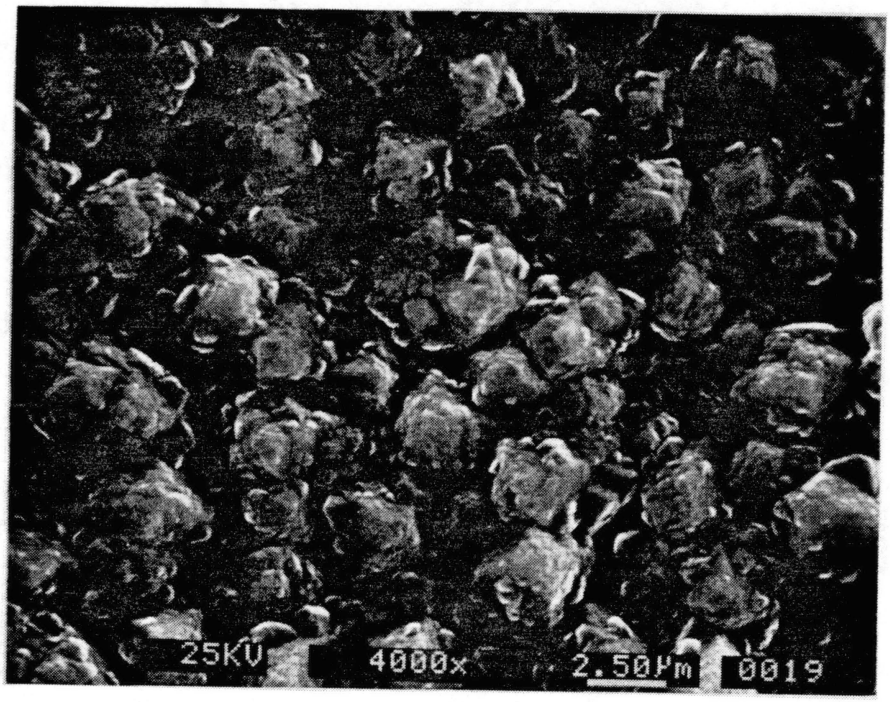

(b) Pressure = 190 psi

Figure 25. Effect of Acetylene Cylinder Pressure

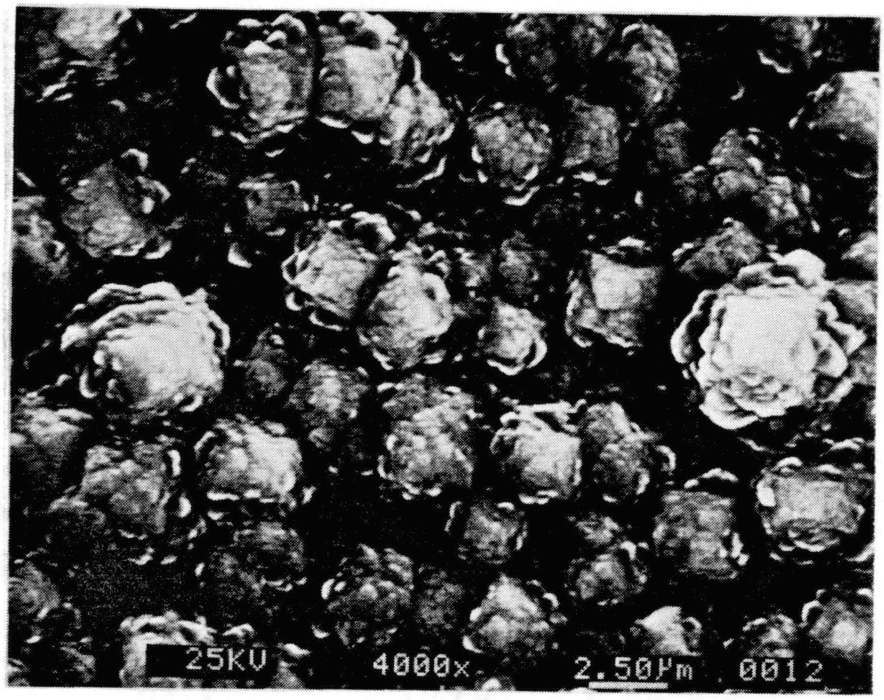

(c) Pressure = 170 psi

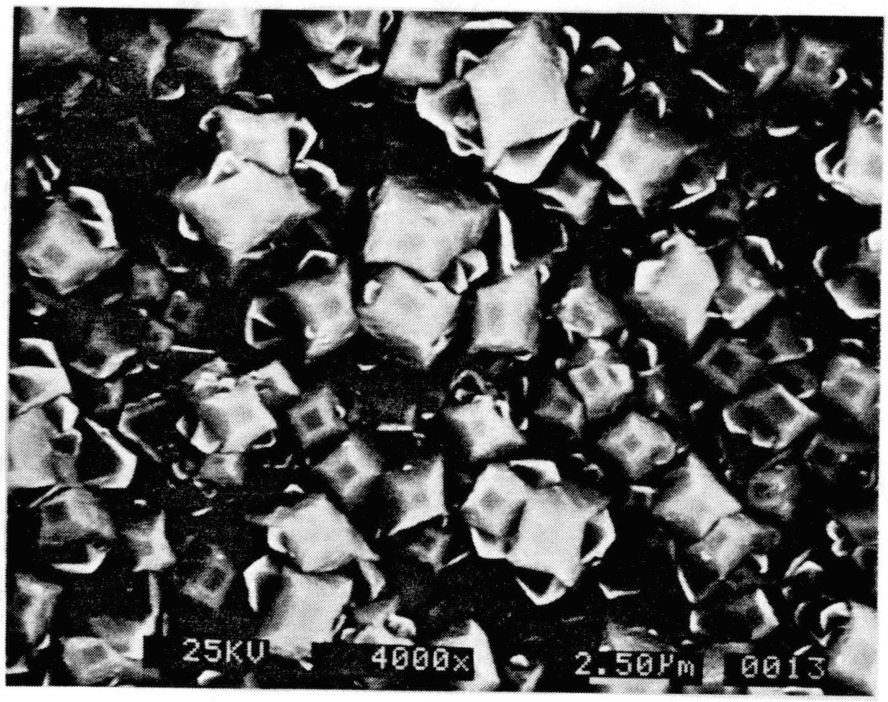

(d) Pressure = 140 psi

Figure 25. Effect of Acetylene Cylinder Pressure (Contd.)

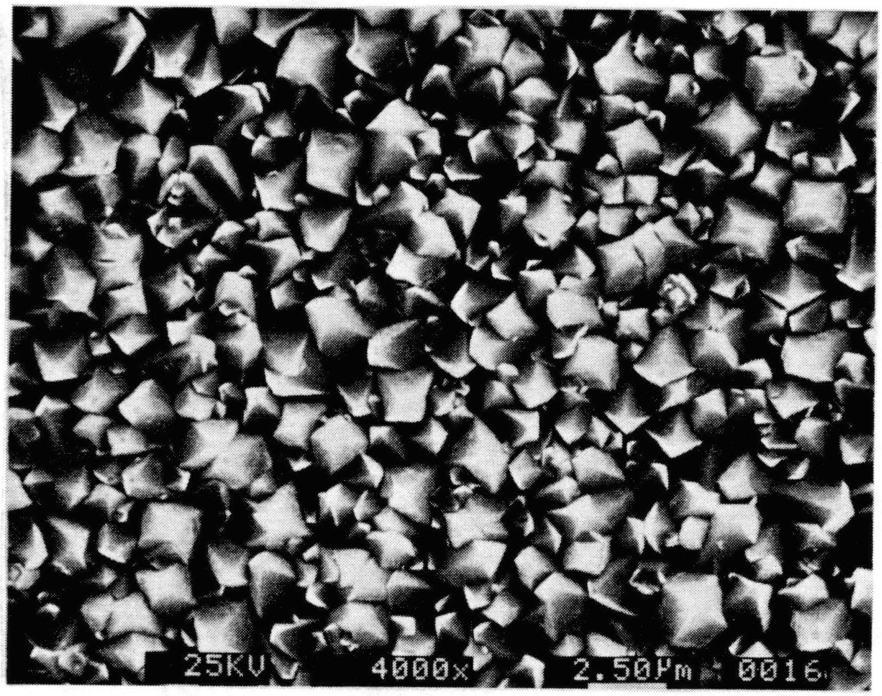

(e) Pressure = 98 psi

Figure 25. Effect of Acetylene Cylinder Pressure (Contd.)

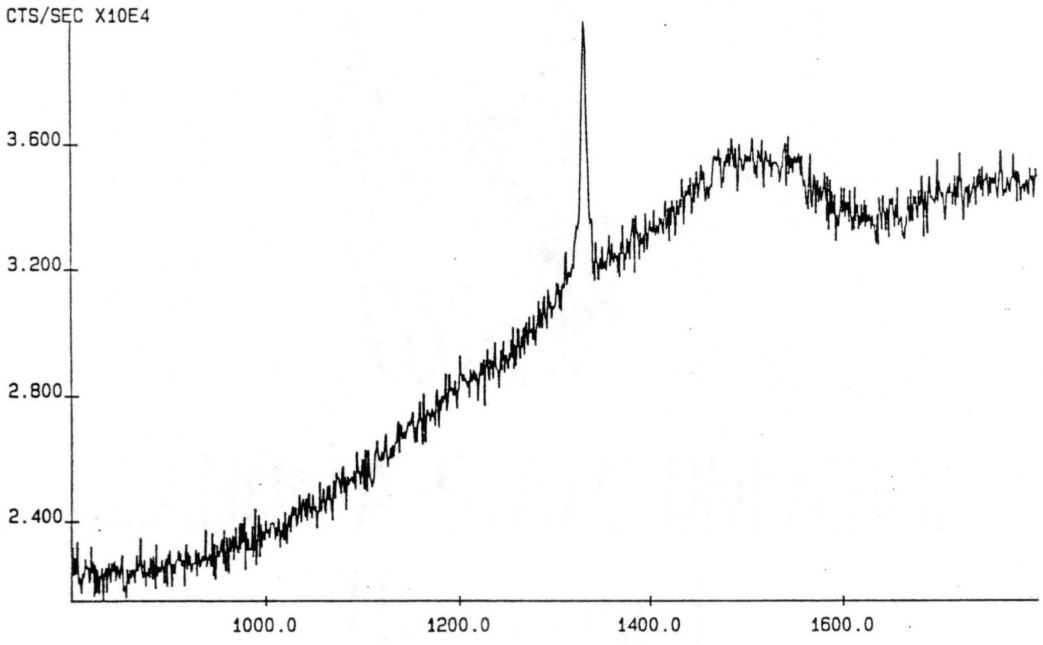

(a) Pressure = 215 psi

Figure 26. Raman Spectra of Film at Different Acetylene Cylinder Pressures (Contd.)

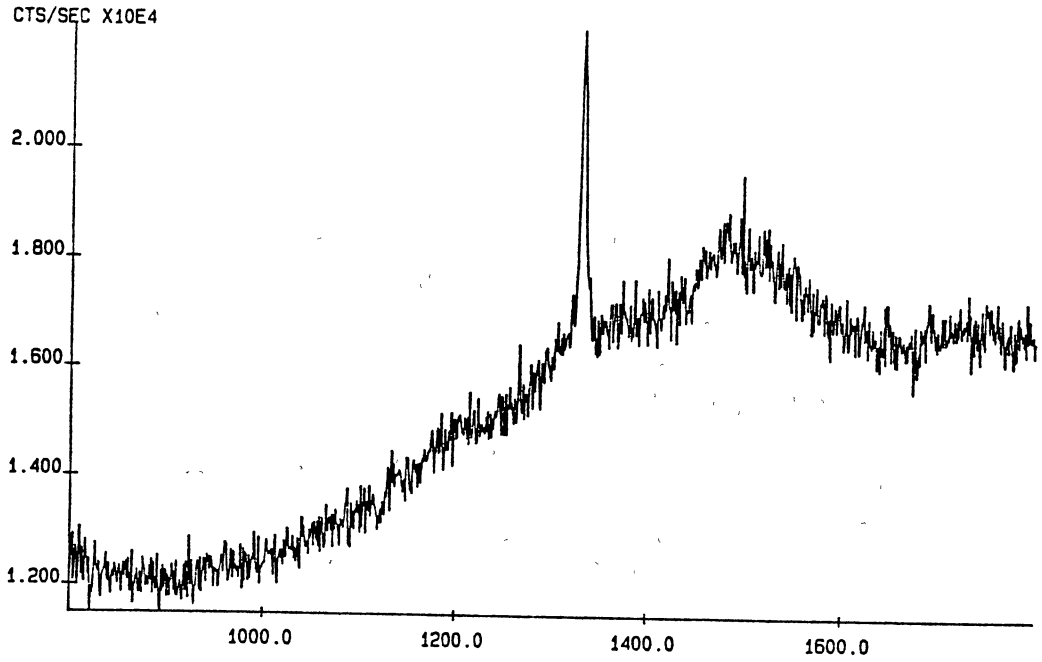

(b) Pressure = 190 psi

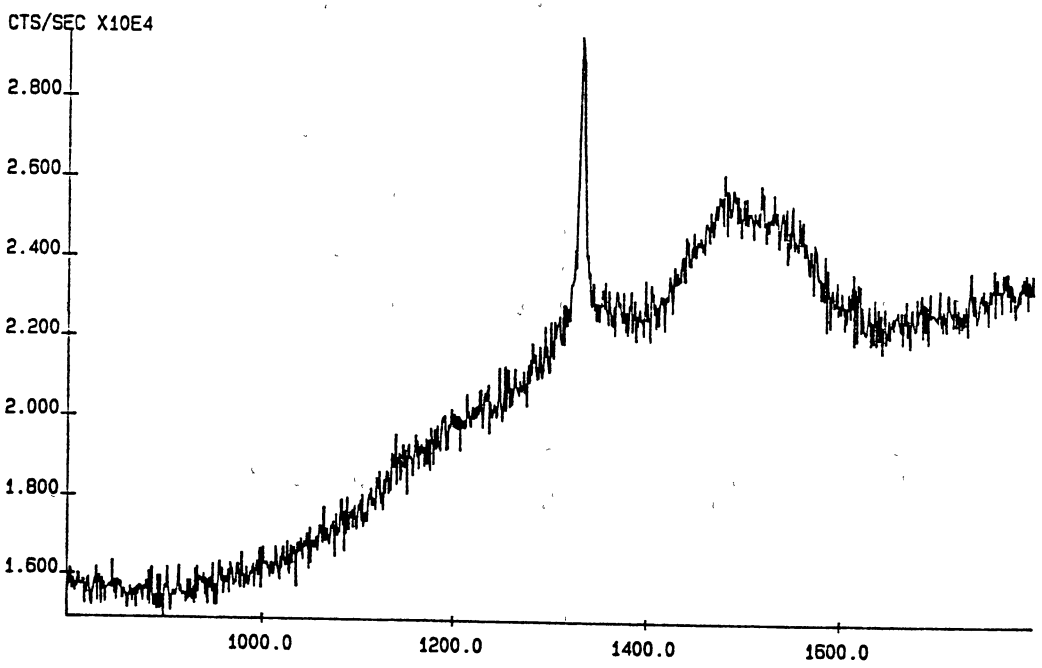

(c) Pressure = 170 psi

Figure 26. Raman Spectra of Film at Different Acetylene Cylinder Pressures (Contd.)

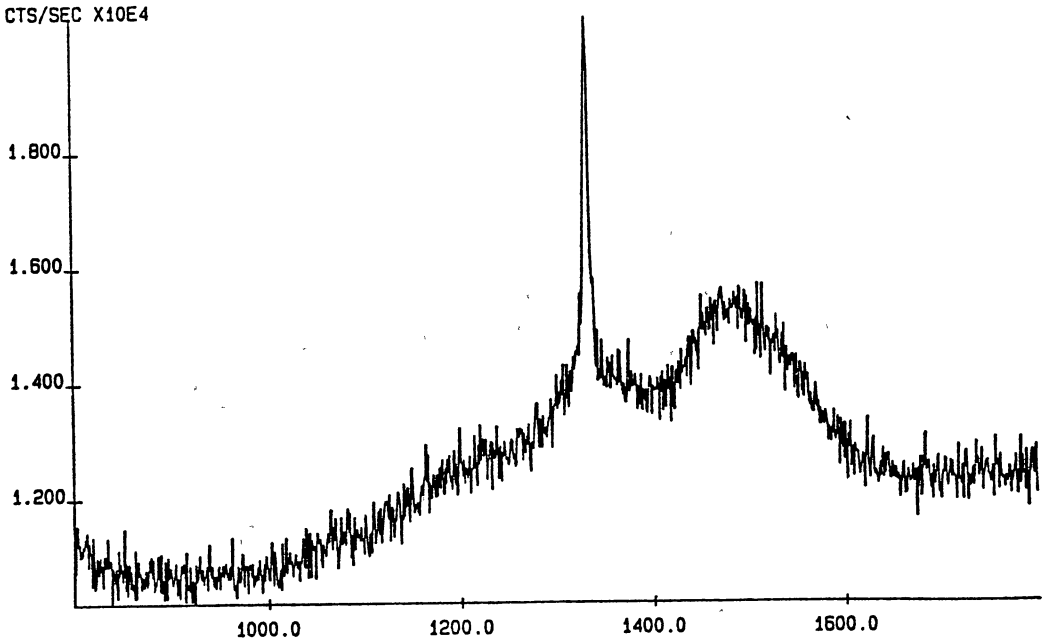

(d) Pressure = 140 psi

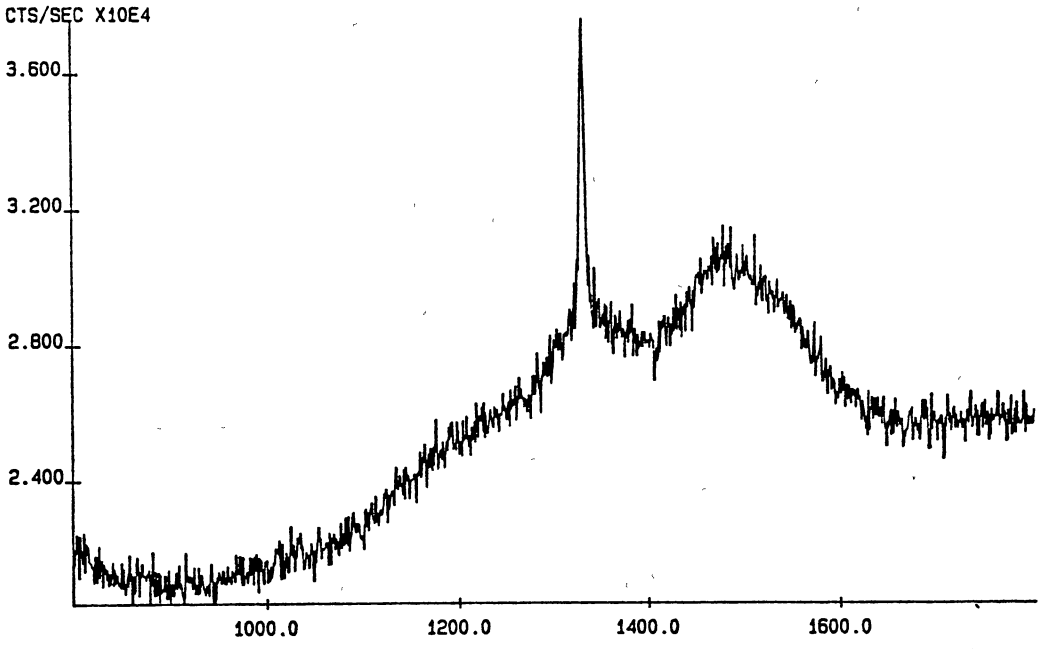

(e) Pressure = 98 psi

Figure 26. Raman Spectra of Film at Different Acetylene Cylinder Pressures (Contd.)

Morphological Variations Across the Diamond Film Surface

The existence of features ranging from cauliflower-like growth to well developed octahedral and cubic facets on the surface of a diamond film grown by combustion synthesis is well known. This peculiar growth behavior has been attributed to the existence of strong radial gradients of substrate temperatures and concentrations of the flame species. Some researchers [59-60] are of the opinion that the cauliflower-like particles observed on most flame formed diamonds are features which have resulted due to high density of secondary nucleation on well formed diamond particles. It is also believed that good quality diamonds grow only at the periphery of the acetylene feather in a vertically blowing flame because of the higher oxygen concentrations existing there [60]. In this investigation an attempt is made to address these issues.

Figure 27 is a SEM micrograph of a diamond film grown at a gas ratio, R=0.98, with a C_2H_2 flow rates of 3 slm. Figure 28 is a schematic of the same film showing four distinct zones. The micrographs of the morphological features in each zone are shown in the Figures 29(a) to (e). In and around zone-IV (which is the central portion of the film), well formed cubo-octahedral crystals were prevalent and the film was clear, white and translucent (Fig. 29(a)). In zone-III, cubo octahedral crystals similar to the ones in zone-IV were observed but they were not well developed (Fig. 29(b)). The cubic features were smaller and the octahedral {111} planes were more dominant. The zone was still translucent, the degree being lower than at zone-IV. In zone-II the morphology changed to highly twinned octahedra with numerous secondary growth features. In the region of transition between zone-II and III, good octahedral crystals were observed (Fig. 29(c)). The region at zone-II and towards the edge was very dark and not transparent. At zone-I, only cauliflower growth was observed (Fig. 29(d)). It is clear that as one moves from the edge of the film to the center, the morphology changes from cauliflower-like through octahedral to cubo-octahedral and ultimately to cubic. In many of the films grown,

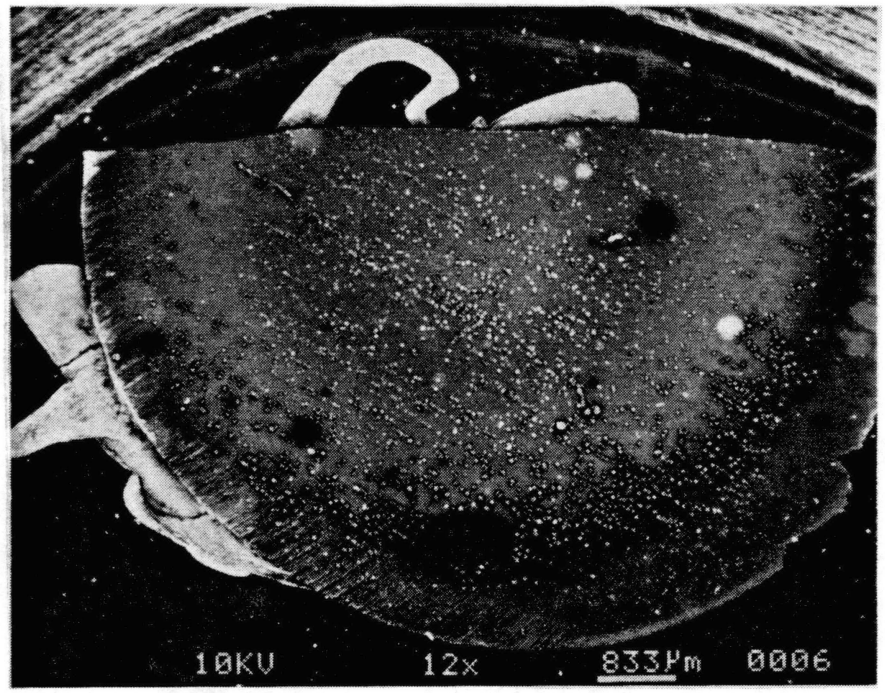

Figure 27. Top View of a Film Grown With R = 0.98

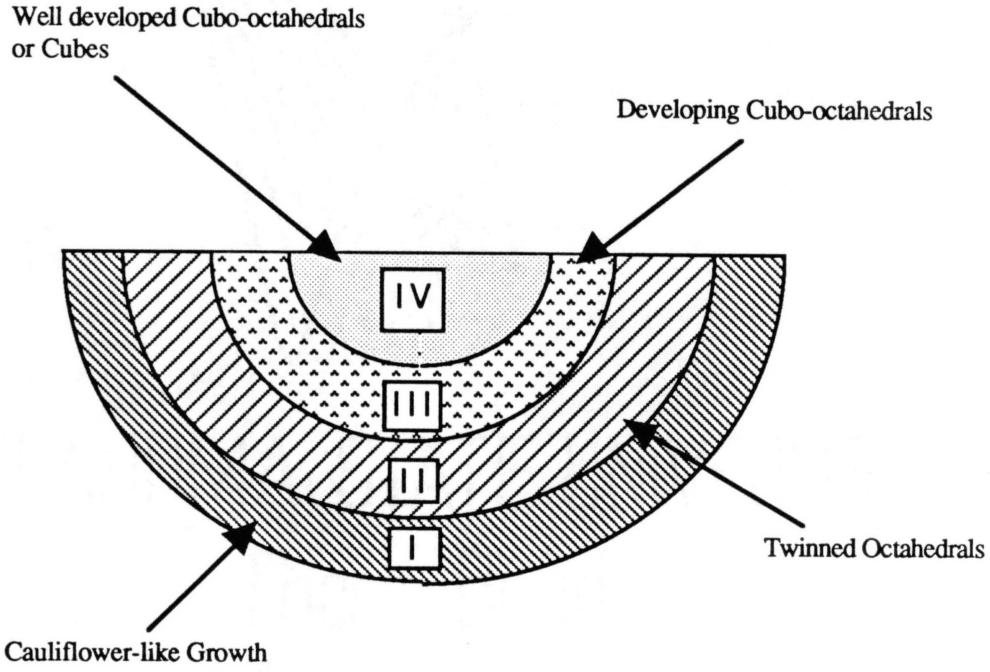

Figure 28. Schematic of the above Film Identifying Four Zones of Observation

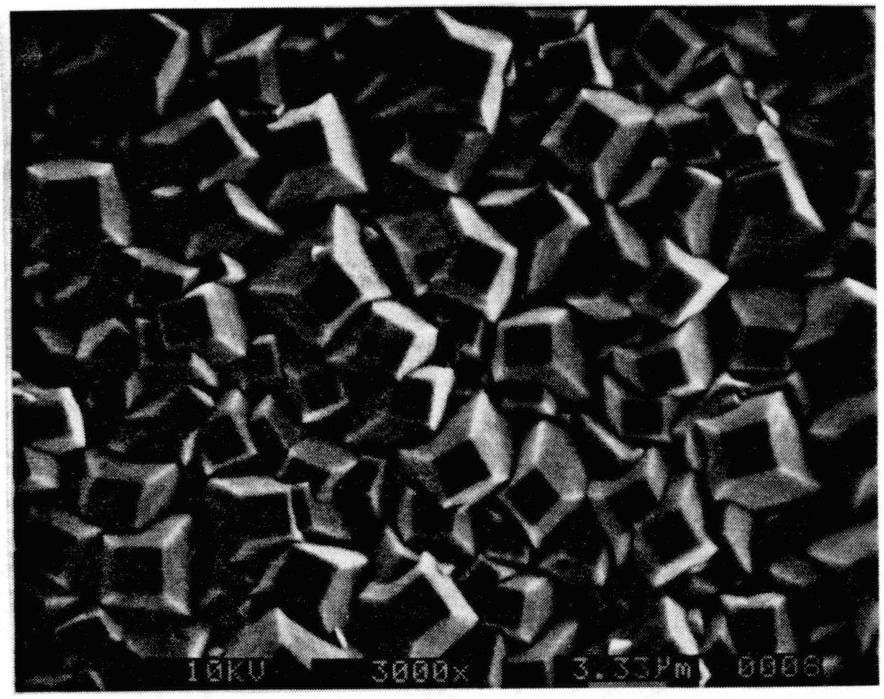

(a) Zone IV

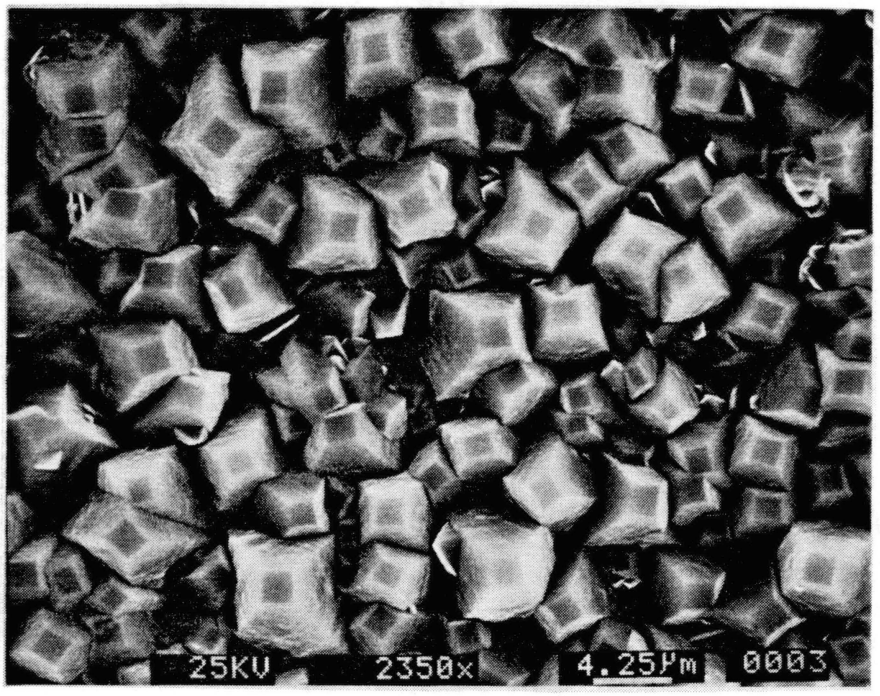

(b) Zone III

Figure 29. Morphologies at Different Zones

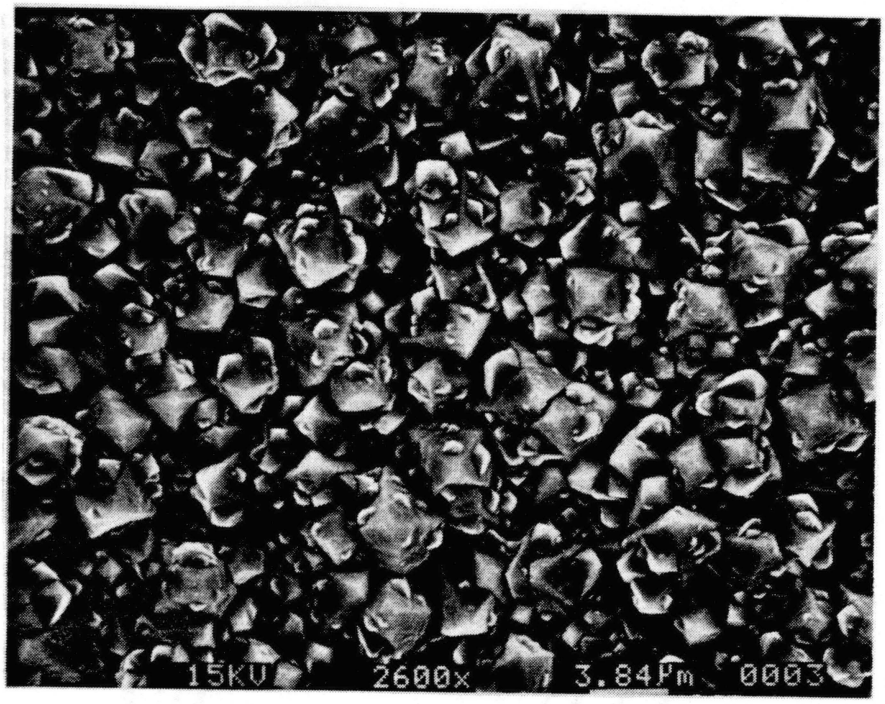

(c) Zone II

(d) Zone I

Figure 29. Morphologies at Different Zones (contd.)

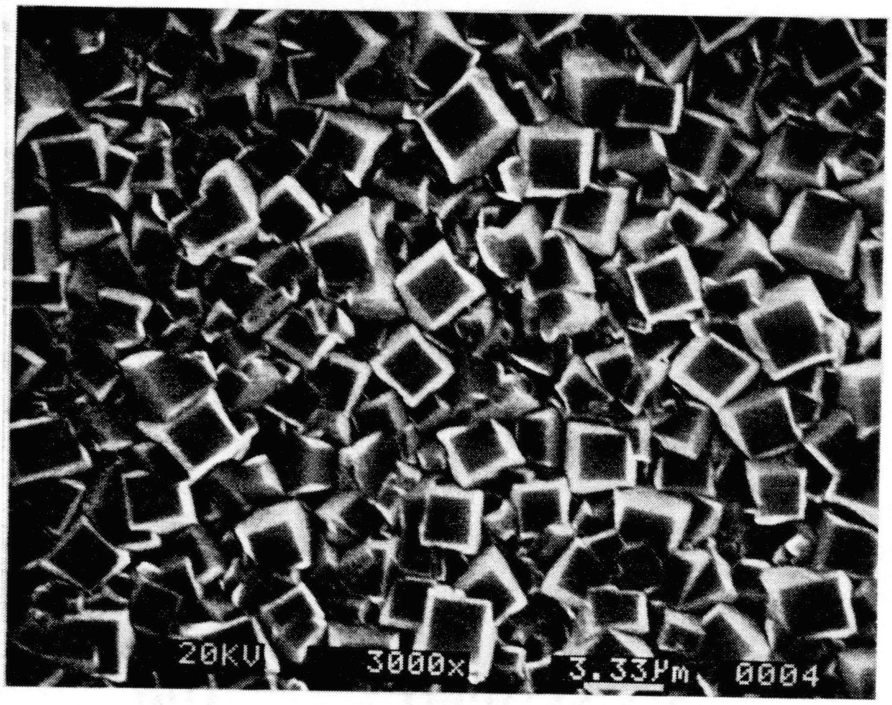

(e) Zone IV (at R = 1)

Figure 29. Morphologies at Different Zones (Contd.)

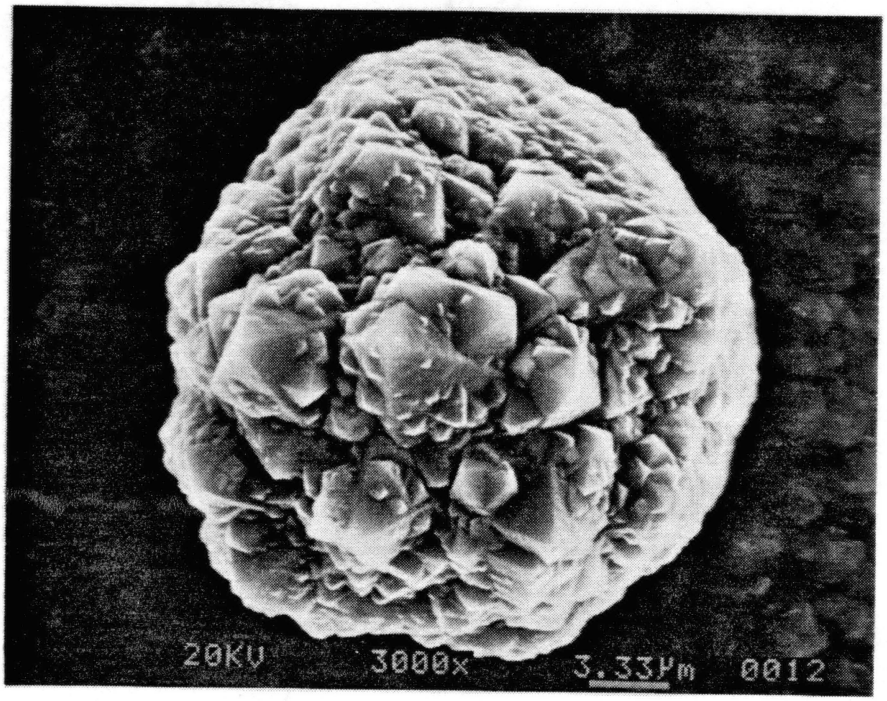

Figure 30. Micrograph of a Cauliflower-like Structure

especially ones with higher oxygen content in the mixture, cubic features were predominant in the center (Fig. 29(e)).

The zones observed on various diamond films, grown under entirely different processing conditions, exhibited identical morphological trends, the only exception being the nature of crystals at the center. Films grown at lower gas ratios (~ R=0.94) showed octahedral orientations while those at higher ratios (~ R=1.00) from cubo-octahedral to cubic. The cauliflower-like forms were present in almost all the films observed the amount varying for different conditions of growth. Similar trends in morphology were recently reported by Hanssen et. al. [66]. At this juncture it will be worthwhile to point out that the substrate temperatures were always maintained in the neighbourhood of 850 to 900° C for all the films grown.

This observation of the morphological differences on the diamond film enables us to develop a hypothesis for the growth mechanism of diamond films and the possibility of tailoring the morphology of the diamond crystallites. A recent publication of Hanssen et. al. [66] further corroborates these findings.

Evolution of the Diamond Crystals

As mentioned earlier, the morphology of flame grown diamonds consists of an assortment of crystal structures ranging from cauliflower-like to octahedrals, cubo-octahedral, cubic, and a range of intermediate morphologies. The cauliflower-like growth features have been previously dismissed as a highly defective form of diamond exhibiting a weak diamond Raman peak at 1332 cm^{-1} [67]. Figure 30 is a micrograph of a large cauliflower-like growth feature. However, the evidence provided in this section suggests that this "cauliflower-like" structure is infact diamond and is a precursor growth feature for the well developed octahedral and cubic crystals.

Figure 31(a) is a SEM micrograph showing some large cauliflower-like structures observed at the periphery of the film, i.e., at zone-I of Figure 28. Observation of the small

cauliflowers in the background at this magnification indicates no apparent crystalline orientation or facets. As can be seen from Figure 31(a) some of the larger cauliflower-like structures have been crowned by octahedra. The {111} faces of these octahedral formations exhibit numerous secondary growth, as is clear from one of the structures on the right of the picture (Fig. 31(a)). It is assumed here that the large growth features are those which have grown at a faster rate than the ones in the background.

In Figure 31(b) some highly twinned octahedral crystals are shown. The {111} faces of these crystals exhibit secondary nucleation which are also octahedral in nature. An examination of the lateral surfaces of these structures indicate close similarity to the corresponding surfaces on the cauliflowers discussed earlier. There are still some cauliflowers visible in the background showing tendency to convert into octahedra. It is believed that the larger structures have prevented the smaller ones from developing fully, because in areas where these large overgrowths were absent, good octahedral crystals had formed as shown in Figure 31(c). All these features were observed in zone-II. From the above observations, it can be deduced that the cauliflowers are infact transforming into octahedral structures under suitable growth conditions. The fact that the conversion is to octahedral and not to cubic is supported by the observation that the {111} surfaces are the most favored growth features under metastable conditions [37, 73]. Also, the temperature and chemical species of the reacting gases may have some influence on this.

The onset of the {100} faces on the octahedral structures is clearly shown in Figure 31(d). As can be seen, the {100} faces are very smooth compared to the {111} planes. These crystals were observed in zone-III towards zone-II and away from zone-IV. Careful observation of the small crystallites below indicate that some of them also have developed flat {100} features on top.

In zone-IV, the {100} planes are larger in area and even the smaller crystallites exhibit the cubo-octahedral morphology (Fig. 31(e)). Though octahedral features still

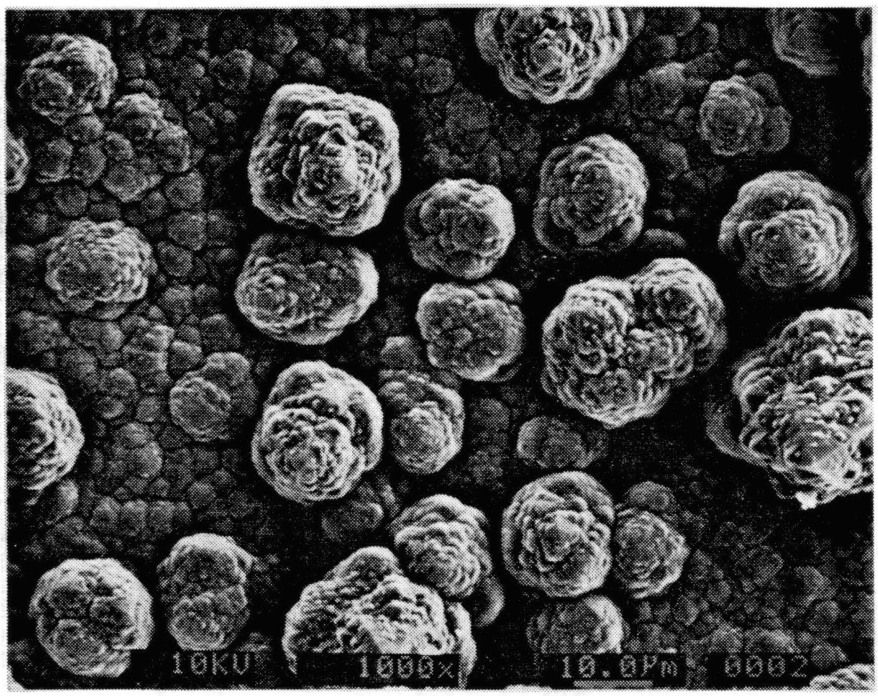

(a)

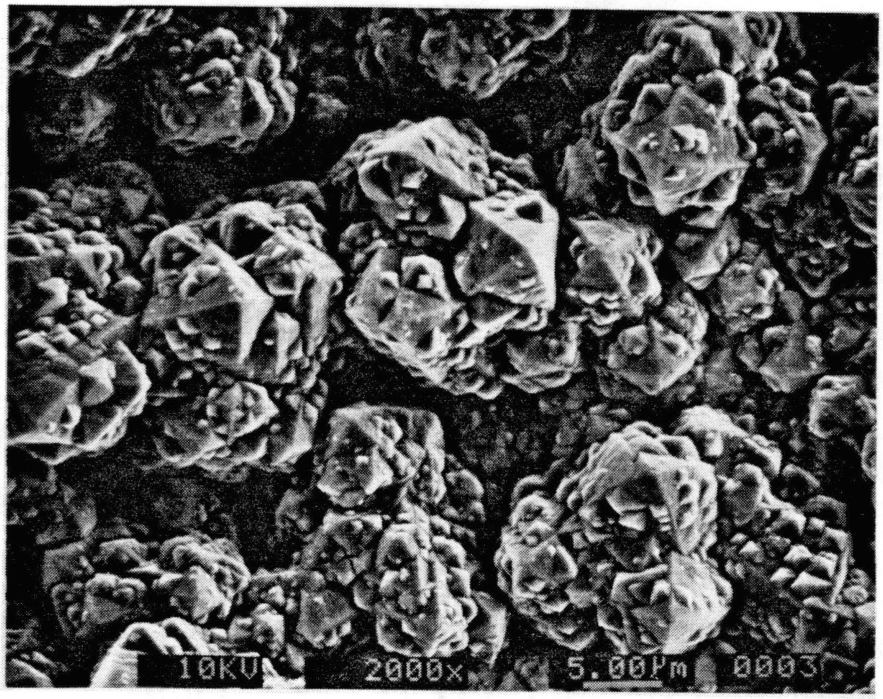

(b)

Figure 31. Evolution of Diamond Crystallites

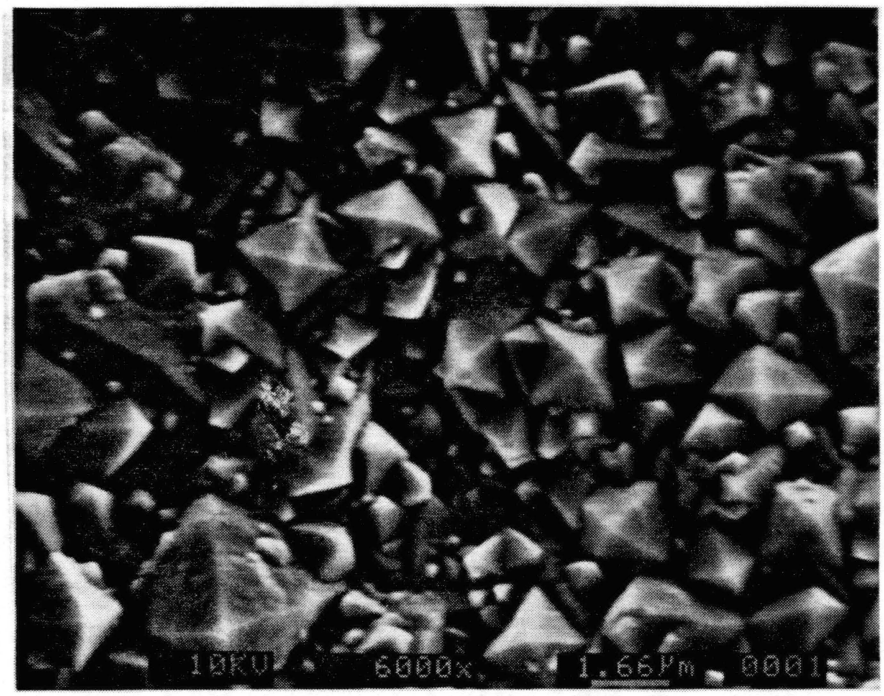

(c)

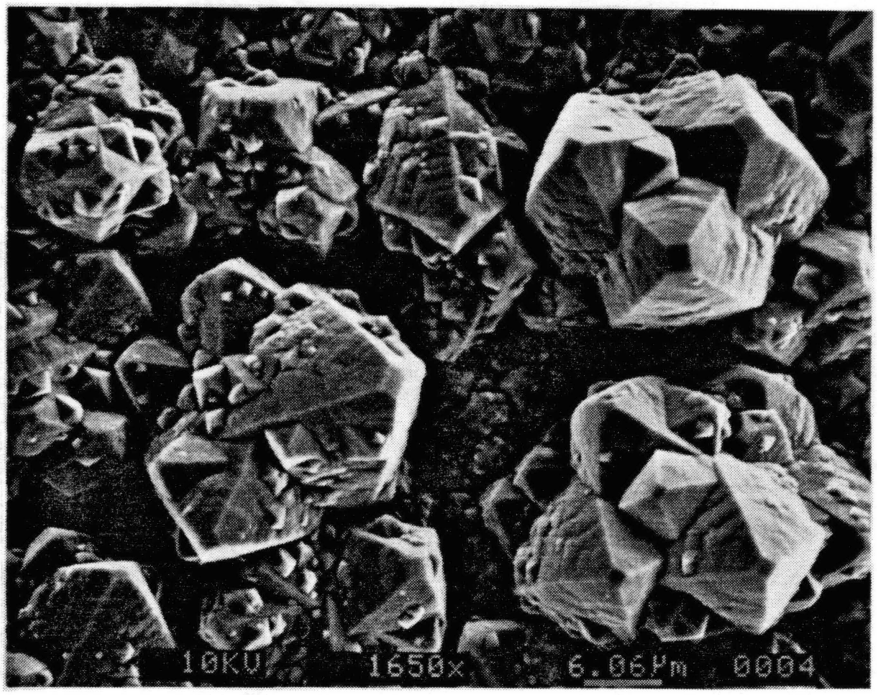

(d)

Figure 31. Evolution of Diamond Crystallites (Contd.)

(e)

Figure 31. Evolution of Diamond Crystallites (Contd.)

dominate the crystallites, it looks as if the corners of the octahedra have been neatly sliced off to display the smooth {100} faces.

To summarize, it has been postulated with the help of SEM micrographs of the diamond films that the octahedral and cubic crystalline forms to evolve from the cauliflower-like structures. Since the octahedral form of diamond is more favored to grow than cubic, the cauliflowers turn to octahedra first. These octahedral facets then change slowly to the cubo-octahedral or cube morphologies. The fact that the film was thicker at the center than at the edge indicates that the cauliflowers at the center grew at much faster rates than their counterparts at the edge, became octahedrals and then started changing to cubo-octahedra.

The process of conversion of the octahedral features to cubo-octahedra or to cubic structures is paramount to our understanding of the diamond film growth. The conditions at the center of the substrate, below the inner cone are severe due to the high temperatures. Under these conditions the likelihood of the diamond oxidizing is very high. Evans and Phaal [104] in 1962 studied the oxidation of diamond. They observed that the {111} surfaces of diamond had the highest oxidation rate, followed by the {110} surface, with the {100} surface having the lowest rate. It is therefore felt that as the deposition continues, the octahedral crystals gradually change to cubic as a result of etching by oxygen present in the feather. This hypothesis finds support from the fact that at higher flow ratios of 1 to 1.02, the {100} faces were of larger size than at lower flow ratios.

Based on earlier observations the following steps in the combustion synthesis of diamond may be occurring:

1. multinucleation resulting in cauliflower growth,
2. preferential growth of the cauliflowers,
3. secondary nucleation of crystallites as the earlier ones attain maximum growth.

This type of growth process was observed earlier by Kobashi et.al.[71] in their microwave CVD experiments.

Morphology as a Function of Cylinder Pressure

In this investigation we found rather accidently, that the diamond morphology was rather sensitive to the acetylene cylinder pressure. This to our knowledge has not been reported in the literature. While conducting the experiments, we observed that under identical conditions of growth some films exhibited cauliflower-like structures while others well formed octahedral or cubic structures. This disparity in the film quality was especially glaring when a new cylinder was used after the gas in the old one had depleted. We observed that with a new acetylene cylinder the deposited film was thick, opaque and black in color and consisted of only cauliflower-like features. As the pressure lowered corresponding to half the cylinder contents, these cauliflowers gradually turned to octahedral morphology and the film started to become translucent, even though it was dark in appearance. A further reduction in cylinder pressure resulted in white, highly translucent films which exhibited well formed cubo-octahedral morphology. This trend again indicates the evolution from the cauliflowers to other crystal morphologies. The conditions of growth were always the same, as mentioned earlier, only the C_2H_2 cylinder was getting depleted.

To understand this unusual growth pattern, the C_2H_2 was analysed using mass spectroscopy at different stages of cylinder pressures. The analysis indicated the presence of acetone, whose content in the gas increased as the pressure went down. The mass spectroscopy result of the gas at 120 psi is shown in Figure 32. The presence of acetone in the gas can be attributed to the fact that acetylene comes dissolved in acetone in the cylinder. At higher flow rates and lower cylinder pressures, there is a possibility that the acetone in vapor form can be pulled out of the cylinder along with the gas. Lower the cylinder pressure, more the likelihood of acetone being pulled out. Another observation which confirmed the presence of acetone was the condensation of the acetone vapors in the gas lines overnight. This clogged the mass flow meters causing them to malfunction.

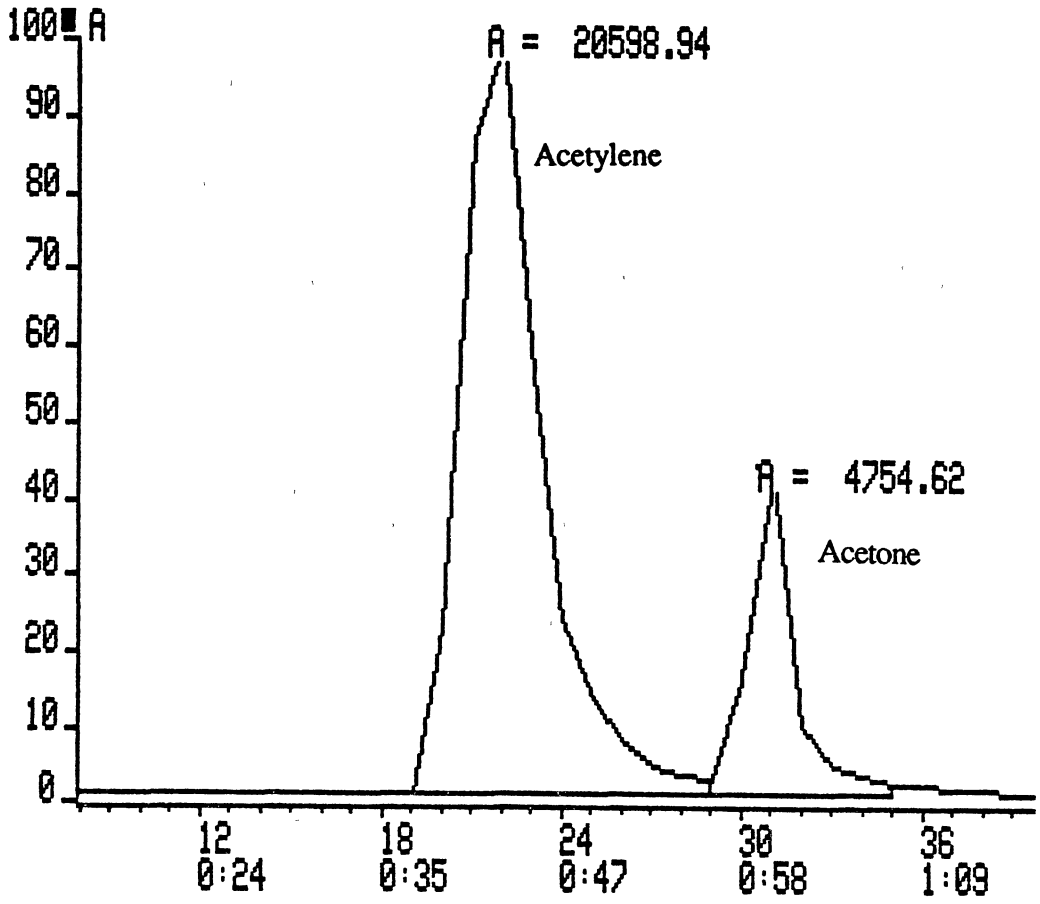

Figure 32. Mass Spectrum of Acetylene Gas at Cylinder Pressure of 120 psi

Morphology as a Function of the Stagnation Zone

The quest to grow diamond films which are uniform in thickness has proved to be elusive till date. This objective is especially difficult to realise in the combustion method because of the presence of strong radial gradients of temperatures and species concentrations. Moreover, the structure of the flame itself being highly variant, precludes the growth of films with uniform morphology and thickness under normal growth conditions. It was therefore felt that a close study of the flame structure would help in understanding the regimes within the acetylene feather where it would be possible to grow films of uniform thickness.

When a flame impinges vertically on a flat substrate at high velocity, it has to change its direction as it approaches the flat surface. A stagnation zone, therefore can be created at the center as shown in Figure 33(a). This zone separates the flame from the substrate. This zone usually termed "dead zone" is often observed in the case of fluids impinging on a plate . For the flame impingement, the shape of this stagnation zone varies depending upon the distance of the inner cone from the substrate and the velocity of flame. It appears to change from a bell-shaped zone (Fig. 33(a)) to a flat one (Fig. 33(b)) as the inner cone is brought nearer to the substrate. Along with the stagnation zone, the outer boundary of the feather also changes shape with the separation of the inner cone.

We found good diamond crystals to form within the stagnation zone with the diamond film to be fairly uniform in thickness in this region. Hanssen et. al. [62] found the temperature to be fairly constant in the central region of the substrate, which in our case may represent the stagnation zone. Beyond this zone the morphology of the film started changing to poorly formed octahedra or cauliflower-like shapes. This was the region, we believe, where the outer boundary of the feather changes directions. The cauliflower-like structures were predominant in the region where the feather moves parallel to the substrate.

From this discussion it appears that in order to synthesize films of uniform thickness, the substrate should be entirely within the stagnation zone. A flat stagnation

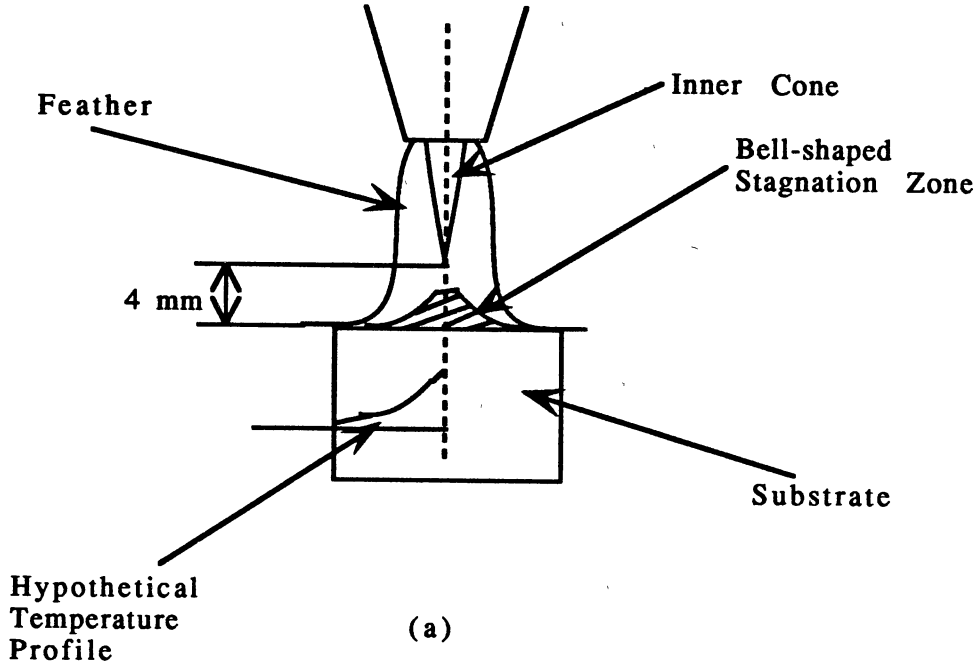

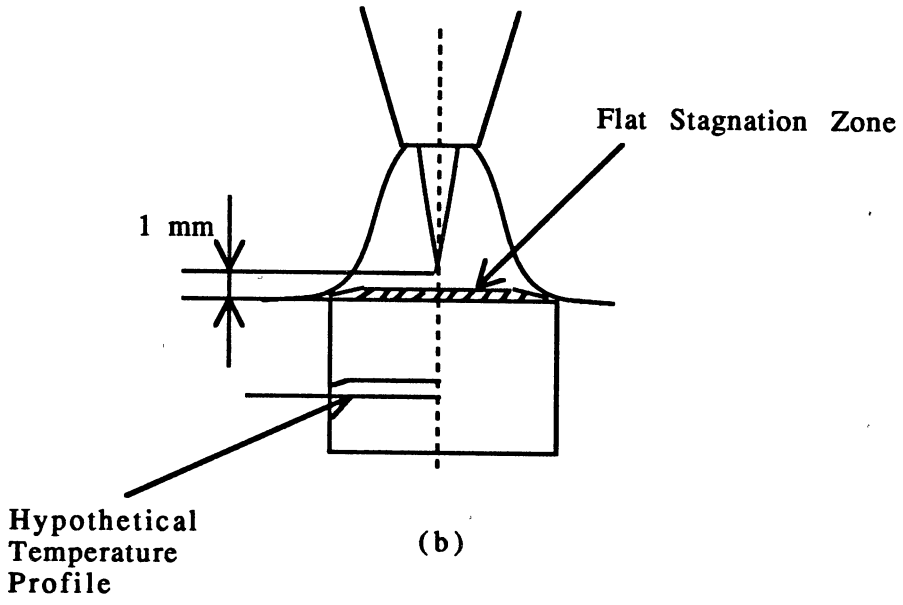

Figure 33. Stagnation Zone Shapes as a Function of Inner Cone Distance From the Substrate

zone parallel to the substrate surface is a better choice than a bell shaped one, as the temperature profile, would be similar in shape to the zone. Thus a flat zone may have a fairly uniform temperature while a bell-shaped zone may have temperature gradients. Using this approach, we grew highly transparent films without any cauliflower-like features by positioning the flame with respect to the substrate in such a manner that a flat stagnation zone covered the entire surface of the substrate. The outer boundary of the feather never intersected the substrate surface.

CHAPTER VI

CONCLUSIONS

The combustion flame method was used for the deposition of good quality diamond films on a molybdenum substrate. The effect of different parameters such as the gas flow ratio, gas flow rate, distance of the inner cone from the substrate, and acetylene cylinder pressure was systematically studied. It was observed that the quality of the diamond film, with the μRaman spectrum as a basis of assessment, improved with higher gas flow ratios ($R \approx 1$), lower gas flow rate, smaller distance of the inner cone from the substrate, and low acetylene cylinder pressure. The transparency and quality of the diamond film was found to be sensitively dependent on the acetylene cylinder pressure with excellent films obtained at the lower values of the cylinder pressure. This improvement in film characteristic is attributed to the presence of acetone vapors in the gas stream.

A careful observation of the diamond film surface revealed four zones of morphologies. The morphology varied from the cauliflower-like structures at the edge to well developed octahedra or cubic structures in the center. The intermediate regions consisted of highly twinned octahedral features. The morphology at the central portion of the film was found to be sensitive to the ratio of oxygen to acetylene. Cubic morphology dominated at high gas ratios ($R \approx 1$) and the octahedral morphology at lower values ($R \approx 0.94$). Cubo-octahedra were prevalent at intermediate ratios. This morphological behavior was consistently observed for different processing conditions with the substrate temperatures averaging about 850° C in all the experiments.

Based on extensive SEM examination of the diamond films it appears that the cauliflower-like structure is a precursor to the well developed {111} and {100} structures.

Depending on the experimental conditions the cauliflower-like structure transforms to either octahedra at ratios of R ≈ 0.94 and to cubic at R ≈ 1. These transformations were observed at low substrate temperature of ~ 850° C, suggesting that substrate temperatures may not be the only cause of the observed morphological behavior. It is proposed that the flame grown diamond films first grow with cauliflower-like features, independent of the experimental conditions. These then transform into octahedral structures with passage of time, as the {111} morphology is the most preferred growth feature. Depending on the gas flow ratios, the octahedral features would transform to cubo-octahedral or cubic morphologies as a result of further growth and/or etching by oxygen present in the gas stream. This observation, we believe, is very significant in tailoring the morphology of the crystallites to a desired configuration.

Since the flame impinges on a flat substrate, it is reasonable to assume that a change in flow field near the substrate can lead to the development of a stagnation zone in the center of the substrate. The size of the zone may depend on various processing parameters. A close study of the flame characteristics, using a No. 4 nozzle, as it impinges on the substrate revealed the presence of a stagnation zone within the flame. This zone was observed to change from a bell-shaped to a flat zone as the distance of the inner cone from the substrate is changed from 4 mm to 1mm. Within the stagnation zone well formed crystallites were observed and the film was transparent. By varying the shape of the stagnation zone, uniform films have been synthesized.

REFERENCES

1. Newton, I., "Optiks", London, (1704).
2. Lavoisier, A. L., Memoire Academie des Sciences, (1772) 564-591.
3. Tennant, S., Phil. Trans. R. Soc., 87, (1797) 97-123.
4. Allen, W., and W. H. Pepys, Phil. Trans. R. Soc, 97, (1807) 267.
5. Davy, H., "The Collected Works of Sir Humphrey Davy", V, (1840).
6. Hannay, J. B., Proc. Roy. Soc., 30, (1880) 188.
7. Moissan, H., C. R. Acad. Sci., Paris, 118, (1894) 320.
8. Crookes, W., "Diamonds," London: Harper & Brothers, (1909).
9. Parsons, C. A., Phil. Trans., 220, (1920) 67.
10. Hershey, J. W., Trans. Kansas Acad. Sci., 40, (1940) 213.
11. Bridgman, P. W., J. Chem. Phys., 15, (1947) 92.
12. Bundy, F. P., Hall, H. T., Strong, H. M., and R. H. Wentorf, Nature (London), 176, (1955) 51-54.
13. Bovenkerk, H. P., Bundy, F. P., Hall, H. T., Strong, H. M., and R. H. Wentorf, Nature (London), 184, (1959) 1094.
14. Decarli, P. S. and J. C. Jamieson, Science, 133, (1961) 1821.
15. Bundy, F. P., Strong, H. M., and R. H. Wentorf, Chemistry and Physics of Carbon, Marcel Dekker, New York, (1973), 213-216.
16. Bridgman, P. W., Sci. Am., 193, (1955) 42-46.
17. W. von Bolton, Z. Elektrochem., 17, (1911) 971.
18. Eversole, W. G., U.S. Patent Nos. 3,030,188 & 3,030,188 (1962).
19. Angus, J. C., Will, H. A., and W.S. Stanko, J. Appl. Phys., 39, (1968) 2915-2922.
20. Chauhan, S. P., Angus, J. C., and N. C. Gardner, J. Appl. Phys., 47, 11 (1976) 4746-4754.

21. Poferl, D. J., Gardner, N.C., and J. C. Angus, J. Appl. Phys., 44, 4 (1973) 1428-1434.

22. Angus, J. C., Gardner, N. C., Poferl, D. J., Chauhan, S. P., Dyble, T. J., Sung, P., Sint. Almazy., 3, (1971) 38-39.

23. Deryagin, B. and D. B. Fedoseev, Sci. Am., 233, 5 (1975) 102-109.

24. Spitsyn, B. V., Bouilov, L. L., and B. V. Deryagin, J. Cryst. Growth, 52, (1981) 219-226.

25. Lux, B. and R. Haubner, Int. J. Ref. Hard. Metals, (May 1989) 158-174.

26. Hirose, Y. and M. Mitsuizumi, New Diamond, 4, 3 (1988) 34-35.

27. Spear, K. E., Earth Miner. Sci., 56, 4 (1987) 53-59.

28. Devries, R. C., Annu. Rev. Mater. Sci., 17, (1987) 161-187.

29. Angus, J. C. and C. C. Hayman, Science, 241, (1988) 913-921.

30. Spear, K. E., J. Am. Ceram. Soc., 72, 2 (1989) 171-191.

31. Matsumoto, S., Sato, Y., Tsutsumi, M., and N. Setaka, J. Mater. Sci., 17, (1982) 3106-3112.

32. Matsumoto, S., Sato, Y., Kamo, M., and N. Setaka, Jpn. J. Appl. Phys., 21, 4 (1982) L183-L185.

33. Bonnot, A. M., Thin Solid Films, 185, (1990) 111-121.

34. Farabaugh, E. N., Feldman, A., and L. H. Robins, SPIE- Diamond Optics, 969, (1988) 24-31.

35. Hirose, Y. and Y. Terasawa, Jap. J. Appl. Phys., 25, (1986) L519-L521.

36. Iijima, S., Aikawa, Y., and K. Baba, Appl. Phys. Lett., 57, 25 (1990) 2646-2648.

37. Lee, Y. H., Bachmann, K. J., and J. T. Glass, Appld. Phys. Lett., 57, 18 (1990) 1916-1918.

38. Okoli, S., Haubner, R., and B. Lux, J. de Physique, 50, 5 (1989) 159-168.

39. Singh, B., Mesker, O. R., Levine, A. W. and Y. Arie, Appl. Phys. Lett., 52, 20 (1988) 1658-1660.

40. Singh, B., Mesker, O., Levine, A. W., and Y. Arie, J. Vac. Sci. Tech., (1988)

41. Singh, B., Arie, Y., Levine, A. W., and O. R. Mesker, Appl. Phys. Lett., 52, 6 (1988) 451-452.

42. Kamo, M., Sato, Y., Matsumoto, S., and N. Setaka, J. Cryst. Growth, 62, (1983) 642-644.

43. Ong, T. P. and R. P. H. Chang, Appl. Phys. Lett., 55, 20 (1989) 2063-2065.

44. Suzuki, J., Kawarada, H., Mar, K., Wei, J., Yokota, Y., and A. Hiraki, Jap. J. Appl. Phys., 28, 2 (1989) L281-L283.

45. Kamo, M., Chawanya, H., Tanaka, T., Sato, Y., and N. Setaka, Mat. Sci. Engg., A105/106, (1988) 535-541.

46. Kawarada, H., Mar, K. S., and A. Hiraki, Jap. J. Appl. Phys., 26, 6 (1987) L1032-L1034.

47. Akatsuka, F., Hirose, Y., and K. Komaki, Jap. J. Appl. Phys., 27, 9 (1988) L1600-L1602.

48. Chang, C. P., Flamm, D. L., Ibbotson, D. E., and J. A. Mucha, J. Appl. Phys., 63, 5 (1988) 1744-1748.

49. Kurihara, K., Sasaki, K., Kawarada, M.,and N. Koshino, Appl. Phys. Lett., 52, 6 (1988) 437-438.

50. Nakao, S., Nodda, M., Kusakabe, H., Shimizu, H., and S. Maruno, Jap. J. Appl. Phys., 29, 8 (1990) 1511-1514.

51. Ohtake, N. and M. Yoshikawa, J. Electochem. Soc., 137, 2 (1990) 717-722.

52. Amaratunga, G., Putnis, A., Clay, K., and W. Milne, Appl. Phys. Lett., 55, 7 (1989) 634-635.

53. Kobayashi, K., Yamamoto, K., Mutsukura, N., and Y. Machi, Thin Solid Films, 185, (1990) 71-78.

54. Matsumoto, S., J. Mater. Sci. Lett., 4, (1985) 600-602.

55. Meyer, D. E., Ianno, N. J., and J. A. Woollam, J. Mater. Res., 3, 6 (1988) 1397-1403.

56. Kitahama, K., Hirata, K., Nakamatsu, H., Kawai, S., Fujimori, N., Imai, T., Yoshino, Y., and A. Doi, Appl. Phys. Lett., 49, (1986) 634.

57. Sawabe, A. and T. Inuzuka, Appl. Phys. Lett., 46, 2 (1985) 146-147.

58. Sawabe, A. and. T. Inuzuka, Thin Solid Films, 137, (1986) 89-99.

59. Yarbrough, W. A., Stewart, M. A., and J.A. Cooper, Surf. Coat. Tech., 39/40, (1989) 241-252.

60. Tzeng, Y., Cutshaw, C., Phiilips, R., Srivinyunon, T., Ibrahim, A., and B. H. Loo, J. Appl. Phys., 56, 2 (1990) 134-136.

61. Ravi, K. V. and A. Joshi, Appl. Phys. Lett., 58, 3 (1991) 246-248.

62. Oakes, D. B., Butler, J. E., Snail, K. A., Carrington, W. A., and L. M. Hanssen, J. Appld. Phys., 69, 4 (1991) 2602-2610.

63. Komanduri, R., Fehrenbacher, L. L., Hanssen, L. M., Morrish, A., Snail, K. A., Thorpe, T., Butler, J. E., and Rath, B. A., Annals of CIRP, West Berlin, 1990,

64. Komanduri, R., Snail, K. A., and L. L. Fehrenbacher, Phil. Mag. Lett., 62, 4 (1990) 283-290.

65. Hirose, Y. and S. Amanoma, J. Appl. Phys., 68, 12 (1990) 6401-6405.

66. Hanssen, L. M., Snail, K. A., Carrington, W. A., Butler, J. E., Kellogg, S., and D. B. Oakes, Thin Solid Films, 196, (1991) 271-281.

67. Hanssen, L. M., Carrington, W. A., Butler, J. E. and K. A. Snail, Mater. Lett., 7, (1988) 289.

68. Carrington, W. A., Hanssen, L. M., Snail, K. A., Oakes, D. B., and J. E. Butler, Metall. Trans., 20A, (1989) 1282-1284.

69. Murakawa, M., Takeuchi, S., and Y. Hirose, Surf. Coat. Tech., 39/40, (1989) 235-240.

70. Matsumoto, S. and Y. Matsui, J. Mater. Sci., 18, (1983) 1785-1793.

71. Kobashi, K., Nishimura, K., Kawate, Y., and T. Horiuchi, Phys. Rev. B, 38, 6 (1988) 4067-4084.

72. Kim, J. S., Kim, M. H., Park, S. S., and J. Y. Lee, J. Appl. Phys., 67, 7 (1990) 3354-3357.

73. Hirabayashi, K., and N. I. Kurihara, Jap. J. Appl. Phys., 29, 10 (1990) L1862-L1865.

74. Hirabayashi, K., and N. I. Kurihara, Jap. J. Appl. Phys., 29, 10 (1990) L1901-L1903.

75. Hirabayashi, K.and N. I. Kurihara, Jap. J. Appl. Phys., 30, 1A (1991) L49-L51.

76. Wild, C., Herres, N., and P. Koidl, J. Appl. Phys., 68, 3 (1990) 973-978.

77. Deryagin, B. V., Bouilov, L. L., and B. V. Spitsyn, Arch. Nauki. Mater., 7, 2 (1986) 111-119.

78. Deryagin, B. V. and D. V. Fedoseev, Izd. Nauka, Moscow, USSR, 1977.

79. Varnin, V. P., Fedoseev, D. V., and I. G. Teremetskaya, Arch. Nauki Mater., 7, 2 (1986) 121-125.

80. Tsuda, M., Nakajima, M., and S. Oikawa, J. Am. Chem. Soc., 108, (1986) 5780-5783.

81. Tsuda, M., Nakajima, M., and S. Oikawa, Jpn. J. Appl. Phys., 26, (1987) L527-L529.

82. Frenklach, M. and K. E. Spear, J. Mater. Res., 3, 1 (1988) 133-140.

83. Aisenberg, S. and R. Chabot, J. Appl. Phys., 42, 7 (1971) 2953-2958.

84. Messier, R., Badzian, A., Badzian, T.,Spear, K. E., Bachmann, P., and R. Roy, Thin Solid Films, 153, (1987) 1-9.

85. Buckley, R. G., Moustakas, T. D., Ye, L., and J. Varon, J. Appl. Phys., 66, 8 (1989) 3595-3599.

86. Harshavardhan, K. S., Vijayaraghavan, M. N., Chandrabhas, N., and A. K. Sood, J. Appl. Phys., 68, 7 (1990) 3303-3306.

87. Knight, D. S. and W. B. White, J. Mater. Res., 4, 2 (1989) 385-393.

88. Ramdas, A. K. and S. A. Solin, Phys. Rev. B, 4 (1970) 1687-1698.

89. Knight, D. S., Drawl, W. R., Badzian, A., Badzian, T. and W. B. White, Symposium on Diamond And Diamond-like Materials Synthesis, Pittsburgh, Materials Research Society, 1988,

90. Nemanich, R. J. and S. A. Solin, Phys. Rev. B, 20, 3 (1979) 392-401.

91. Wagner, J., Ramsteiner, M., Wild, Ch. and P. Koidl, Phys. Rev. B, 40, 3 (1989) 1817-1824.

92. Frenklach, M., J. Appl. Phys., 65, 12 (1989) 5142-5149.

93. Badzian, A. R. and R. C. Devries, Mater. Res. Bull., 23, (1988) 385-398.

94. Setaka, N., J. Mater. Res., 4, 3 (1989) 664-670.

95. Mucha, J. A., Flamm, D. L., and D. E. Ibbotson, J. Appld. Phys., 65, 9 (1989) 3448-3452.

96. Kawato, T. and K. Kondo, Jap. J. Appl. Phys., 26, 9 (1987) 1429-1432.

97. Zhang, F., Zhang, Y., Yang, Y., and G. Chen, Appl. Phys. Lett., 57, 14 (1990) 1467-1469.

98. Celli, F. G., Pehrsson, P. E., Wang, H. T., and J. E. Butler, Appl. Phys. Lett., 52, 24 (1988) 2043-2045.

99. Harris, S. J., Weiner, A. M., and T. A. Perry, Appl. Phys. Lett., 53, (1988) 1605-1608.

100. Matsui, Y., Yuuki, A., Sahara, M., and Y. Hirose, Jap. J. Appl. Phys., 28, 9 (1989) 1718-1724.

101. Matsui, Y., Yabe, H., and Y. Hirose, Jap. J. Appl. Phys., 29, 8 (1990) 1552-1560.

102. Cappelli, M. A. and P. H. Paul, J. Appl. Phys., 67, 5 (1990) 2596-2602.

103. Gaydon, A. G. and H. G. Wolfhurd, "Flames: Their Structure, Radiation, and Temperature", Chapman and Hall Ltd., London, U. K., (1970).

104. Evans, T. and C. Phaal, Fifth Biennial Conference on Carbon, Pennsylvania State University, (1962), 147-153.

105. J. E. Field, "The Properties of Diamond," Academic Press, (1979).

106. Bachmann, P. K. and R. Messier, Chem. Engg. News, May 15 (1989), 24-39.

107. Evans, T. and P. F. James, Proc. Roy. Soc., A277, (1964) 260-269.

108. "The Oxy-Acetylene Handbook", The Linde Air Products Company, New York, (1943).

109. M. W. Geis, Appl. Phys. Lett., 55, 6 (1989) 550-552.

APPENDIXES

APPENDIX A

PROPERTIES OF DIAMOND

Diamond is a material with many unique properties, and these have made it pre-eminent as a gem stone, an industrial tool, and as a material for solid state research. The fact that diamond can be grown synthetically as single crystals and now as polycrystalline films, often with chosen properties, has broadened the scope of application of this exquisite material.

About 95% of diamond consumed for industrial application is as an abrasive, for such operations as lapping and polishing, grinding, sawing, drilling and as a single point machining tool. However, the balance of consumption of industrial diamond finds applications as heat sinks, bearings, hardness indenters, surgeon's knives, etc., in which the hardness of diamond is often important but there is no abrasive action.

In this Appendix, the various properties of diamond which have been exploited for industrial applications will be presented. A comprehensive work on the properties of diamond can be found in the book by J. E. Field [105].

Classification of Diamonds

Based on their optical and electrical properties and their impurity content, diamonds are classified into four types of single crystal material and two types of polycrystalline material [105, 106]:

Type Ia. About 98% of the natural diamonds are of this type. They contain nitrogen as an impurity in fairly substantial amounts (~ 0.1%) in the form of small aggregates or platelets. The nitrogen which is not paramagnetic, strongly absorbs ultra-violet and infra-red light. These diamonds are optically transparent at wavelengths > 320 nm. At room temperature, the thermal conductivity is ~1000 Watts m^{-1} K^{-1}.

Type Ib. Almost all synthetic (HP-HT) diamonds are of this type. They contain paramagnetic nitrogen on isolated substitutional lattice sites upto ~0.2%. Optical, thermal, and electrical properties are similar to type Ia diamonds.

Type IIa. Very rare in nature and is practically free of nitrogen. These are transparent to ultra-violet above 225 nm. Thermal conductivity at room temperature is 2000 Watts m^{-1} K^{-1}.

Type IIb. Extremely rare in nature, these diamonds contain a very low concentration of nitrogen (lower than type IIa). They have a bluish color due to the presence of boron which makes them a p-type semiconductor.

Carbonados and Ballas. These are naturally occurring polycrystalline diamonds. Carbonados which contain graphite and other impurities are tougher than single crystal diamonds. Ballas are round, dense, randomly oriented polycrystalline diamonds. They have very high impact resistance and do not cleave.

Mechanical Properties

Specific values of the mechanical properties of diamond are listed in Table I [30]. Two of the exceptional properties of diamond are its extreme hardness and its very high thermal conductivity. These properties coupled with the low coefficient of thermal expansion and friction have been effectively exploited in its use as an abrasive and for wear resistant applications.

The fracture behavior of diamond is dominated by cleavage on the {111} plane, although cleavage has also been observed on the {110} plane. This behavior is not clear as the energy differences for the different planes are small. The most likely answer may be due to defects on the {111} plane giving preferential weakening. Cleavage cracks in diamond can propagate at very high velocities (~ 7200 ms^{-1}). Comparison of the strengths

of good quality diamonds indicate the best value of the tensile strength to be roughly 300 kg mm^{-2} [105].

TABLE I

MECHANICAL PROPERTIES OF DIAMOND

Properties	Values
Hardness	Indentation hardness, 8000 kg/mm^2
Coefficient of Friction	~ 0.1 in air ~ 1 in vacuum
Elastic Modulii ($\times 10^{11}$ Pa)	
C_{11}	10.8
C_{12}	1.25
C_{44}	5.77
Pressure Coefficient, dC/dP	
C_{11}	6.0(0.7)
C_{12}	3.1(0.7)
C_{44}	3.0(0.3
Temperature Coefficient,	
C_{11}	-1.4(0.2)
C_{12}	-5.7(1.5)
C_{44}	-1.25(0.1)
Young's Modulus, E (Pa)	10.5×10^{11}
Poisson's Ratio,	0.104
Bulk Modulus (Pa)	4.42×10^{11}

The adhesion and friction of diamond depend both on the bulk and surface properties of diamond. In air, the friction of diamond on diamond is relatively low, $\mu \approx 0.1$. The friction depends on crystal face and orientation. On the octahedral face the friction is low and there is no anisotropy. The lowest friction is along the <011> direction and the highest along the <100> direction. In vacuum, the friction can reach high values ($\mu \approx 1$) [105].

At room temperature, diamond behaves as an elastic brittle solid. However, at 1800° C, in vacuum, dislocations become relatively mobile and it is possible to produce appreciable plastic deformation.

Thermal Properties

At room temperature, the thermal conductivity of type IIa diamond is four to five times better than that of copper. The maximum thermal conductivity occurs at 80 K. However, the thermal conductivity drops significantly even if small amounts of nitrogen is present as an impurity. The presence of ^{13}C isotope of carbon also affects the thermal conductivity of diamond. The thermal properties of diamond are listed in Table III [30].

The coefficient of linear expansion of diamond at room temperature is only 8×10^{-7} K^{-1}. In contrast copper has an expansion coefficient of 170×10^{-7} K^{-1}, at room temperature. The special low expansion alloy Invar (a nickel-steel alloy) has an expansion coefficient similar to that of diamond at 9×10^{-7} K^{-1} [105].

Optical and Electrical Properties

The transparency of diamond is one important reason why it makes a pre-eminent gem. Diamonds with low nitrogen content are transparent down to 220 nm. If they have nitrogen impurities they absorb at wavelengths lower than 320 nm. Diamond also, has an high refractive index, ~2.4.

A pure, perfect diamond is an extremely good insulator with resistivities greater than 10^{14} ohm-meters being frequently observed. However, diamond can be made semiconductive by doping it with phosphorus (n-type) or with boron (p-type). The mobility of these positively and negatively charged carriers are equal and high in diamond. Table III [30] lists the electrical and optical properties of diamond.

TABLE II

THERMAL PROPERTIES OF DIAMOND

Properties	Values
Thermal Conductivity (W/ cm. K)	
Typical values at 293 K	
Type Ia	6-10
Type IIa	20-21
Thermal Expansion ($\times 10^{-6}$ K^{-1})	
193 K	0.4(0.1)
293 K	0.8(0.1)
400-1200 K	1.5-4.8
Debye Temperature, at T > 600 K (K)	1880
Bulk Modulus, B (Pa)	4.4×10^{11}
Cp -Cv at T > 1100 K (J / mol. K)	4.2×10^{-4} T
Cp at 1800 K	24.7
Cp at 3000 K	26.3

Chemical Properties

Diamond is extremely inert chemically and is not affected by any acids or chemicals. Substances such as sodium nitrate are known to affect diamond in the molten state at temperatures as low as ~ 450° C. O_2 , CO, CO_2 , H_2 , H_2 O, and Cl_2 at high temperatures have been used to etch diamonds [30]. In oxygen itself, diamond starts to be oxidized at ~ 700° C [104].

TABLE III

ELECTRICAL AND OPTICAL PROPERTIES OF DIAMOND

Properties	Values
Lattice Constant (nm)	0.3567
Density (g/cm^3)	3.515
Band Gap (eV)	5.45
Saturated electron velocity ($\times 10^7$ cm/s)	2.7
Carrier Mobility ($cm^2/V.s$)	
Electron	2200
Hole	1600
Breakdown ($\times 10^5$ V/cm)	100
Dielectric Constant	5.5
Resistivity (Ω cm)	10^{13}
Refractive Index	2.42

Two groups of metal have been found to chemically attack diamonds. The first group consists of carbide formers and include tungsten, tantalum, titanium, and zirconium. At high temperatures, these metals form carbides. The second group includes iron, cobalt, manganese, nickel, and chromium, and also the platinum group of metals. In the molten state these metals are true solvents for carbon.

When diamond is heated to high temperatures it transforms to graphite. Results of experiments on the heating of diamond in vacuum [107], show that the onset of graphitization is detectable around 1500° C and the rate of graphitization increases rapidly until around 2000° C diamond completely transforms into graphite in a short time.

APPENDIX B

INSTRUMENT SPECIFICATIONS

Mass Flow Meters

Model	:	MKS 2259C
Full Scale Ranges	:	10000 sccm (acetylene) and 5000 sccm (oxygen)
Accuracy	:	± 0.8% of F. S. at 760 torr/0° C
Resolution	:	0.1% of F. S.
Settling Time	:	< 2 seconds within 2% of set point
Maximum Inlet Pressure	:	150 psig

Mass Flow Programmer

Model	:	MKS 147B
Number of Channels	:	4 - flow (independent or in ratio)
Measuring Rate	:	250 msec/measurement
Output Rate	:	4 measurements/sec
Input Voltage	:	4 × 0 - 5 VDC (flow signal)
Output Voltage	:	4 × 0 - 5 VDC (flow set point)

Dual Wavelength Infrared Pyrometer

Model	:	Williamson Tempmatic 8000 Series
Accuracy	:	0.75% full scale
Repeatability	:	0.25% full scale
Working Distance	:	6" to 1-1/2 feet
Response Time	:	Adjustable 0.2 to 5 seconds
Range	:	550 - 1100° C and 900 - 2400° C
Spot Size at 18" Distance	:	0.25"

μRaman Spectrometer

Model	:	RAMANOR U 1000 (Instruments SA Inc.)

Focal Length	:	1000 mm
Aperture Size	:	f/8
Grating Size	:	$110 \times 110\ mm^2$
Number of Grooves/mm	:	1800
Resolution	:	0.15 cm^{-1} on the Hg line at 5791 Å
Dispersion	:	9.2 cm^{-1}/mm at 514.5 nm
Scanning Period	:	0.1 to 4800 cm^{-1}/min

APPENDIX C

COMPARISON OF THE PROPERTIES OF DIAMOND AND CUBIC BORON NITRIDE

TABLE IV

SELECTED PROPERTIES OF DIAMOND AND CBN

	Diamond	cBN
STRUCTURAL		
Structure	cubic Fd3m	cubic F43m
Unit Cell (Å)	3.567	3.615
Density (gm/cm^3)	3.52	3.48
Cleavage	{111}	{011}
MECHANICAL		
Hardness (kg/mm^2)	8500+	4500
Bulk Modulus GPa	435	367
THERMAL		
Conductivity at 25 °C (W/cm/°C)	20 (Type IIa)	8
Expansion at 400 °C (cm/cm/°C)	3.5	4.8
Graphitization	1400-1800 °C	>1550 °C
OPTICAL		
Refractive Index	2.417	2.117
Band Gap eV	5.47	6.1 - 6.6
ELECTRICAL		
Resistivity (ohm-cm)	10^{13}	10^{10}
Dielectric Constant	5.5	4.5

VITA 2

SRIHARI NANDYAL

Candidate for the Degree of

Master of Science

Thesis : COMBUSTION SYNTHESIS OF DIAMOND FILMS

Major Field : Mechanical Engineering

Biographical :

Personal Data: Born in Nandyal, Andhra Pradesh, India, December 20, 1963, the son of Seshasayan and Vijayalakshmi Nandyal.

Education: Received Bachelor of Engineering degree in Mechanical Engineering from Karnataka Regional Engineering College at Surathkal, India in July, 1985; completed requirements for the Master of Science degree at Oklahoma State University in December, 1991.

Professional Experience: Assistant Engineer,
Tata Engineering and Locomotive Company, Jamshedpur, India;
August 1985 to August 1988;
Teaching Assistant, Department of Mechanical and Aerospace Engineering,
Oklahoma State University, September, 1988 to May 1991.